TECHNISCHE UNIVERSITÄT MÜNCHEN

Lehrstuhl für Entwicklungsgenetik

Acute effects of psychopharmacological compounds on ionotropic receptor signalling and synaptic plasticity related mechanisms

Sascha Tanasic

Vollständiger Abdruck der von der Fakultät Wissenschaftszentrum Weihenstephan für Ernährung, Landnutzung und Umwelt der Technischen Universität München zur Erlangung des akademischen Grades eines

Doktors der Naturwissenschaften

genehmigten Dissertation.

Vorsitzender: Univ.-Prof. Dr. H. Luksch

Prüfer der Dissertation:

1. apl. Prof. Dr. J. Graw
2. Univ.-Prof. Dr. M. Klingenspor
3. apl. Prof. Dr. G. Rammes

Die Dissertation wurde am 23.07.2012 bei der Technischen Universität München eingereicht und durch die Fakultät Wissenschaftszentrum Weihenstephan für Ernährung, Landnutzung und Umwelt am 18.01.2013 angenommen.

Index

1 Scope of the work

This work aims to deepen our knowledge about the function of psychopharmacological compounds, such as antidepressants (Sogaard, Werge *et al.* 2006), to bring new insights on their mechanisms of action at both molecular and cellular levels. Although a wide variety of antidepressants are used to treat depression, a serious medical condition that occurs more frequently in modern society, the lack of knowledge how these drugs actually affect the neuronal network is alarmingly high.

Here the immediate effects of antidepressants were investigated during synaptic plasticity related mechanisms both in neurons and in astrocytes after acute application. Furthermore, this work focused on preferential targets of antidepressants embodied in specific membrane structures of the targeted cells. Indeed in this field of research it is important to improve the drug design to ensure the development of better, faster and of course safer compounds, and have a critical view on drugs that are prescribed to thousands of patients without certitudes about their mode of action.

In 2007, Allen *et al.* described how neurotransmitter signalling might rely on the localization of target receptors, for example in the so-called lipid rafts, a cholesterol enriched microdomain within the plasma membrane (Allen, Halverson-Tamboli *et al.* 2007).

To observe possible effects on novel molecular targets this work focused to what extent lipid raft integrity contributes to functional properties of different ionotropic receptors and to the effects of antidepressants (fluoxetine, desipramine) and the benzodiazepine diazepam. In this context, the impairment of lipid rafts integrity, induced by the cholesterol-depleting agents methyl-ß-cyclodextrine (MßCD) or simvastatin (Sim), should markedly affect receptors function and thus change the drug efficacy on the different types of receptors. Such findings could influence pharmacological research in general and change the basic approaches of drug testing and development. This may also contribute to a better understanding of the mode of action of certain psychopharmacological compounds at a molecular level.

Substances affecting single neuronal receptors consequentially also have the capacity to influence entire neuronal networks. Synaptic plasticity is not only a convenient model for the dynamics in a neuronal network, but is also suggested to be highly involved in the pathology of depression. Long-term potentiation (LTP), one

form of synaptic plasticity, is thought to be a cellular correlate of learning and memory. LTP is a process underlying synaptic changes and molecular signalling pathways activation. By monitoring LTP in the CA1 region of the hippocampus (where the best-studied form of LTP occurs) and focusing on the cellular activity in the participating cells, it might be possible to narrow down the potential targets of acutely applied ADs. Among all intracellular pathways, some are of particular interest in the context of neuronal activity and synaptic plasticity. 42-kDa and 44-kDa mitogen-activated protein kinase (Extracellular-regulated protein Kinase 1/2, ERK1/2), members of the MAPK family, and *Arc/Arg3.1* (activity-regulated cytoskeleton-associated protein/activity regulated gene 3.1) are not only molecular markers for cell activity, but are also part of the signalling pathways involved in the expression and maintenance of LTP. Investigating those molecular key mechanisms during the activity of a neuronal network under the influence of the antidepressant desipramine could elucidate new targets and mechanisms involved in the acute effects of psychopharmacological drugs and the processes involved in the course of depression.

For decades non-neuronal or glia cells, such as Astrocytes, were not considered as major players in the signalling processes of neuronal networks. Growing evidence has shown that both astrocytes and neurons are both important to conduct neurotransmission in the central nervous system (CNS). This “team play” requires a coordinated bimodal communication between these two very different cell types to coordinate the complicated mechanisms during synaptic plasticity. Eph/ephrin signalling, especially the EphA4/EphrinA3 system, has recently been identified as one possible pathway for neuron-astrocyte communication. Signalling between the neuronal receptor EphA4 and its astrocytic ligand EphrinA3 might be a communication link between neurons and astrocytes. Their involvement in LTP has been recently shown by Filosa and colleagues in 2009. Thus, a possible influence of an antidepressant such as desipramine on this signalling pathway could place astrocytes into a new focus of research in drug development.

2 Introduction

Dysfunctions in hippocampal physiology seem to be largely involved in the pathology of affective disorders (Videbech and Ravnkilde 2004). Other studies showed that patients suffering from depression showed deficiencies in verbal learning (Deckersbach, Savage *et al.* 2005). Affective or mood disorders have seemingly been associated with structural changes not only at the molecular, but also at the synaptic level (Duman, Malberg *et al.* 1999; Gould and Tanapat 1999; Bianchi, Hagan *et al.* 2005).

In the 1960s the conclusion of monoamine neurotransmitter (serotonine, noradrenaline, dopamine) deficiency in depressive patients was the first step to modern mood disorder therapy (Schildkraut 1965). Although this hypothesis is still valid, it does not provide enough clues to unravel the origins of depressive disorders or to explain some of the accessory phenomena such as the ineffectiveness in individual patients and the general delayed onset of antidepressants (Hirschfeld 2000). The heterogenous etiology of mood disorders diagnosed as depression seems to be one of the biggest challenges in this field of research.

Nevertheless the approaches for successful therapies are still improving. Based on the monoamine hypothesis the first pharmaceuticals were designed to increase the monoamine concentration in the brain. In the 1950s in addition to the monoamine oxidase inhibitors (MAOIs) tricyclic antidepressants such as imipramine and desipramine (DMI) were introduced. Tryciclic ADs enhance the monoamine neurotransmitter concentration by inhibiting the reuptake of monoamines from the synaptic cleft. In the late 1970s selective serotonine reuptake inhibitors (SSRIs) such as fluoxetine were additionally introduced because they showed fewer side-effects than the tricyclic ADs (Hyttel 1977; Georgotas, Krakowski *et al.* 1982).

In addition to their effects on monoamine reuptake many ADs affect also various neuronal receptors. Some have antogonistic effects on a receptor such as desipramine (DMI), imipramine and fluoxetine which are known to reduce serotonine-induced Na^+- and Ca^{2+}-currents by antagonizing the serotonin 5-HT_3 receptor (Eisensamer, Rammes *et al.* 2003). Tricyclic ADs such as DMI and imipramine have also been shown to block N-methyl-D aspartate receptor (NMDAR) a subtype of ionotropic glutamate receptor (Watanabe, Saito *et al.* 1993). Thus, one specific AD does not necessarily affect only one target receptor and can have a huge impact on signal transmission in the brain.

2.1 The role of lipid raft microdomains in receptor signalling

2.1.1 Principles of ionotropic receptor signalling

A fundamental process for the maintenance of the complex and steady transmission of neuronal signals in the central nervous system (CNS) is the cooperative function between excitatory and inhibitory circuits in neuronal networks. Neurotransmission is subject to electrochemical processes conducted by specific receptors. The transmission of information between neurons occurs *via* action potentials which emerge from changes in the neuronal membrane potential, induced through voltage-gated ion channels. The propagation of these action potentials from one neuron to another occurs either through electrical, or more often, chemical synapses. Chemical synapses use neurotransmitters for indirect and unidirectional signal transmission. When an action potential reaches the presynaptic terminal of a neuron the neurotransmitter is released and diffuses through the synaptic cleft to the postsynaptic membrane. Once released in the synaptic cleft, the neurotransmitter binds to specific ionotropic receptors, permeable only for certain ionic species. This specificity enables the flux of ions which causes a change in membrane potential.

Basically there are two different neurotransmitter systems in the CNS: excitatory and inhibtory. Excitatory neurotransmitter systems promote neuronal activity through an influx of positive ions into the postsynaptic cell, while inhibitory systems attenuate activity (influx of negative ions) both as a result of activation of ligand-gated channels (LGCs). LGCs can be classified into three basic groups according to different parameters.

-Ion selectivity: receptors like glutamate, 5-HT_3 and acetylcholin receptors are specific for cations (Ca^{2+}, Na^{+}, K^{+}) and promote excitation, while receptors like glycine and gamma-aminobutyric acid receptors ($GABA_A$) only gate anions (Cl^{-}) and promote inhibition.

-Ionotropic LGCs: these are receptors (e.g. $GABA_A$, 5-HT_3) where the ion channel and the ligand binding site form a unit consisting of multiple proteins. After binding of the neurotransmitter, a conformational change results in the opening of the channel pore.

-Metabotropic LGCs (or G protein coupled receptors): in this case, the binding of the ligand on the receptor (for example $GABA_B$ and certain 5-HT receptors) leads

to the activation of G proteins and intracellular signalling cascades and finally to the modulation of plasma membrane ionic channels.

In summary LGCs mediate synaptic transmission by regulating the flux of anions and cations through the cell membrane after binding with neurotransmitters (Greger 1996; Klinke 1996).

2.1.2 The link between lipid raft microdomains and receptor signalling

For decades the classic "fluid mosaic" model of the cell membrane supported the theory of a simple lipid bilayer-construct in which functional proteins floated freely on a “sea” of lipid molecules (Singer and Nicolson 1972). However, the ongoing research of all these membrane associated proteins, showed a great scale of structure and clusters of organization for some of the observed molecules. This could not be possible with the idea of freely floating proteins. Soon a model for this organizational structure in the membrane was proposed: The lipid raft microdomain.

The lipid raft model suggests the clustering of specific molecules being part of a signalling pathway to facilitate rapid and efficient signal transduction through spatial proximity of the interacting components. This would be a prerequisite for the enhancement of signal specificity by confining the localization of certain receptors into raft-like domains containing a defined subset of signalling molecules. Consequently nonspecific signalling would be avoided by limiting the access of receptors and other reactive molecules to different signalling pathways (Pike 2003).

In conclusion lipid rafts are necessary for the compartmentalization of the cell membrane to ensure specificity and functionality of particular signalling pathways of the cells. Lipid rafts are specific microdomains embedded in the cell membrane which consist of an enriched cholesterol and glycosphingolipid domain (Pike 2004) (Fig. 1). Lipids and proteins can move in and out of these domains, thereby forming distinct clusters which determine their biophysical properties. Biochemically, lipid rafts are often defined as insoluble by non-ionic detergents upon sucrose density gradient centrifugation at 41C° (Brown and Rose 1992). These heterogeneous and highly dynamic structures float within the membrane bilayer and contain various functional molecules (Kusumi and Suzuki 2005). Their size can vary between 25 and 100nm in diameter depending on their type (Simons and Toomre 2000; Nicolau, Burrage *et al.* 2006).

Increasing evidence suggest that the membrane localization of distinct neuro-transmitter receptors within lipid rafts can influence their function by affecting neurotransmitter binding, receptor trafficking and clustering (Tsui-Pierchala, Encinas *et al.* 2002; Allen, Halverson-Tamboli *et al.* 2007).

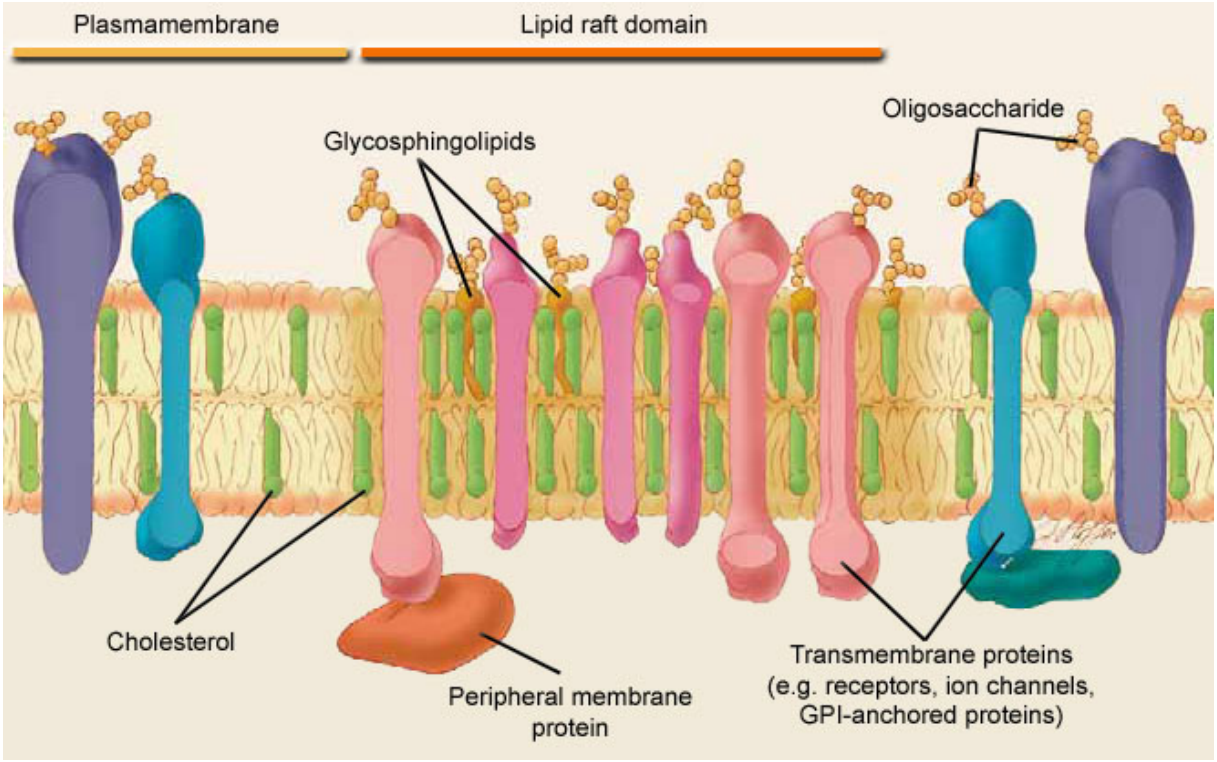

Fig.1. Model of a lipid raft microdomain embedded in the phospholipid bilayer. The raft consists of a cholesterol enriched domain with a high amount of glycosphingolipids. Accumulated proteins in rafts can be more organized and form clusters containing effector proteins interacting with molecules outside the lipid raft or with specific receptor compositions that may act as signalling pathway modules (Pines, Oplinger *et al.* 2005).

This hypothesis led to various studies focusing on the role of lipid rafts in receptor signalling, which proposed two common types of lipid rafts (Fig. 2):
non-caveolar (or planar) rafts and *caveolea*. The biochemical marker and major component of *caveolae* is caveolin and apart from hippocampal neurons, they are primarily found in non-neuronal cells like astrocytes, oligodendrocytes and endothelial cells (Trushina, Du Charme *et al.* 2006). In contrast planar rafts consist of flotillin and are more abundant in neuroblastoma cells and neurons (Lang, Lommel *et al.* 1998).

Until today almost all ionotropic receptors have been associated with lipid rafts and despite some discrepancies concerning the localization of certain receptors,

which are probably caused by procedural variations, it is very likely that the lipid-protein interactions occuring in lipid rafts could influence ionotropic receptor conformation and therefore agonist potency or efficacy (Allen, Halverson-Tamboli *et al.* 2007).

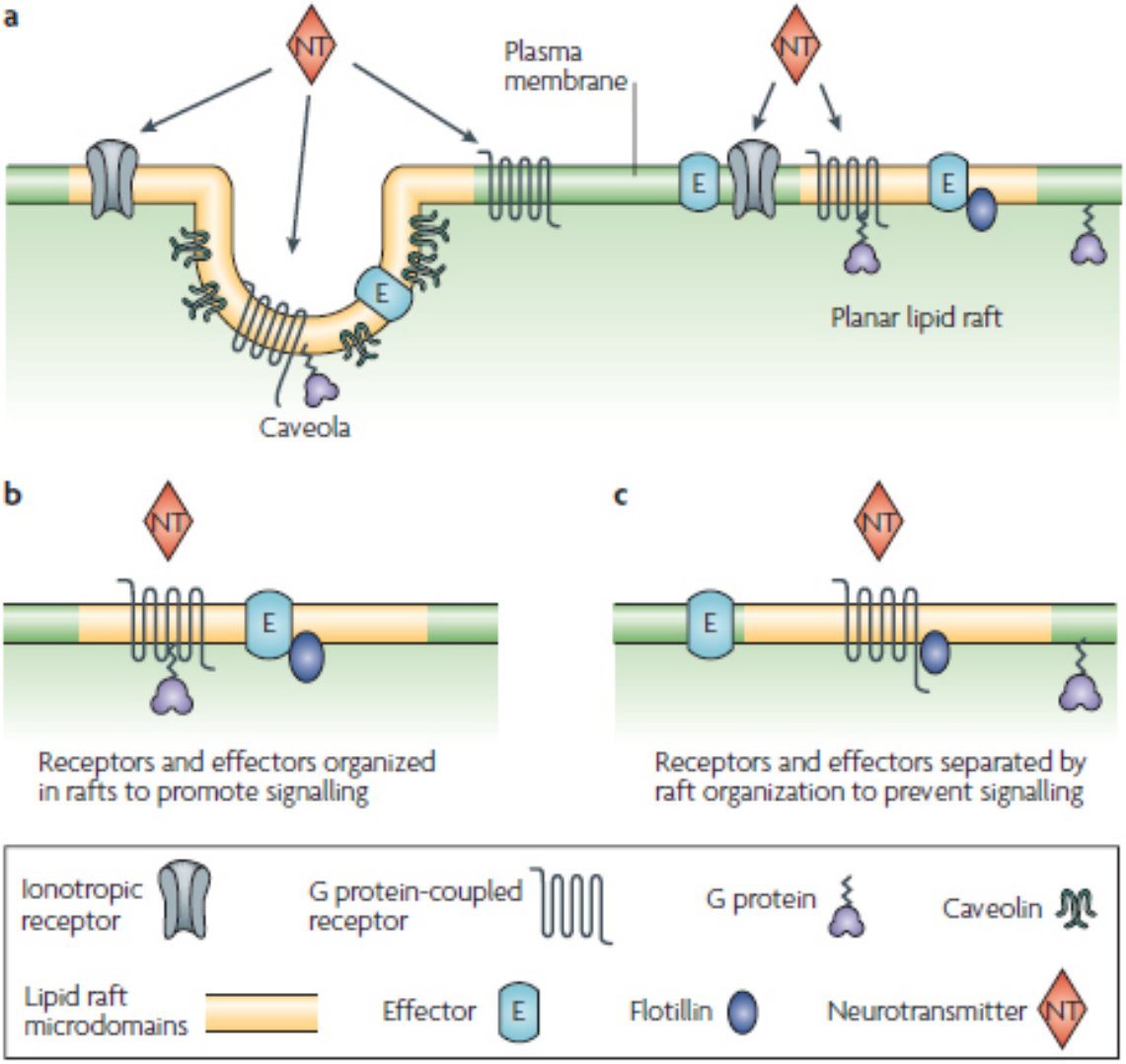

Fig.2. Lipid raft microdomains and membrane organization of neurotransmitter signalling molecules. a Showing the two common raft domains in mammalian cells: planar lipid rafts and caveolae. Both possess a similar lipid composition. Planar rafts are essentially continuous with the plane of the plasma membrane and lack distinguishing morphological features. Caveolae are small, flask-shaped membrane invaginations of the plasma membrane that contain caveolins. Caveolin molecules can oligomerize and are thought to be essential in forming these invaginated membrane structures. Caveolins and flotillin can recruit signalling molecules into lipid rafts. Many neurotransmitter receptors (both ionotropic and G-protein-coupled), G proteins, and signalling effectors such as secondmessenger-generating enzymes are found in lipid rafts. Neurotransmitters might activate receptors that are located both within and outside lipid rafts. **b** The lipid raft signalling hypothesis proposes

that these microdomains spatially organize signalling molecules at the membrane, perhaps in complexes, to promote kinetically favourable interactions that are necessary for signal transduction. **c** Alternatively, lipid raft microdomains might inhibit interactions by separating signalling molecules, thereby dampening signalling responses (Allen, Halverson-Tamboli *et al.* 2007).

2.1.3 Lipid rafts and ionotropic receptors as targets for psycho-pharmacological compounds

Psychopharmacological substances such as ADs and benzodiazepines can have a great effect on the function of a range of ionotropic receptors (Walters, Hadley *et al.* 2000; Nothdurfter, Tanasic *et al.* 2010). Considering the important role lipid rafts may play in receptor signalling, it is very likely that certain psychopharmacological compounds may act differently on receptors localized in raft-like domains, than on non-raft receptors. In addition the potential involvement of lipid rafts in certain brain disorders such as unipolar depression, schizophrenia and bipolar affective disorder has also prompted studies to explore how these microdomains contribute to various psychiatric diseases (Allen, Halverson-Tamboli *et al.* 2007).

In fact, it has been shown that lipid rafts do play a role in the mode of action of ADs. A study from 2008 indicates that the G-protein subunit $G\alpha_s$ is most likely shifted to lipid rafts, where it couples to adenylyl cyclase to a lesser extent, in post mortem brain tissue of patients who had suffered from major depression (Donati, Dwivedi *et al.* 2008). Chronic treatment with ADs may enhance $G\alpha_s$ signalling through preventing the accumulation of $G\alpha_s$ in lipid rafts (Donati and Rasenick 2005). Moreover, a variety of ADs and antipsychotics accumulate in raft-like domains together with the serotonin type 3 (5-HT_3) receptor as detected by sucrose density gradient centrifugation (Eisensamer, Uhr *et al.* 2005). The last finding is of particular interest since various classes of ADs and antipsychotics have been shown to act as non-competitive antagonists on this neurotransmitter receptor (Fan 1994; Breitinger, Geetha *et al.* 2001; Eisensamer, Rammes *et al.* 2003; Rammes, Eisensamer *et al.* 2004).

The 5-HT_3 receptor is a pentameric ligand-gated nonspecific cation channel, which functions either as homomeric 5-HT_{3A} or as heteromeric 5-HT_{3AB} receptor (van Hooft and Vijverberg 2000; Hannon and Hoyer 2008). Electrophysiological and immunohistochemical evidence indicate that the majority of native 5-HT_3 receptor complexes do not contain the 5-HT_{3B} subunit (Hussy, Lukas *et al.* 1994; Fletcher and

Barnes 1998; Reeves and Lummis 2006). In the CNS, the 5-HT_{3A} receptor is highly expressed in the area postrema, the caudate nucleus, the hippocampus, and the amygdala (Barnes and Sharp 1999).

In 2005 Dalskov and his associates have localized the $GABA_A$ receptor in lipid raft microdomains in rat cerebellar granule cells by using subcellular fractionation. Their observation suggests “hot spots” of $GABA_A$ clusters on the cell surface (Dalskov, Immerdal *et al.* 2005). GABA is the major inhibitory neurotransmitter in the vertebrate CNS, and altered GABAergic neurotransmission has been implicated in neurological and psychiatric disorders such as epilepsy, schizophrenia and mood disorders (Fritschy and Brunig 2003; Sogaard, Werge *et al.* 2006). $GABA_A$ receptors are responsible for the fast inhibitory effects on synaptic transmission and can be influenced by many pharmacological compounds, mostly molecules such as barbiturates, anesthetics and benzodiazepines (e.g. diazepam) (Johnston 1996). The direct mechanism of the functional changes of $GABA_A$ receptor activity is still not understood, but the involvement of lipid rafts may play a role on the mode of action at the $GABA_A$ receptor.

Another very prominent receptor has been showed to be embedded into lipid rafts: the N-methyl-D-aspartic acid receptor (NMDAR). NMDAR-mediated synaptic responses are fundamental for long-term potentiation in the hippocampus (see next chapter) and can be influenced by tricyclic ADs such as desipramine (DMI) (Watanabe, Saito *et al.* 1993). However, there is some uncertainty regarding the subcellular localization of the different NMDAR subunits and several research groups have published conflictive observations concerning the raft or non-raft localization of the NR1 and NR2B subunits of the NMDAR (Suzuki, Ito *et al.* 2001; Hering, Lin *et al.* 2003; Frank, Giammarioli *et al.* 2004; Guirland, Suzuki *et al.* 2004).

2.2 Synaptic plasticity

The perception of our proximity and the amount of information we actually process, is continuously and unconsciously regulated by our brain without us being aware of it. It constantly filters and stores information, forms our behaviour and eventually defines who we are as individuals. These features of the CNS are thought to depend on the variability or “plasticity” of synaptic connections.

Dysfunctions in synaptic plasticity always result in severe neurological disorders like mental retardation, Alzheimer´s disease, chronic pain states and cognitive deficits. On that account understanding how patterns of neuronal activity are translated into persistant changes in synaptic connectivity is one of the most important challenges in basic and clinical neuroscience (Bliss, Collingridge *et al.* 2007; Citri and Malenka 2008).

Some features of synaptic plasticity build the foundation for the ability to store memories, since it is one of the main variable forces of neurotransmission at synapses (Martin, Grimwood *et al.* 2000). These mechanisms, facilitating memory storage, require a contemporary protein synthesis and a promptly responding gene transcription to stabilize synaptic long-term changes (Adams and Dudek 2005).

Long-term potentiation (LTP) is thought to be a cellular correlate of learning and memory and is supposedly being orchestrated by these mechanisms.

2.2.1 Long-term potentiation (LTP)

LTP was described for the first time by Bliss and colleagues in 1973, when they revealed that tetanic electrical stimulation of the perforant pathway of presynaptic fibres caused elevated responses in postsynaptic granule cells in the dentate gyrus of the hippocampus. They called this phenomenon long-term potentiation because the increase in postsynaptic currents they recorded was continously stable over a long time period.

LTP is an example of a long lasting increase in synaptic efficacy, which can be elicited with brief pulses of high frequency stimulation (Bliss and Lomo 1973; English and Sweatt 1996). A formal hypothesis embodying this idea was advanced by the psychologist Donald Hebb in 1949. According to Hebb’s famous postulate, “When an axon of cell A is near enough to excite a cell B and repeatedly or persistently takes part in firing it, some growth process or metabolic change takes place in one or both

cells such that A's efficiency, as one of the cells firing B, is increased.". Hence, LTP is sometimes also referred to as Hebbian synaptic plasticity.

LTP has been subjected to more intense studies in the hippocampus (especially the dentate gyrus and CA1 and CA3 subfields) than elsewhere in the brain. Although the laminated structure of the hippocampus makes it particularly convenient for the study of LTP, there is no reason to suppose that hippocampal synapses occupy a privileged position in the hierarchy of plasticity. LTP has been described in many other brain regions, including cerebellum, amygdala, sensory cortex, motor cortex, prefrontal cortex, and nucleus accumbens (Andersen 2007). To find out more about this supposed model of learning and memory, its molecular mechanisms were focus of many researchers, but although this effect has been extensively investigated there are still a lot of unknown variables in the equation.

Experiments conducted in the late 1980s revealed a number of inhibitors capable of suppressing LTP in the CA1 area of the hippocampus. After treatment with NMDAR inhibitors, Ca^{2+} chelators, calmodulin antagonists and various protein kinase inhibitors LTP induction could be blocked (Collingridge, Kehl *et al.* 1983; Malenka, Kauer *et al.* 1989; Malenka, Lancaster *et al.* 1992). Moreover mutant mice lacking NMDAR showed both impairment of learning and memory and attenuation of LTP (Sakimura, Kutsuwada *et al.* 1995; McHugh, Blum *et al.* 1996). Thus, the induction of LTP in the CA1 area of the hippocampus requires activation of NMDARs, the entry of Ca^{2+} into postsynaptic neurons, and activation of protein kinases like CaM kinase II (CaMKII) and protein kinase C (PKC) (Miyamoto 2006).

However, induction of LTP is just the first phase. The long lasting mechanism supporting an elavated excitatory postsynaptic potential (EPSP) has to be maintained. Stimulation of NMDAR with NMDA or glutamate increases transiently the phosphorylation of 42-kDa Extracellular-Regulated protein Kinase (ERK), a member of the Mitogen-Activated Protein Kinase (MAPK) family, as well as the Ca^{2+}-independent form of CamKII in cultured hippocampal neurons (Fukunaga, Stoppini *et al.* 1993). A western blot study showed that, after LTP induction in hippocampal slices delivered by high frequency stimulation (HFS) to the Schaffer collateral pathway, the activity of MAPK increased but did not last the whole period of LTP induction (English and Sweatt 1996; English and Sweatt 1997; Liu, Fukunaga *et al.* 1999).

Cyclic AMP (cAMP) response element binding protein (CREB) phosphorylation in response to HFS-induced LTP follows is a downstream element of this very complex signalling pathway and can be activated via a MAPK-dependent or a MAPK-independent manner, through CamKII and IV, both regulated by NMDAR activity (Miyamoto 2006).

CaMKII phosphorylates the GluR1 subunit of α-Amino-3-hydroxy-5-methyl-4-isoxazolepropionic acid receptor (AMPAR) in the postsynaptic membrane as well (Barria, Muller *et al.* 1997; Lee, Barbarosie *et al.* 2000). One hypothesis postulates a following recruitment and increased integration of AMPAR in the synaptic membrane over yet unexplained mechanisms, which leads to the long lasting elevation of postsynaptic conductivity (Davies, Carling *et al.* 1989; Liao, Scannevin *et al.* 2001; Lu, Man *et al.* 2001).

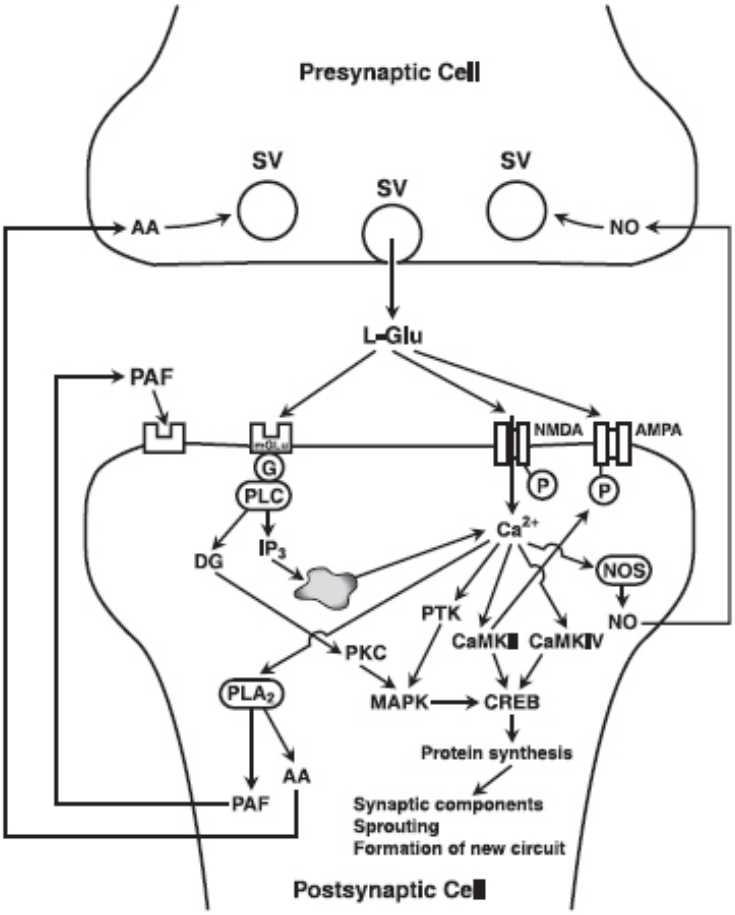

Fig.3. Schematic view of the possible hypothesis for signalling pathways involved in LTP induction and maintainance. Neurotransmitter L-glutamate (L-Glu) is released from presynaptic vesicles (SV). NMDA glutamate receptors are activated and consequently Ca^{2+} enters the postsynaptic neuron and activates CamKII. CamKII can phosphorylate AMPA glutamate receptors with concominant activation. In parallel intracellular processes are

initiated which supposedly maintain LTP via gene expression and novel protein synthesis (Kandel, Albright *et al.* 2000; Lynch 2004). In this mechanism the activation of CaMKII and MAPK seems to be substantial, that in turn activates the essential transcription factor CREB (Miyamoto 2006).

For any form of synaptic plasticity based upon learning and memory processes, as is LTP, long lasting and persistent modifications of synaptic physiology is a necessity. These long-lasting changes would depend on fast induction of gene transcription and subsequent protein synthesis for synaptic sprouting and formation of new circuits. Antidepressants have been shown to have both acute and long-term effects on LTP, but it is still unclear how exactly ADs influence the mechanism of LTP and why there is such a heterogenity in the results (Birnstiel and Haas 1991).

2.2.2 Arc: Neuronal activity marker and LTP regulator

Arc/Arg3.1 (Activity-regulated cytoskeleton-associated gene/Activity regulated gene 3.1) belongs to one of the most important effector family known in neurobiology: the immediate early-genes (IEG). IEG are defined as genes that are transiently and rapidly activated at the transcriptional level following robust neurotransmitter, synaptic or growth factor stimulation (Sheng and Greenberg 1990). *In vivo*, *Arc/Arg3.1* is activated/or expressed in populations of neurons that mediate learning (such as in the hippocampus) and behavioral-specific networks (such as in the cortex) (Ramirez-Amaya, Vazdarjanova *et al.* 2005; Tagawa, Kanold *et al.* 2005). The expression of *Arc/Arg3.1* is confined to the brain and testis and is almost exclusively restricted to CaMKII-positive glutamatergic neurons in the hippocampus and the neocortex, with very sparse or no expression in glial cells (Vazdarjanova, Ramirez-Amaya *et al.* 2006; Shepherd and Bear 2011).

Initially used as an activity neuronal marker, it has become the focus of many scientific studies because of its vast involvement in several critical neuronal mechanisms. After synaptic stimulation *Arc/Arg3.1* mRNA is rapidly induced and distributed to the dendrites where it may be locally translated to facilitate specific synapse alterations (Link, Konietzko *et al.* 1995; Rodriguez, Davies *et al.* 2005).

Arc/Arg3.1, for simplicity henceforth referred to as *Arc*, regulates actin cytoskeletal dynamics underlying formation of long-term potentiation (LTP), regulation of AMPAR endocytosis and homeostatic plasticity (Bramham, Alme *et al.* 2010). Homeostatic plasticity can be described as the ability of neurons to self

regulate their own excitability. Through activity-mediated local synthesis and degradation of proteins (e.g. receptors), synaptic inputs may directly remodel the protein consistency, and thereby the functional properties, of dendritic spines and their surroundings.

Arc transcription can be caused by LTP induction via high frequency afferent stimulation (HFS), activation of NMDAR and extracellular signal-regulated kinase (ERK) (Steward, Wallace *et al.* 1998; Steward and Worley 2001) and in response to neuronal activity, as shown in primary neuronal cultures (Rao, Pintchovski *et al.* 2006). *Arc* mRNA is also rapidly expressed in neurons following seizures, brain-derived neurotrophic factor (BDNF) and learning and memory experiences (Link, Konietzko *et al.* 1995; Lyford, Yamagata *et al.* 1995; Kubik, Miyashita *et al.* 2007). It can also be pharmacologically induced by the group 1 metabotropic glutamate receptor (mGluR) agonist dihydroxyphenylglycine (DHPG), or after the activation of the adenylyl cyclase by forskolin (Waltereit, Dammermann *et al.* 2001; Rao, Pintchovski *et al.* 2006; Yasuda, Fukuchi *et al.* 2007). In pheochromocytoma 12 cells and hippocampal neurons, an increase in intracellular calcium and cAMP levels was also shown to induce *Arc*, dependent on ERK activation and NMDAR phosphorylation by the protein kinase A (PKA) pathway (Waltereit, Dammermann *et al.* 2001; Bloomer, VanDongen *et al.* 2008).

However, Arc activation is not exclusively reliant on NMDA receptor activity. In dissociated hippocampal neurons, membrane depolarization, calcium influx through voltage-gated calcium channels and cAMP also cause *Arc* mRNA transcription. Both cAMP and calcium are triggered by PKA. Additionaly, MAPK is involved in transcriptional activation via cAMP (Waltereit, Dammermann *et al.* 2001).

Arc mRNA can be detected in a time frame of one hour following transcription in dendrites of dentate granule cells and up to 300µm away from the cell somata (Link, Konietzko *et al.* 1995; Wallace, Lyford *et al.* 1998). *Arc*, as every RNA that is transported to the dendrites, is a messenger ribonucleoprotein (mRNP, or transport RNP) that contains several components for the translational machinery, RNA binding proteins involved in decay and localization, and molecular motors for RNA transportation.

Through local actin polymerization and NMDAR signalling, *Arc* accumulates in dendritic regions where synapses have been recently activated (Steward, Wallace *et al.* 1998), which makes it an interesting indicator for quantification of neuronal

activity. A work of Lopez de Heredia *et al.* from 2004 suggests that this specific localization results from microtubule-dependent fast transport followed by F-actin-dependent docking (Lopez de Heredia and Jansen 2004).

Experiments in the CA1 region of the hippocampus in acute brain slices from *Arc* knockout mice show that the late phase of LTP is inhibited, while early phase LTP is enhanced (Plath, Ohana *et al.* 2006). Inhibition of *Arc* by *Arc* antisense oligodeoxynucleotides results in the attenuation of LTP maintainance, without affecting LTP induction (Guzowski, Lyford *et al.* 2000; Messaoudi, Kanhema *et al.* 2007).

This suggests a required Arc translation during a certain time window for LTP. Despite a well timed gene expression, LTP consolidation needs enduring structural changes which are dependent on F-actin accumulation, as well as ARC protein synthesis (Fukazawa, Saitoh *et al.* 2003; Bramham, Worley *et al.* 2008). These processes include growth of postsynaptic dendritic spines and expansion of the postsynaptic density (Matsuzaki, Honkura *et al.* 2004; Bourne and Harris 2008). When LTP consolidation is inhibited a loss of emerging F-actin at medial perforant path synapses corresponding to dephosphorylation of cofilin can be observed (Messaoudi, Kanhema *et al.* 2007). This suggests that *Arc* promotes LTP consolidation by regulating actin dynamics in neuronal synapses.

Through interrelation with certain components of the endocytotic machinery (endophilin 2/3 and dynamin), *Arc* is capable of regulating the receptor composition at the cell surface. By internalization of AMPAR it can control the activity-dependent depression of excitatory synaptic transmission during homeostatic plasticity and mGluR-dependent long-term depression (LTD) (Chowdhury, Shepherd *et al.* 2006; Rial Verde, Lee-Osbourne *et al.* 2006; Turrigiano 2008).

In hippocampal neuronal cultures, decrease in neuronal firing activitiy during tetrodotoxin treatment enhances *Arc* expression, while increase in activity in the presence of a $GABA_A$ receptor blocker decreases *Arc* expression. Overexpression of *Arc* inhibits an actvity blockade by enhancing AMPAR function while in *Arc* knockout neurons the regulation of AMPAR homeostasis is terminated (Chowdhury, Shepherd *et al.* 2006). Recent studies show that *Arc* transcription is controlled by AMPA and NMDA receptor activation in a complex system with a feedback mechanism, controlling *Arc* transcription and NMDAR/AMPAR homeostasis (Rao, Pintchovski *et al.* 2006).

Chronic treatment of animals with ADs showed enhanced TrkB receptor signalling and an upregulation of its endogenous ligand, BDNF, expression in the hippocampus, dentate gyrus and cortex, prominantly after treatment with SSRIs. While BDNF, besides being able to induce LTP, has numerous other functions, TrkB regulates the expression of key genes to rescue or promote plasticity in the affected regions (Dagestad, Kuipers *et al.* 2006; Castren, Voikar *et al.* 2007).

Stress or traumatic events are thought to contribute to depressive disorders *via* downregulation of BDNF, although the removal of BDNF in rat forebrain does not mediate depressive like behaviour (Krishnan and Nestler 2008).

Arc is not only an important effector gene in context with BDNF-induced LTP in the dentate gyrus, but is also upregulated in the forebrain after increased TrkB signalling following antidepressant treatment (Pei, Zetterstrom *et al.* 2003; Alme, Wibrand *et al.* 2007). The capability of regulating synaptic plasticity and receptor trafficking in addition to the facts previously mentioned, suggest that Arc may not be only a simple tool for monitoring neuronal activity, but also has to be considered as a major player in the mechanisms involved in the mode of action of antidepressants.

2.2.3 Astrocyte/neuron communications in synaptic plasticity

For a long time glial cells, including astrocytes, have been thought to be only responsible for structural integrity in the CNS, but over the last decades growing evidence showed a much more important role for the non-neuronal cells in the brain.

Interactions between astrocytes and neurons are fundamental for both synapse or spine development and synaptic transmisson (Allen and Barres 2005). Astrocytes regulate synaptic transmission by releasing specific factors and substances, called “gliotransmitters”, such as D-serine for example (Halassa, Fellin *et al.* 2007). They can also exert a more direct influence on neurons by sensing synaptic activity via detection of glutamate release from presynaptic terminals and respond with the release of certain gliotransmitters altering/or modifying neuronal activity (Halassa, Fellin *et al.* 2007; Barres 2008). One major factor in the bidirectional communication between these two very different cell types is based on a recently discovered signalling system: The Eph/ephrin signalling. Ephrin ligands and their cognate Eph receptors are involved in axon guidance during neuronal development and the regulation of neuronal plasticity and synapse dynamics in the adult brain (Yamada and Nelson 2007; Klein 2009).

Eph receptors belong to the family of receptor tyrosine kinases and are divided into two groups: EphA and EphB receptors. The ligands for the EphAs are almost exclusively A-type ephrins (EphrinA1-5) which are ligated at the surface of the cellmembrane by a glycosylphosphatidylinositol (GPI) anchor, whereas EphBs bind to the B-type ephrins EphrinB1-3 (Pasquale 2008).

One prominent feature of this signalling system is that Eph receptors are also acting as a ligand in the same manner that an ephrin ligand can act as a receptor allowing reverse and forward signalling with the same set of molecules (Fig. 4) (Klein 2009). Most Eph receptors are primarily responsible for neuron-neuron signalling, while the receptor EphA4 is solely involved in neuron-astrocyte communication (Fig. 5).

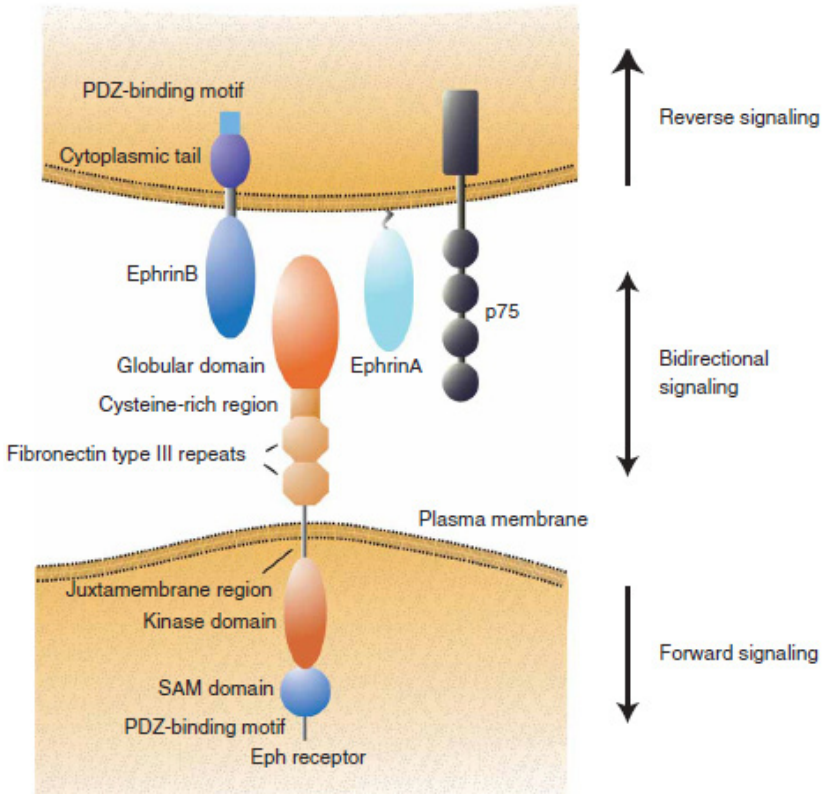

Fig.4. Schematic diagram depicting the concept of the bidirectional signalling between two cells. One cell is expressing EphrinA and EphrinB proteins. The two proteins vary in respect to the structure of their membrane anchors. In contrast the Eph receptors have a very similar molecular configuration. When ephrins interact with the globular domain of the Eph receptor this can trigger reverse signalling into the ephrin-expressing cell, forward signalling towards the Eph receptor cell, or bidirectional signalling. The p75 neurotrophin receptor has been shown to play a role in reverse signalling during retinotopic mapping (Klein 2009).

As an exception the EphA4 can be activated by A-type and most of the B-type ligands (Pasquale 2008). EphA4 is abundant in dendritic spines of hippocampal neurons, whereas one of its ligands, EphrinA3, is localized within astrocytes close to these spines (Murai, Nguyen *et al.* 2003). EphrinA3 induced EphA4 activation in hippocampal brain slices reduces spine length and density. Inactivation of EphA4 produces spine elongations and dynamic morphological changes in cell shape, implicating that EphA4/EphrinA3 signalling is critical for spine morphology (Murai, Nguyen *et al.* 2003; Klein 2009). EphrinA3 activates the EphA4 receptor *via* the recruitment of cyclin-dependent kinase 5 (Cdk5) and enhances the activity of Cdk5 kinase by tyrosine phosphorylation (Fu, Chen *et al.* 2007). This inhibits ß1-integrin activity and further downstream signalling pathways and enables actin reorganization in the spine and thus modulation of spine morphology (Bourgin, Murai *et al.* 2007).

Although astrocytes have been shown to participate in synapse function and development, their involvement in synaptic plasticity is yet not clear. In 2009 Filosa *et al.* showed that the EphA4 mediated neuron-glia interaction modulates LTP in postsynaptic CA1 region through regulation of astrocytic glutamate transporters (Filosa, Paixao *et al.* 2009).

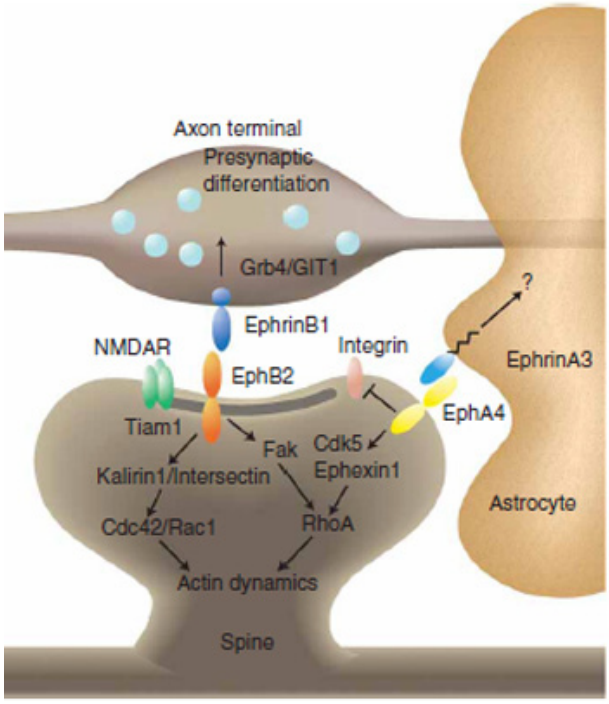

Fig.5. EphrinB/EphB signalling between neuronal spine and axon and EphA4 acting as a link to astrocyte-neuron communication. The signalling pathways of EphB have been investigated to a greater extent and have an influence on filopodial motility and interact with NMDARs (Kayser, Nolt *et al.* 2008). EphA4 activated by astrocytic ephrinA3 triggers forward

signalling involving recruitment of Cdk5, ephexin1 and RhoA which elicits the regulation of actin dynamics. Both EphA4 and part of the EphB signalling pathways have an impact on actin reorganization and therefore on spine dynamics in a different manner dependent on the source of the output signal. While EhprinB reverse signalling could be responsibel for presynaptic differentiation, ephrinA3 reverse signalling may modulate astrocytic functions (Klein 2009).

Rapid removal of glutamate from the synaptic cleft after synaptic activation by glial transporters is essential to avoid spill-over and excitotoxicity (Bergles and Jahr 1998; Tzingounis and Wadiche 2007). During neuronal activity, including LTP, the glutamate uptake by astrocytes increases (Pita-Almenar, Collado *et al.* 2006). The molecular mechanisms involved in this process are still only sparsely understood.

However, it seems that EphA4 is required for LTP in the hippocampus, as well as ephrinA3 which also affects the glutamate currents in astrocytes. While overexpression of ephrinA3 decreases glial glutamate transporter abundance, loss of EphA4 does the contrary (Filosa, Paixao *et al.* 2009). In summary astrocytes do not only control spine morphology and synaptic functions via the Eph/ephrin signalling, they also seem to play a major role in synaptic plasticity related mechanisms, which we are just about to begin to comprehend. The role of astrocytes and their communication with neuronal cells as possible targets of antidepressants is yet unclear.

3 Materials and methods

3.1 Basic introduction to patch-clamp technique

The patch-clamp technique allows the analysis of transmembrane ion currents generated through the activation of ionic channels. This method was established by Erwin Neher and Bert Sakmann in the 1970s. The basic principle of this technique is to electrically seal the aperture of a fine glass pipette with a small piece ("patch") of the cell membrane. With a special patch-clamp amplifier, the electric polarisation at the cell membrane can be measured (Hamill, Marty *et al.* 1981).

From a simplistic point of view, the cell membrane can be considered as an isolator between the intra- and extracellular space. Depending on the ionic composition of these two compartments an electrochemical gradient exists. Activation of ion channels located in the membrane thus causes an ion influx or efflux driven by the gradient. The resulting current change is recorded by the patch-clamp amplifier and the difference is balanced by a compensatory current that equals the original current change. This is accomplished with a negative feedback mechanism during which the transmembrane voltage is measured and constantly compared with the "clamped" voltage (setting of the default voltage). As an example, a cell is clamped at -70mV and the application of an agonist results in the influx of positive ions. The cell is more depolarised from the original potential and the difference between this new potential and the original potential has now to be compensated. This is achieved by the amplifier which has to inject the corresponding negative current. Accordingly, a so called (positive) inward current is displayed as a negative deflection on the recording device by definition (Fig. 6).

The earlier mentioned electrical seal is an important advantage compared to older techniques and considerably reduces background noise during recordings. This seal is obtained by applying a negative pressure in the glass pipette, aspirating the cell membrane and resulting in a very stable contact between the pipette and the membrane surface. Ideally, the electric resistance between the pipette and the membrane is several giga Ohm (GΩ). Hence, also referred to as "giga seal".

Depending on the research question different patch-clamp configurations or settings can be used. The Outside-out configuration can be used to measure currents of single ion channels. In this configuration, a fragment of cell membrane is excised

and sealed to the pipette tip with the exterior side of the cell membrane in contact with the bath solution.

In the whole-cell-configuration, the integrity of the cell is preserved and only the small patch of membrane under the pipette is broken by a small suction. By that, the inside of the pipette is in contact with the intracellular medium of the cell, creating a homogenous intracellular content defined by the solution in the glass pipette. Thus, the total sum of currents over the membrane of the entire cell through multiple channels is recorded at once. Now every change in the ionic composition of the cytoplasm of the cell, for example triggered by opening of the channels/receptors via an agonist, results in a measurable current running through the pipette solution to the silver-chlorided electrode. The electrode conducts the electric current to the amplifier and an analysing unit which is able to visualise these currents with specific analysis programs (Numberger 1996) (Fig. 6). Besides the two mentioned configurations there are two other settings (cell-attached and inside-out configurations) which will not be presented here.

For this work, the whole-cell configuration was chosen, as the sum of all receptors in the cell might represent changes in lipid raft integrity much more effectively.

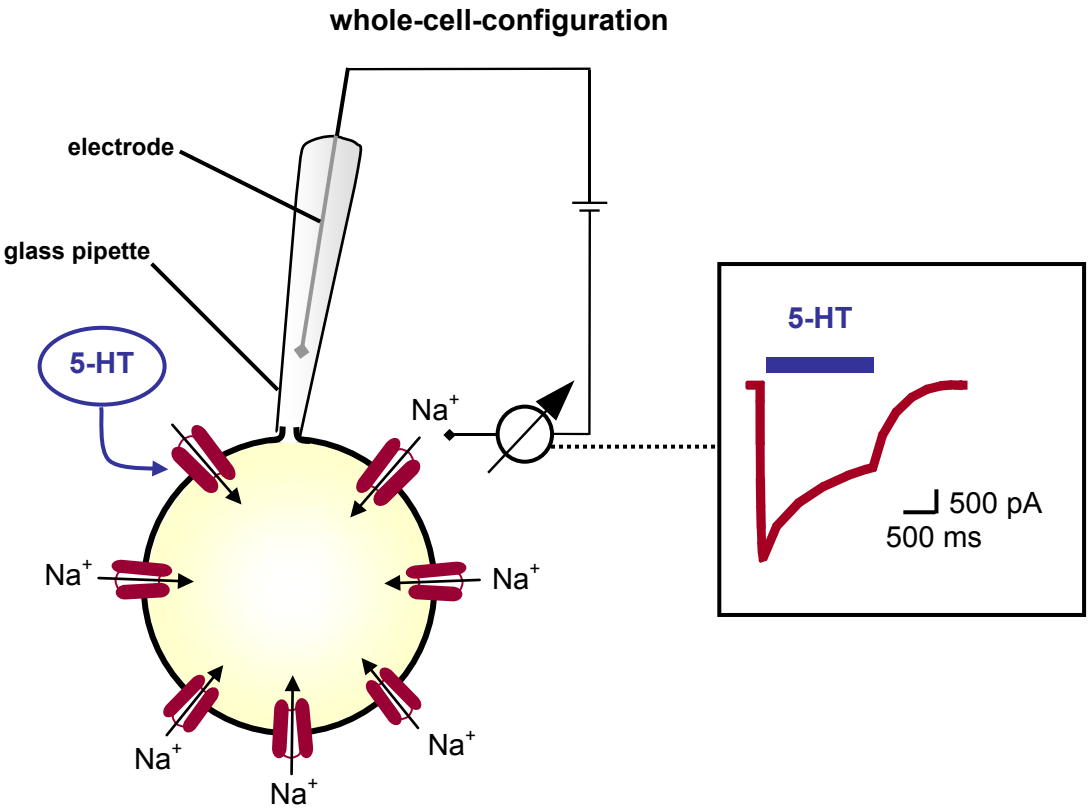

Fig.6. Whole-cell configuration of the patch-clamp technique. Serotonin (5-HT) evoked sodium (Na^+) influx through the activation of 5-HT receptors, as an example for a whole-cell patch-clamp experiment.

3.1.2 Whole-cell patch-clamp analysis

Analysis of patch-clamp recordings can be achieved with various programs. Recorded currents are processed for the essential parameters. The peak equals the maximum amplitude of the current and charge represents the area under the curve. τ_{on} is the onset constant, meaning the time needed to reach the maximum amplitude after application of the agonist, while τ_{off} is the deactivation time after agonist withdrawal (offset). After maximum stimulation in presence of the agonist, the desensitisation period is initiated (τ_{des}). τ parameters are needed to interpret receptor kinetics (Fig. 7). Few programs use plateau parameter instead of charge, depending on the default settings at the used patch-clamp setup. The plateau is the steady state phase of the current after the fast transient peak of the current, and is defined by its amplitude and its duration.

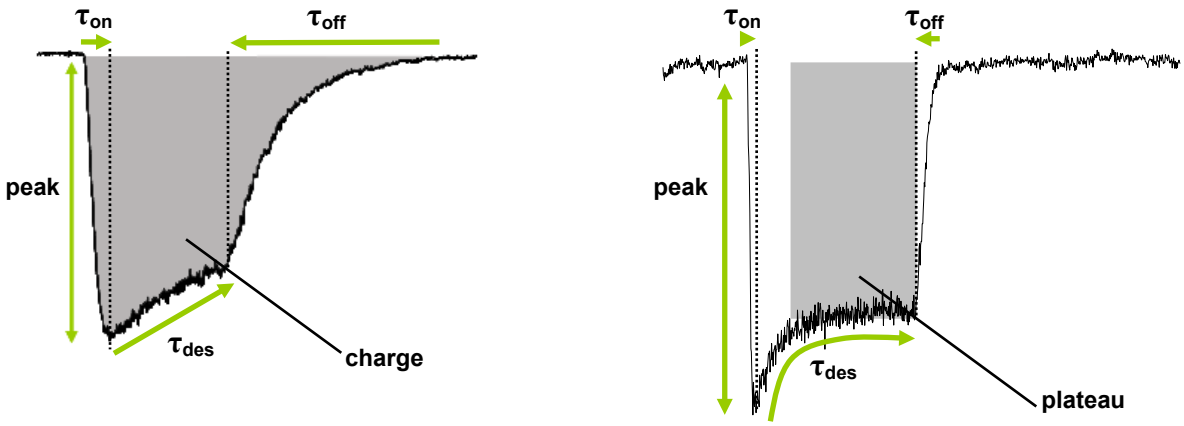

Fig.7. Two representative currents showing used parameters for whole-cell patch-clamp analysis. Left panel shows a GABA-evoked current with depicted parameters of amplitude (peak), onset (τ_{on}), offset (τ_{off}), desensitisation (τ_{des}) and charge (grey area). Right panel shows representative NMDA evoked current with plateau (grey rectangle) instead of charge parameter.

3.1.3 Fast-application setup

Analysis of receptor kinetics largely depends on the application device for the receptor agonist and the drugs being tested. In this work a custom made piezo-triggered theta-glass application device was used. Common "single tube" systems

may allow a complete change of solution surrounding the cell. However, their disadvantage lies in the representation of the deactivation time. It is either dependent on passive diffusion or it is limited by the time the solutions are exchanged in the tubes. A much faster solution is the use of a theta-glass connected to a valve-guided perfusion system and a piezo-switch for fast change of the theta-glass position. The theta-glass provides a laminar flow that separates the buffer solution and the solution containing the agonist. Activation of the piezo-switch moves the theta-glass into a different position and thus changes the solution surrounding the cell (Fig. 8). This system allows a higher temporal resolution by accomplishing application times of less then 10ms and a faster washout of the agonist. Therefore, recordings with this setup allow a more physiological representation of the activation and deactivation kinetics of a receptor. In addition the perfusion system allows the application of multiple substances in various concentrations during a single experiment.

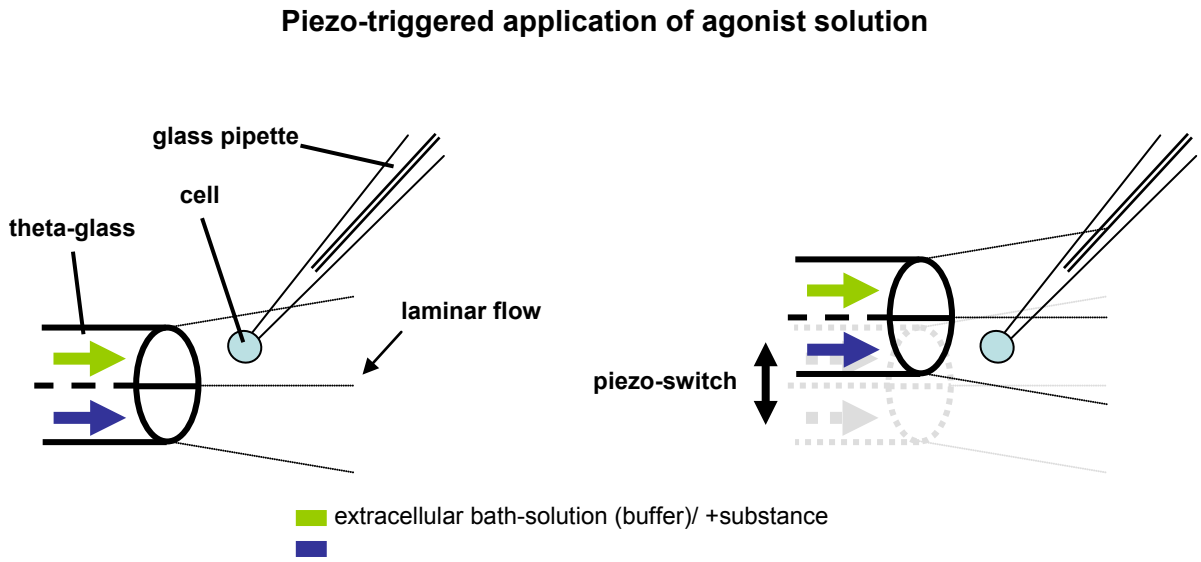

Fig.8. Scheme showing the principle of a fast-application setup. The cell is lifted with the glass-pipette under visual control *via* a micro-manipulator and positioned in front of the theta-glass into the stream containing the extracellular bath-solution. By triggering the piezo-switch the cell is bathed with agonist solution, which evokes the corresponding currents of the activated receptors.

3.2 Materials and methods: Effect of cholesterol depletion on receptor function and effects of psychopharmacological compounds

3.2.1 Chemicals and drugs

Desipramine and Fluox were obtained from Sigma-Aldrich (Deisenhofen, Germany). For stock solutions DMI and Fluox (10mM) were dissolved in H_2O. Diazepam (Diaz; 5mM; Sigma-Aldrich) was dissolved in 80% ethanol (*p.A.*, Klinikum Schwabing, Städtisches Klinikum München GmbH, Germany). Ingredients of bath solution were ordered from Carl Roth GmbH, Karlsruhe, Germany.

3.2.2 Cell culture

N1E-115 mouse neuroblastoma cells naturally expressing the 5-HT_{3A} receptor and WSS-1 cells (HEK 293) stably expressing the rat $GABA_A$ receptor alpha 1, beta 2 and gamma 2 subunits were obtained from ATCC LGC Promochem, Wesel, Germany. HEK 293 cells stably transfected with the human 5-HT_{3A} receptor were kindly provided by Dr. Theo Rein and constructed as described according to Lankiewicz *et al.* (Lankiewicz, Lobitz *et al.* 1998). Cells were cultured in Dulbecco's Modified Eagle's Medium (DMEM; Invitrogen, Karlsruhe, Germany) supplemented with 10% fetal calf serum (FCS; Invitrogen), 1% sodium pyruvate (Invitrogen) and antibiotics (Gibco® Antibiotic-Antimycotic, Invitrogen). Cells were reseeded onto fresh Petri dishes (Josef Peske, Aindlingen-Arnhofen, Germany) twice a week after treatment with 1% trypsin-EDTA (Invitrogen). Cells were cultured at 37°C, 5% CO_2, and 95% humidity.

Primary hippocampal neurons were kindly provided by Merz Pharmaceuticals GmbH, Frankfurt and obtained from rat embryos (E20-E21, Sprague-Dawley strain) and were transferred to Ca^{2+}- and Mg^{2+}-free Hank's-buffered salt solution (Invitrogen). Cells were dissociated in 0.66% trypsin/0.1% DNAse (AppliChem GmbH, Darmstadt, Germany) following 0.05% DNAse/0.3% ovomucoid incubation. After centrifugation, cells were resuspended in MEM (Invitrogen) and plated on poly-DL ornithine/laminin coated Petri dishes. Cells were cultured in $NaHCO_3$/HEPES-buffered MEM supplemented with 5% FCS and 5% horse serum (Invitrogen). Glial mitosis was inhibited by cytosine-β-D-arabinofuranoside (Sigma-Aldrich).

3.2.3 Cholesterol depletion

For cholesterol depletion cells were either treated with MßCD (Sigma-Aldrich) or Simvastatin (Sigma-Aldrich). When MßCD was used, cells were incubated with 0.5mM up to 7.5mM for 12h at 37°C in serum-free DMEM. For Simvastatin (Sim) induced cholesterol depletion, cells were kept in serum-free DMEM for 12h before Sim was added at a concentration of 500nM for 24h at 37°C. For depletion of WSS-1 cells 0.5mM MßCD was used. Due to reasons of cell viability the concentration for primary hippocampal neurons had to be lowered to 0.1mM MßCD.

3.2.4 Electrophysiological recordings of 5-HT_3 receptor

Cells were kept in DMEM without FCS for 12 h prior to the recordings. Serotonin (5-HT) induced inward Na^+ -currents were recorded from lifted cells in the whole-cell voltage clamp configuration under visual control using an inverted microscope (Zeiss, Jena, Germany) and a micro-manipulator (Eppendorf, Hamburg, Germany). N1E-115 cells were kept in a bath solution containing 162mM NaCl, 5.3mM KCl, 0.67mM Na_2HPO_4, 0.22mM KH_2PO_4, 15mM HEPES, and 5.6mM glucose. The bath solution for HEK 293 cells stably expressing the human 5-HT_{3A} receptor consisted of 140mM NaCl, 2.8mM KCl, 10mM HEPES, and 5.6mM glucose. Both solutions were adjusted to pH 7.2 with NaOH. Patch electrodes were pulled from borosilicate glass (Hilgenberg, Malsfeld, Germany) using a horizontal pipette puller (Zeitz-Instruments, Augsburg, Germany) to yield pipettes with a resistance of 3–6MΩ. Pipettes were filled with a solution containing 130mM CsCl, 2mM $MgCl_2$, 10mM EGTA, 10mM HEPES, 2mM K-ATP, 0.2mM Tris GTP, 10mM glucose, pH of 7.2, which was adjusted with CsOH.

After the whole-cell configuration was established, the cells were lifted with the micro-manipulator and 30µM 5-HT for N1E-115 cells or 10 µM 5-HT for HEK 293 cells stably expressing the human 5-HT_{3A} receptor were applied using a fast application setup as described above. The respective concentrations of 5-HT were applied since these were used for the determination of the IC50 value for the inhibition of the 5-HT response by psychopharmacological drugs in a previous study of our group, which was in the low micromolar range (Rammes, Eisensamer *et al.* 2004). Cells were positioned in front of a piezo translator-driven double-barreled application pipette used to expose the lifted cell either to 5-HT-free or 5-HT-containing bath solution. A 2s 5-HT application was delivered every 90s.

When stable control currents were established (at least four successive stable recordings) valves in the perfusion system were switched to tubes containing buffer solution and agonist solution containing the corresponding drug. The respective concentrations of 1µM DMI and 3µM Fluox used to modulate 5-HT_3 receptor function during electrophysiological recordings were chosen according to the IC50 values of a previous study of Eisensamer *et al.* and are achieved in the brain (Baumann, Gaillard *et al.* 1983; Karson, Newton *et al.* 1993; Eisensamer, Rammes *et al.* 2003). DMI and Fluox were diluted with bath solution to the required concentration. After wash-in of the drugs and onset of the pharmacological effect again four successive stable currents were recorded before start of wash-out with buffer and agonist (recovery current).

Current signals were recorded at a holding potential of -50mV with an EPC-9 amplifier (Heka, Lamprecht, Germany) and were analyzed using the Heka 8.5 PulseFit and IgorPro v. 5.04B (Wavemetrics, Lake Oswego, OR, USA) software on a Power Macintosh G3 computer. Only results from stable cells showing at least 50% recovery of responses to 5-HT following the removal of drugs entered the final analysis. To compensate for this effect the percentage of antagonism at each concentration was based on both the control and the recovery current by assuming a linear time course for the rundown.

Effects of drugs are analysed by IgorPro by establishing the mean of the last two recordings of both the control recording and recovery currents after wash-out and comparing this value with the mean of the last two stable recordings after drug application. The peak amplitude and charge evoked by 5-HT in the absence of antidepressants were set as 100%. Statistical data were analyzed with Excel® (Microsoft®, USA) using the unpaired Student t-test.

3.2.5 Electrophysiological recordings of $GABA_A$ receptor

Voltage clamp recordings were made in the whole-cell configuration at a holding potential of -50mV in WSS-1 cells. Application time of agonist and drug were 500ms if not stated otherwise with an interval of 15s. GABA concentrations used for dose-response analysis were 10µM, 30µM, 100µM, 300µM and 3mM. Standard concentrations of GABA were used for $GABA_A$ receptor-mediated currents analysis: 30µM or 100µM. The intracellular solution used for these recordings was composed of: 140mM KCl, 11mM EGTA, 10mM HEPES, 2mM $MgCl_2$ and 0.1mM ATP, pH 7.35,

adjusted with KOH. The corresponding extracellular bath solution was: 162mM NaCl, 5.3mM KCl, 0.67mM NaH_2PO_4, 0.22mM KH_2PO_4, 5.6mM glucose, 15mM HEPES, and 2mM $CaCl_2$, pH 7.4. Analysis was statistically processed as stated in the chapter before.

3.2.6 Electrophysiological recordings of NMDA receptor in primary hippocampal neurons cultures

Voltage clamp recordings were made in the whole-cell configuration at a holding potential of -70mV in primary hippocampal neurons. Application time of agonist was 2s with an interval of 30s. Intracellular solution for NMDA: 120mM CsCl, 10mM EGTA, 1mM $MgCl_2$, 0.2mM $CaCl_2$, 10mM glucose, 22mM TEA-Cl (TetraEthylAmmonium chloride), 2mM ATP and 0.2mM cAMP, pH 7.35 (adjusted with CsOH). The corresponding extracellular bath solution was: 140mM NaCl, 3mM KCl, 10mM glucose, 10mM HEPES, 0.2mM $CaCl_2$ and 4.5mM sucrose, pH 7.35 (adjusted with KOH). D-Serine (5μM) was added to all solutions as the co-agonist of NMDA receptors. NMDA currents were analysed using plateau instead of charge parameter due to a different default setting in the recording software. Analysis was statistically processed as stated in the chapter before.

3.3 Basic introduction to field potential recordings and induction of LTP

Field potentials are extracellular potentials recorded from groups of neurons in response to synaptic stimulation. In laminated structures such as the hippocampus, field potentials provide detailed information on cellular activity.

A field potential is generated by extracellular current flowing across the tissue resistance between the recording electrode and, in general, the ground electrode. Although measurable extracellular voltages are generated by action potentials in a single neuron, and form the basis of single unit recording, synaptic currents generated by single neurons are generally too small to be detected. In the hippocampus, the synchronous and localized currents generated by synaptic activation of a population of pyramidal or granule cells give rise to a characteristic and easily measurable negative field potential. Such negative field potentials is taken as a sign of excitatory synaptic activity and is called a field excitatory postsynaptic potential (fEPSP).

The main advantage of using field potentials is that an extracellular potential recording may give an accurate index of synaptic activity with regard to amplitude, time, and polarity (Andersen 2007).

LTP is defined as a persistent increase in the strength of synaptic activity recorded from individual or from a population of neurons. LTP can be induced in a number of ways, most conveniently by a tetanic stimulation (typically a train of multiple stimuli at a constant frequency). The single application of a one second 100Hz stimulus is sufficient to induce robust LTP in CA1 hippocampal region (Bliss and Collingridge 1993).

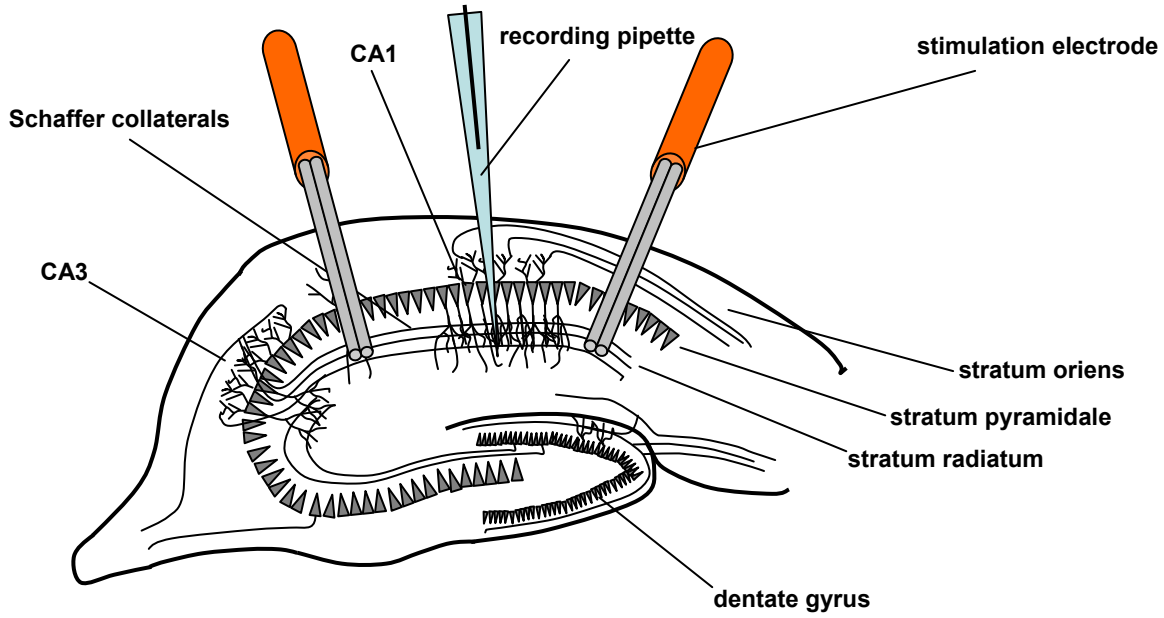

Fig.9. Experimental setup for two-electrode fEPSP measurements in hippocampal CA1 region in acute brain slice.

Two bipolar tungsten stimulation electrodes are placed at the borders of CA1 region. Recording pipette is placed in between. Alternating stimuli allow two parallel recordings of fEPSPs and two LTP experiments within the same slice.

3.4 Materials and methods: Acute effects of the antidepressant desipramine on synaptic plasticity related mechanisms

3.4.1 Brain slice preparation

Saggital hippocampal slices (350µM thick) were obtained from male 4-6 week old CD1 mice (animal facility of the Max Planck Institute of Biochemistry, Martinsried, Germany) that were anaesthetized with isoflurane before decapitation. The brain was rapidly removed, and slices were prepared in ice-cold Ringer solution using a vibroslicer (Microm HM 650 V, Walldorf, Germany).The composition of the Ringer solution was 124mM NaCl, 3mM KCl, 26mM $NaHCO_3$, 2mM $CaCl_2$, 1mM $MgSO_4$, 10mM D-glucose, and 1.25mM NaH_2PO_4, aerated with a 95% O_2–5% CO_2 mixture at all times resulting in a final pH of 7.3 (carbonate buffer).

All slices were placed in a holding chamber for at least 60 min and were then transferred to a customised immersion superfusing chamber for extracellular recordings. The flow rate of the solution through the chamber was 1.5ml/min. Extracellular recordings were made using glass microelectrodes (2–3MΩ) filled with Ringer solution. All experiments were performed at room temperature. DMI stocksolution (10mM) was diluted directly into Ringer solution to 3µM or 10µM end concentration.

3.4.2 Electrophysiological recordings

fEPSPs were evoked by stimulating the Schaffer collateral commissural pathway (Sccp) in the dendritic region of hippocampal CA1, by test stimuli (4–5V, 20µs) delivered via two bipolar tungsten electrodes (at 0.033Hz per electrode) insulated to the tip (tip diameter 50µm). For the induction of LTP, high-frequency stimulation (HFS; 100Hz/100 pulses, 1s) conditioning pulses were delivered to the same Sccp. inputs. For all recordings, both stimulating electrodes were used to utilize the input specificity of LTP and thereby allow the measurement of an internal control within the same slice. HFS was delivered from one of the electrodes under conditions in the absence DMI and potentiation of the responses was monitored for at least 60min after the tetanus. DMI (3µM or 10µM) was then applied *via* the bath solution for 60min before attempting to induce LTP in the second input following HFS delivered with the second electrode.

The recordings were amplified, filtered (3kHz), and digitized (9kHz) using a laboratory interface board (ITC-16, Instrutech Corp., NY, USA) and the "LTP-program"-software (Anderson and Collingridge 2001), available from http://www/ltp-program.com. Stimuli were applied in an alternating manner to each input. Two signals of the respective input were averaged to one for analysis making 1 every minute. Data were re-analyzed offline with the analysis program Igor Pro v6.1 (Wavemetrics, Lake Oswego, OR, USA) software. Measurements of the slope of the fEPSP were taken between 20 and 80% of the peak amplitude. Slopes of fEPSPs were normalized with respect to the last 10min of the 20min control period before tetanic stimulation (Fig. 10). Statistical data were analyzed with Excel® (Microsoft®, USA) using the paired Student t-test.

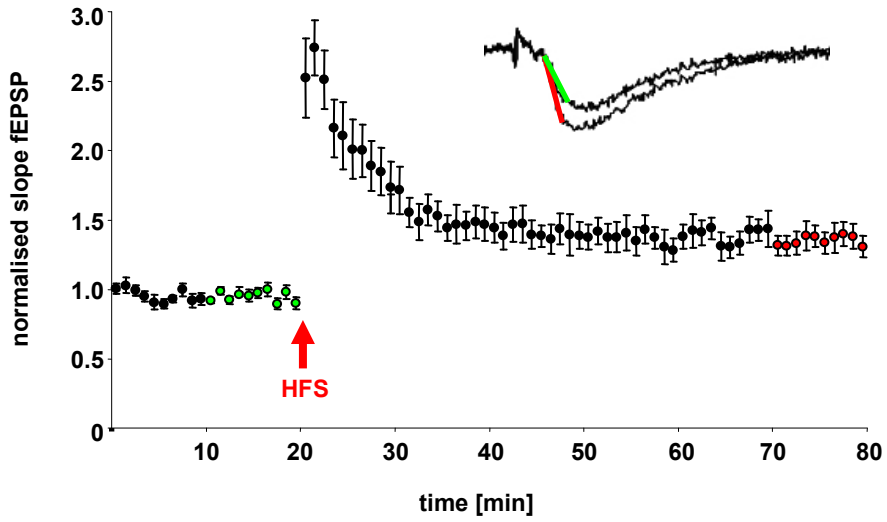

Fig.10. Representative LTP experiment with a single stimulus. Slope of fEPSPs are normalised to the mean of the last 10 measurements before induction of LTP *via* HFS (baseline, green). The compared LTP effect is generated out of the mean of the last 10min of the LTP recording (50-60min after HFS, red). Exemplary fEPSPs in the upper right show slope of baseline (green) before and 60min after HFS (red).

3.4.3 Immunofluorescence analysis of pMAPK in acute brain slices incubated with DMI alone and before and after LTP induction

Brain slices were obtained as described previously in chapter 4.4.1 and treated with 10µM DMI (Sigma) for 10, 15, 30 and 60 minutes alone (Fig. 9a), or taken after defined check points (immediately before HFS and 5, 10 and 30min after HFS) during electrophysiological recordings with (Fig. 9c) or without (Fig. 9b) DMI.

Immediately after acquiration of slices they were washed briefly in ice cold PBS which contained 1mM NaF. Brain slices were then fixed overnight at 4°C in a solution with 4% paraformaldehyd (PFA, Sigma) and 10% sucrose.

The following steps were all performed on ice. Brain slices were washed three times for 5min in PBS/NaF, solubilized with 0,1% TX 100 and washed again three times in PBS/NaF, quenched for 10min with 0,5% H_2O_2, washed again briefly, and blocked for two hours with 2% normal goat serum (Vector, Peterborough, UK).

Incubation with Phospho-p44/42MAP (Erk1/2; Thr202/tyr204) antibody (Cell Signalling, Boston, USA) in PBS/normal goat serum 1:150 was performed at 4°C overnight under constant shaking. Subsequently, slices were washed three times for 10min in PBS and incubated for 2h at room temperature with Biotin-SP conjugated goat anti rabbit IgG (Jackson Immuno Research Europe, London, UK) secondary antibody 1:100 in PBS/normal goat serum 1:150. Sections were washed (see above), and stained for two hours at room temperature with Avidine Alexa Fluor 488 conjugate (Molecular Probes, Invitrogen) 1:1000 and 4`,6-Diamidino-2-phenylindole dihydrochlorid (DAPI, Sigma-Aldrich) 1:1000, washed extensively in PBS and mounted on cover slides with IF/IHC Aqua Polymount (Polysciences Europe GmbH, Eppelheim, Germany).

3.4.3.1 Immunofluorescence analysis of ERK1/2 in acute brain slices

Images of stained slices were acquired with a confocal microscope (Olympus IX81, software, FluoView FV1000 2.1.2.5; Olympus Deutschland GmbH, Hamburg,). Thereafter, cells were counted with FluoView FV1000 software and images were processed using Photoshop® (Adobe). Cell count was performed in *stratum pyramidale* and *stratum radiatum* of hippocampal CA1 region separately.

CA1 region of each slice was subdivided into three images and cell count from corresponding pictures were combined. Total amount of ERK1/2 positive (pMAPK) cells was quantified by counting total DAPI and ERK1/2 positive cells in merged channel. Cells were counted manually and normalized after control slices. Only the total number of cells being ERK1/2 positive were characterized not the efficacy of individual and already active cells. The results show the overall number of active cells in the chosen regions of interest (Fig. 11). Statistical analysis was performed with SPSS 16.0 for Windows®, one-way ANOVA (Dunnett´s post hoc).

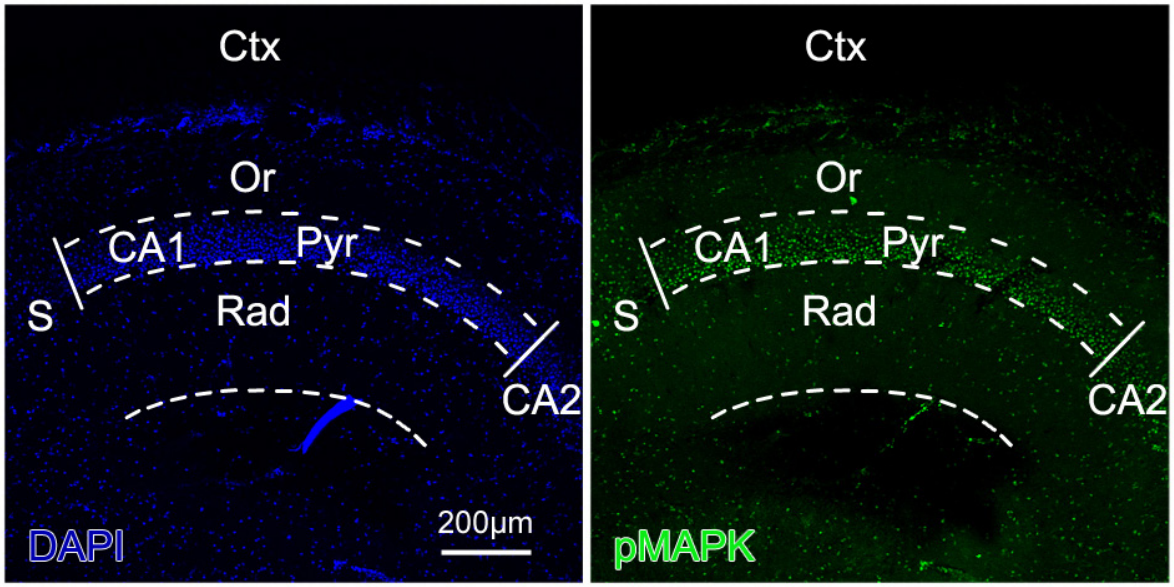

Fig.11. Immunofluorescence staining of CA1 region in hippocampus. Left panel shows DAPI (blue) cell staining for analysis of total cell amount. Right panel shows same slice with phosphorylated ERK1/2 (anti-Phospho-p44/42MAP pMAPK, green). Ctx= cortex, S= *subiculum*, Pyr= *stratum pyramidale*, Rad= *stratum radiatum*, Or= *stratum oriens*.

3.4.4 *In situ* analysis of *Arc* mRNA in acute brain slices before and after LTP with or without DMI

3.4.4.1 Design of *Arc* Probe

Oligonucleotides complementary to mRNA encoding gene for mouse *Arc* (5`GACTCACAACT GCCACACAAC 3` and 5`ACCAGCACAAGGTAATTGGAG 3` complementary to bases 1524–2702 of mouse cDNA) were used. PCR (standard cycles) products from mouse hippocampal cDNA were transformed with Strata Clon PCR Cloning Kit (Stratagene, Waldbronn, Germany). Clones were cultured and purified according to cloning kit protocol, and resulting DNA was sequenced. For *in situ* probe DNA was cut with Bam HI. To generate cRNA riboprobes a commercial transcription kit (Maxiscript T7/T3 RNA labeling kit, Ambion®, Invitrogen) was used. Riboprobes were purified with Mini Quick Spin RNA columns (Roche, Penzberg, Germany).

3.4.4.2 Fluorescent *in situ* hybridisation (FISH)

Brain sections were obtained as described in chapter 4.4.1 and washed twice shortly in SSC/DEPC H_2O (Sigma). Immediately slices were fixed with 4% PFA containing 10% sucrose for 2h on ice while shaking. FISH was performed with TSA-Cyanine3 Kit (Perkin Elmer, Rodgau, Germany).

All further steps were performed on ice. Slides were washed three times for 10min in 2x SSC and pretreated with acetic anhydride (Sigma) solution (0.23g NaCl solubilized in 25ml DEPC H_2O, add 370µl TEA and, directly before use, 125µl acetic anhydride) for 30min. After three washing steps (each 5min) in DEPC water slices were incubated in ice-cold methanol/acetone (1:1) and washed with 2x SSC briefly (once on ice and twice at room temperature).

Slices were prehybridized (prehybridisation solution, Sigma) in a humid chamber for 45min while shaking at room temperature. RNA probe (500ng) was mixed with 120µl hybridization buffer (Sigma), denaturated for 5min at 90°C and added to the slices. Incubation in a humid chamber was performed overnight at 56°C while shaking. Slices were washed three times in 2x SSC and treated with RNAse A (10µg/ml, Roche) 45min at 37°C.

Afterwards brain slices were washed two times for 10min at room temperature in 0.5x SSC, three times for 20min at 56°C and again 10min at room temperature.
Endogenous peroxidases were quenched by treatment with 3% H_2O_2 in 2x SSC for 20min, followed by washing twice for 5min in 2x SSC and once in TNS (0.1M Tris, 0.15M NaCl pH 7.5, Perkin Elmer).

Slices were blocked with TNB blocking reagent (Perkin Elmer) 2h at room temperature and incubated overnight with anti DIG HRP (Roche) 1:90 in TNB.
After three washing steps in TNST (0.05% Tween, Perkin Elmer) each for 15min slices were treated according to the manufacturers instructions with Cy3 tyramine in amplification diluent 1:50, combined with DAPI 1:1000. Before mounted on microscope slide in IF/IHC Aqua Polymount (Polysciences Europe GmbH) brain slices were washed three times for 15min in TNST. Cells were counted manually and normalized after control slices. Only the total number of cells being *Arc* positive (clear *Arc* mRNA signal in cytosol) were characterized. The results show the overall number of active cells in *stratum pyramidale*. Statistical data were analyzed with Excel® (Microsoft®, USA) using the paired Student t-test.

3.4.5 Analysis of EphA4 phosphorylation *via* Ephrin A3 in hippocampal slices with or without DMI treatment by means of immunoprecipitation

Brain slices were obtained as described previously in chapter 4.4.1. Hippocampal slices of each hemisphere were separated into two incubation chambers (four slices per hemisphere from two different animals per experiment).

One chamber was used as control chamber the other was used for incubation with DMI or recombinant human EphrinA3-FC chimera (R&D Systems GmbH, Wiesbaden, Germany). 10µM DMI was applied for 1h to slices and treatment with EphrinA3 lasted for 45min. Slices incubated with both DMI and EphrinA3, were incubated with 10µM DMI for 1h following 45min of EphrinA3 treatment to induce EphA4 phosphorylation. Immediately after incubation slices were transferred into a Petri dish containing fresh PBS on ice for dissection of the hippocampus. Hippocampal sections were frozen at -80°C instantly.

For immunoprecipitation following solutions had to be prepared:

-Lysis buffer: 50mM Tris pH 7.4 (2.5ml 1M/50ml), 150mM NaCl (0.44g)

Directly before use lysis buffer was additionally mixed with 1% Triton X 100, Protease and Phosphatase Inhibitor (one pellet each, Roche)

-Washing solution 2: 50mM Tris, pH 7.4, 0.5M NaCl (1.46g/50ml), 0.1% TX 100
-Washing solution 3: 50mM Tris, pH 7.4, 0.1% TX 100

Sepharose beads (Protein A Sepharose CL 4B, Amersham Biosciences, GE Healthcare, Munich, Germany) for protein separation (40µl beads netto per sample) were washed twice with lysis buffer (without additives) and 100µl of lysis buffer (with additives) were added before centrifugation at 6000rpm for 2min.

Monoclonal mouse anti-EphA4 unconjugated antibody (Novex®, Invitrogen, Karlsruhe, Germany) was pre-diluted in lysis buffer (5-10µl antibody in 300µl buffer), added to beads and incubated for 3h at 4°C and 1h at room temperature. After incubation the antibody/beads mixture was washed with 100µl lysis buffer were added before centrifugation at 6000rpm for 2min

Hippocampal sections are transferred into 800µl lysis buffer (on ice) for tissue preperation and drawn back and forth 10 times with a hypodermic 25-gauge needle into a 1ml syringe. For solubilisation samples were incubated 30-60min on ice and vortexed from time to time. After centrifugation at 14000rpm for 15min pellets were resuspended 4 times with 300µl lysis buffer and a 1ml syringe.

The supernatant was centrifuged 20min with 14000rpm and resulting pellet was kept and applied additionally to sample when necessary. The lysate was added

to the sepharose beads, filled up to 1ml of volume with lysis buffer if necessary and rotated at 4°C over night.

Subsequently three washing steps with washing solution 2 were conducted with centrifugation at 2000rpm for 2min followed by two washing steps with washing solution 2 and 3 (2000rpm for 5min). During the last washing step sample container should be exchanged.

Laemmli buffer diluted 2:5 (10ml of 5x buffer contain 2ml 1M Tris pH 6.8, 2.5ml 20% SDS, 5.7ml 87% glycerine, 200µM 0.5M EDTA, 0.77g DTT, 3.3mg bromphenol blue) was added incubated at 95°C for 10min. Samples must not be put on ice again to prevent re-binding of proteins to the beads. Finally the samples were rotated in brief to separate the beads and the supernatant was taken for Western blot application.

The western blot procedure was adapted from protocols previously described (Di Benedetto, Kallnik *et al.* 2009). In brief, total protein content was quantified with Lowry standard assay (500-0119, Bio-Rad, Hercules, USA) and 15µg of each protein lysate were denatured in Laemmli buffer (90°C for 2min), separated with 10% SDS-PAGE and then transblotted to a nitrocellulose membrane (Protran BA, Whatman, GE Healthcare, Munich, Germany). To reduce background, membranes were blocked with 5% bovine serum albumin (BSA) in Tris-buffered saline with Tween-20 (TBS-T: 10mM Tris-Cl, pH 7.5; 150mM NaCl; and 0.1% Tween-20) overnight at 4°C. Thereafter, they were incubated for 2h at room temperature (RT) with mouse anti-phosphotyrosine antibody, clone 4G10®, biotin conjugate (Millipore, Schwalbach, Taunus, Germany) or a anti-EphA4 receptor, mouse unconjugated monoclonal antibody (Invitrogen) as standard internal control and for semi-quantitative analysis after stripping.

Blots were washed in TBS-T and incubated with HRP-conjugated goat anti-rabbit (Jackson ImmunoResearch Europe Ltd., Suffolk, UK) for 1h at RT. After washing in TBS-T, they were visualized with enhanced chemiluminescence (ECL) detection reagent (Amersham Biosciences) and films were scanned and processed by densitometric analysis using ImageJ software (Rasband, W.S., ImageJ, U. S. National Institutes of Health, Bethesda, USA, http://imagej.nih.gov/ij/).

4 Results

4.1 Impact of lipid raft integrity on ionotropic receptor function and its modulation by psychopharmacological compounds

4.1.1 Effects of cholesterol depletion on 5-HT_3 receptor function

Withdrawal of cholesterol from cell membranes by means of MßCD is a commonly used approach for lipid raft disruption. In this work it was investigated whether cholesterol depletion by MßCD affects 5-HT_3 receptor function using whole-cell voltage-clamp recordings. Treatment of N1-E115 cells kept in DMEM without fetal calf serum (FCS) with 0.5mM MßCD for 12h markedly reduced the peak amplitude and increased onset, desensitization and deactivation kinetics of serotonin-evoked cation currents under cholesterol depleted conditions, whereas the charge parameter remained unaffected (Fig. 12a, Table 1).

When cells were kept in DMEM supplemented with 10% FCS, effects of MßCD-induced cholesterol depletion were less distinctive. Nevertheless, MßCD treatment still reduced the amplitude of the currents, although to a smaller degree than without FCS. In contrast to cholesterol depleted conditions alone, a faster receptor desensitization and deactivation were observed in presence of FCS (Fig. 12b, Table 1).

As an alternative approach for cholesterol depletion the hydroxyl-methylglutaryl-coenzyme A reductase inhibitor simvastatin (Sim) was applied, which inhibits endogenous cholesterol synthesis. Treatment with 500nM Sim for 24h reduced serotonin-evoked cation currents in a similar way as with MßCD (Table 1).

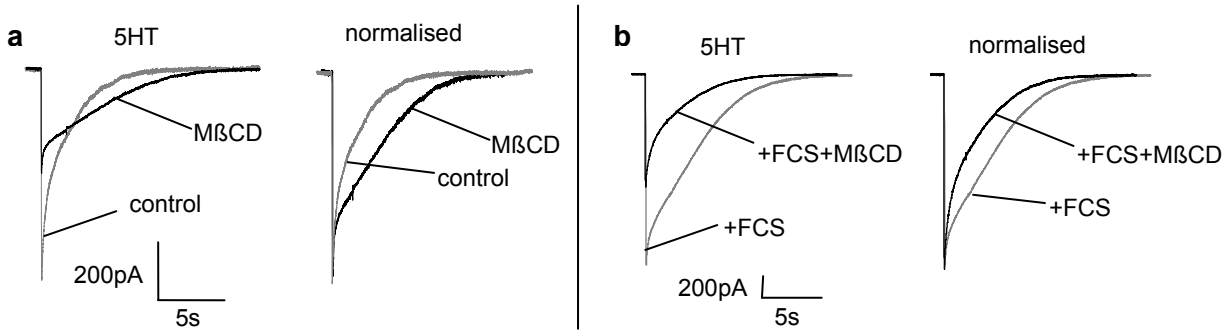

Fig.12. Treatment with MßCD decreases serotonin-evoked cation currents in N1E-115 cells. Cation currents were recorded in a whole-cell voltage-clamp configuration. 30µM

serotonin was applied for 2s. **(a)** Effect of cholesterol depletion with MßCD. The left panel shows representative recordings of an untreated cell (control = without FCS) and of a cell pre-treated with 0.5mM MßCD for 12h (MßCD). The right panel shows the same recording normalized to control. **(b)** Effect of MßCD in the presence of FCS is hindering cholesterol depletion. The left panel shows representative recordings of an untreated cell in the presence of FCS (+FCS) and of a cell pretreated with 0.5mM MßCD for 12h (+FCS+MßCD). Cells were kept in DMEM with FCS for 12h both for control and MßCD incubation before the recordings. The left panel shows currents of a representative experiment, the right panel shows the same recording normalized to the untreated cell + FCS.

	Control	+MßCD	+Sim	+FCS	+FCS+MßCD
τ_{on} (ms)	26.6±4.4	80.7±17.5 (303.4%)[a]	26.0±3.8 (97.7%)[a]	19.8±1.7	21.8±2.4 (110.1%)[b]
τ_{des} (ms)	546.0±30.0	1429.4±196.4 (261.8%)[a]	1215.8±166.1 (222.7%)[a]	1337.8±216.1	876.1±92.5 (65.5%)[b]
τ_{off} (ms)	1938.0±65.3	4010.2±262.1 (206.9%)[a]	3480.2±281.2 (179.6%)[a]	3715.5±150.5	3091.9±172.6 (83.2%)[b]
peak (pA)	-714.7±60.1	-242.9±51.0 (34.0%)[a]	-363.1±111.3 (50.8%)[a]	-1845.3±127.4	-1262.5±116.7 (68.4%)[b]
charge (pC)	-1695±502.7	-1395±371.8 (82.3%)[a]	-1229±500.8 (72.5%)[a]	-8295±808.2	-3123±623.9 (37.6%)[b]

Table 1. Effect of MßCD on serotonin-evoked cation currents in N1E-115 cells. Time constants (τ) of onset (τ_{on}), desensitization (τ_{des}) and offset (τ_{off}), peak amplitudes and charges of serotonin-evoked cation currents in N1E-115 cells under the following conditions: control: cells were kept in DMEM without FCS for 12h; +MßCD: cells were treated with MßCD 0.5mM for 12h in DMEM without FCS; +Sim: cells were treated with Sim 500nM for 24h in DMEM without FCS; +FCS: cells were kept in DMEM supplemented with 10% FCS; +FCS+MßCD: cells were kept in DMEM supplemented with 10% FCS and were treated with 0.5mM MßCD for 12h. Results are shown as the mean±SEM (n=10 independent experiments for each condition, except for +Sim where n=8). [a]Percent of control. [b]Percent of +FCS. Parameters compared to control: +MßCD: τ_{on} p=0.019, τ_{des} p=0.002, τ_{off} p<0.001, peak p<0.001, charge p=0.666; +Sim: τ_{on} p=0.931, τ_{des} p=0.004, τ_{off} p<0.001 , peak p<0.001, charge p=0.661; +FCS: τ_{on} p=0.373, τ_{des} p=0.015, τ_{off} p<0.001, peak p<0.001, charge p<0.001; +FCS+MßCD: τ_{on} p=0.373, τ_{des} p=0.016, τ_{off} p<0.001, peak p<0.001, charge p=0.119.

4.1.2 Effects of cholesterol depletion on the antagonistic effects of ADs on the 5-HT$_3$ receptor

To address the question of whether impairment of lipid raft integrity affects the modulation of the 5-HT$_3$ receptor by ADs the impact of cholesterol depletion on the functional antagonistic effect of desipramine (DMI) and fluoxetine (Fluox) on this receptor was investigated.

DMI reduced the peak and the charge, but increased the speed of decay of serotonin-evoked currents in N1E-115 cells as reported previously (Eisensamer, Rammes *et al.* 2003) (Fig. 13a and d, Table 2).

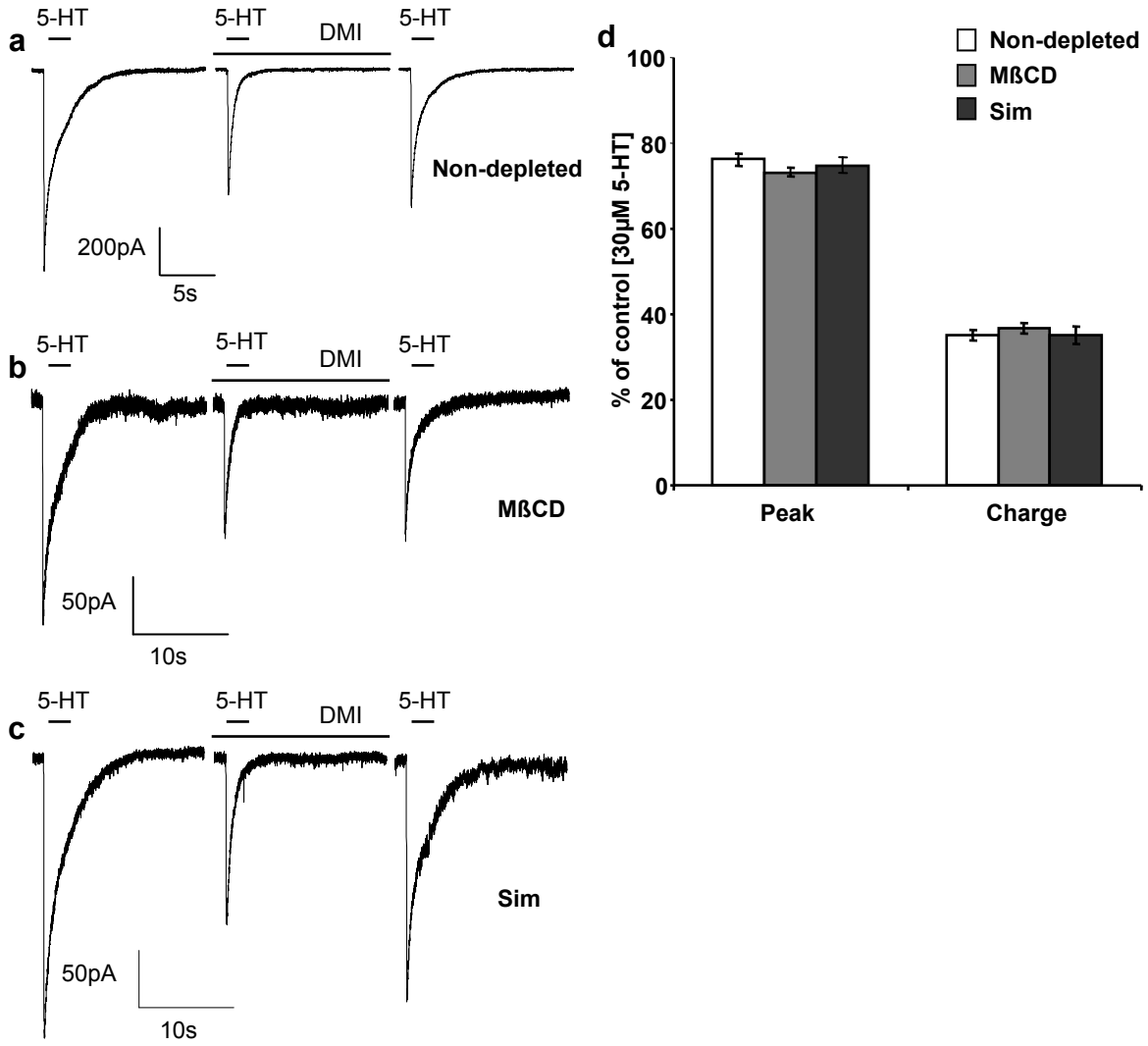

Fig.13. The modulation of serotonin-evoked currents by DMI is not altered after cholesterol depletion of N1E-115 cells. Cation currents were recorded in the whole-cell voltage-clamp configuration. 5-HT (30µM) was applied for 2s in the absence or presence of 1µM DMI. **(a)** Antagonistic effect of DMI on the 5-HT$_3$ receptor in non-depleted cells. The

upper bars indicate the presence of 5-HT, the lower bar indicates the presence of DMI. Representative recordings before and after application of DMI and subsequent washout are shown. **(b)** Antagonistic effect of DMI after cholesterol depletion with MßCD. Cells were treated with 0.5mM MßCD 12h before the recordings. **(c)** Antagonistic effect of DMI after Sim treatment. Cells were treated with 500nM Sim for 24h before the recordings. **(d)** Quantification of the effect of DMI on peak amplitude and charge of serotonin-evoked currents in non depleted cells (white bars) and after cholesterol depletion with MßCD for 12h (grey bars) or 500nM Sim (statin) for 24h (black bars). n=6 independent experiments for each condition and data are shown as mean±SEM% of "control" values obtained in absence of DMI. DMI reduced peak amplitude and charge to a similar extent in all three experimental conditions compared to control (absence of DMI). Non depleted cells: Peak=76.62±1.36%; Charge=35.09±1.26%. MßCD: Peak=74.21±0.96% (p=0.229), Charge=36.72±1.26% (p=0.538); Sim: Peak=74.83±1.74% (p=0.597), Charge=35.16±2.13% (p=0.970).

Although treatment with 0.5mM MßCD for 12h markedly diminished serotonin-evoked currents, the DMI-induced inhibition and kinetic changes were still retained following cholesterol depletion by MßCD (Fig. 13b, Table 2). The same DMI effects were also observed after cholesterol depletion with Sim (Fig. 13d, Table 2). Moreover, the antagonistic effect of DMI on these currents was maintained following MßCD treatment of HEK 293 cells, stably expressing the human 5-HT_3 receptor (see chapter 4.1.6).

	DMI	DMI+MßCD	DMI+Sim
τ_{on} %	162.2±1.7	156.5±9.0	160.7±11.0
τ_{des} %	77.9±2.1	79.1±2.8	78.7±16.5
τ_{off} %	89.9±18.1	60.9±16.1	54.9±8.1

Table 2. 5-HT_3 receptor decay of DMI effect in control cells and depleted cells. Time constants (τ) of onset (τ_{on}), desensitization (τ_{des}) and offset (τ_{off}) of serotonin-evoked currents in N1E-115 cells under the following conditions: application of DMI, DMI+MßCD: application of DMI to cells pretreated with MßCD 0.5mM, DMI+Sim: application of DMI to cells pretreated with Sim 500nM. Results are shown as mean±SEM% of control (see Figure 13 d) of six independent experiments. Parameters compared to DMI effect in non depleted cells (DMI):

DMI+MßCD: τ_{on} % p=0.768, τ_{des} % p=0.727, τ_{off} % p=0.343; DMI+Sim: τ_{on} % p=0.914, τ_{des} % p=0.984, τ_{off} % p=0.453.

Comparable findings were obtained with the selective serotonin reuptake inhibitor Fluox. A decrease in the peak amplitude and charge and an acceleration of receptor desensitization could be observed both in non-depleted cells (Fig. 14a and c, Table 3) and under conditions of MßCD-induced cholesterol depletion (Fig. 14b and c, Table 3).

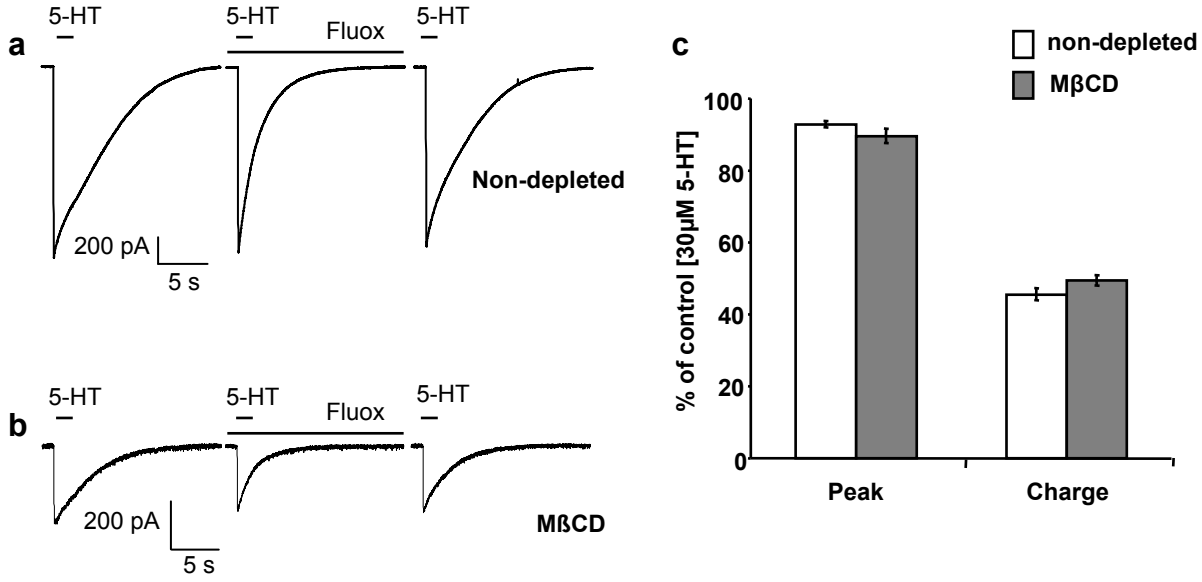

Fig.14. The modulation of serotonin-evoked currents by Fluox is not altered after cholesterol depletion of N1E-115 cells. Cation currents were recorded in the whole-cell voltage-clamp configuration. 5-HT (30µM) was applied for 2s in the absence or presence of 3µM Fluox. **(a)** Antagonistic effect of Fluox on the 5-HT_3 receptor in non-depleted cells. The upper bars indicate the presence of 5-HT, the lower bar indicates the presence of Fluox. Representative recordings before and after application of Fluox and subsequent washout are shown. **(b)** Antagonistic effect of Fluox after MßCD treatment. Cells were treated with 0.5mM MßCD for 12h before the recordings. **(c)** Quantification of the effect of Fluox on peak amplitude and charge of the serotonin-evoked currents in non depleted cells (white bars) and after treatment with MßCD (grey bars). n=6 independent experiments for each condition and data are shown as mean±SEM% of "control" values obtained in absence of Fluox. Fluox effect in non depleted cells: Peak=92.89±1.62 %, Charge=45.49±1.65%. Fluox reduced peak amplitude and charge to a similar extent in both experimental conditions. Fluox+MßCD: Peak=89.54±1.93% (p=0.435), Charge=49.38±1.42% (p=0.177).

	Fluox	Fluox+MßCD
τ_{on} %	98.1±5.1	100.6±3.9
τ_{des} %	96.1±12.9	84.6±1.3
τ_{off} %	47.3±1.2	54.0±4.2

Table 3. Time constants (τ) of onset (τ_{on}), desensitization (τ_{des}) and offset (τ_{off}) of serotonin-evoked currents in N1E-115 cells. Conditions: Fluox: application of Fluox, Fluox+MßCD: application of Fluox to MßCD (0.5mM)-depleted cells. Results are shown as mean±SEM% of control in absence of Fluox. n=6 independent experiments. Parameters compared to Fluox effect in non depleted cells (Fluox column): Fluox+MßCD: τ_{on}% p=0.810, τ_{des}% p=0.568, τ_{off}% p=0.224.

4.1.3 Effects of cholesterol depletion on $GABA_A$ receptor function

Another receptor associated with lipid rafts is the $GABA_A$ receptor which is also a well known target for ADs. Impairment of lipid raft integrity by treatment of WSS-1 cells with 0.5mM MßCD for 12 h diminished GABA-evoked chloride currents as seen for the 5-HT_3 receptor, but did not alter the desensitization properties of the receptor (Fig. 9a). The shift of the GABA dose-response curve to the right after MßCD treatment (Fig. 9b) indicates a reduced potency of the agonist.

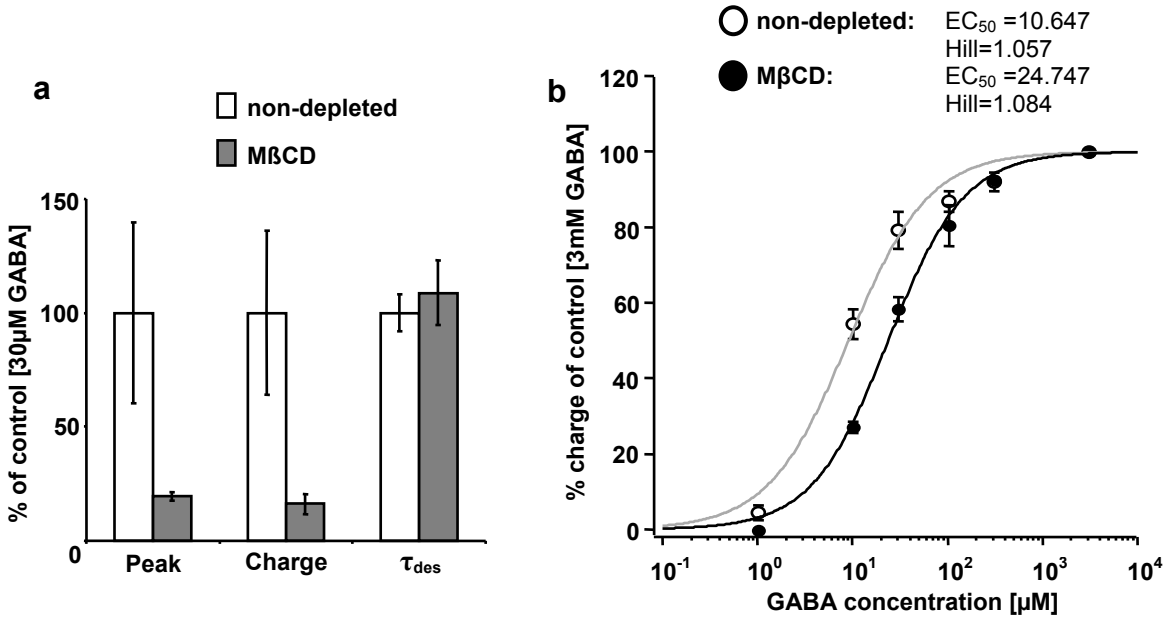

Fig.15. Effect of cholesterol depletion by MßCD on $GABA_A$ receptor. GABA-evoked chloride currents were recorded in the whole-cell voltage clamp configuration. **(a)** Treatment with MßCD significantly decreased GABA-evoked (30µM GABA for 500ms) chloride currents in WSS-1 cells. Desensitization (τ_{des}) of $GABA_A$ receptor is not altered by depletion with MßCD. Data are presented as mean±SEM% of "control" values obtained in non-depleted cells. Non-depleted cells: Peak=100±39.57%, Charge=100±35.90%, τ_{des}=100±8.14%.. MßCD-depleted cells: Peak=19.51±2.04% (p=0.003), Charge=16.13±4.42% (p=0.004), τ_{des}=108.89±1.42% (p=0.411). n=6 independent experiments for each parameter. **(b)** Dose-response curve of the GABA-evoked current charge through the $GABA_A$ receptor in non-depleted WSS-1 cells (open circles; grey curve) and in MßCD-depleted WSS-1 cells (solid circles; black curve). Results are normalized to the maximal current charge induced by the application of 3mM GABA and presented as mean±SEM. n=7 independent experiments. MßCD EC_{50}=24.75±3.49 compared to non depleted cells EC_{50}=10,647±2,066 (p=0.003).

4.1.4 Effects of cholesterol depletion on the potentiating effect of diazepam at the $GABA_A$ receptor

Benzodiazepines are potent positive allosteric modulators of $GABA_A$ receptors (Dalskov, Immerdal *et al.* 2005). As previously shown, 1µM Diazepam (Diaz) markedly potentiated GABA-evoked chloride currents in WSS-1 cells (Davies, Hoffmann *et al.* 2000) (Fig. 16a, c). This potentiating effect of Diaz on GABA-evoked currents was even more pronounced after cholesterol depletion with MßCD (Fig. 16b, c).

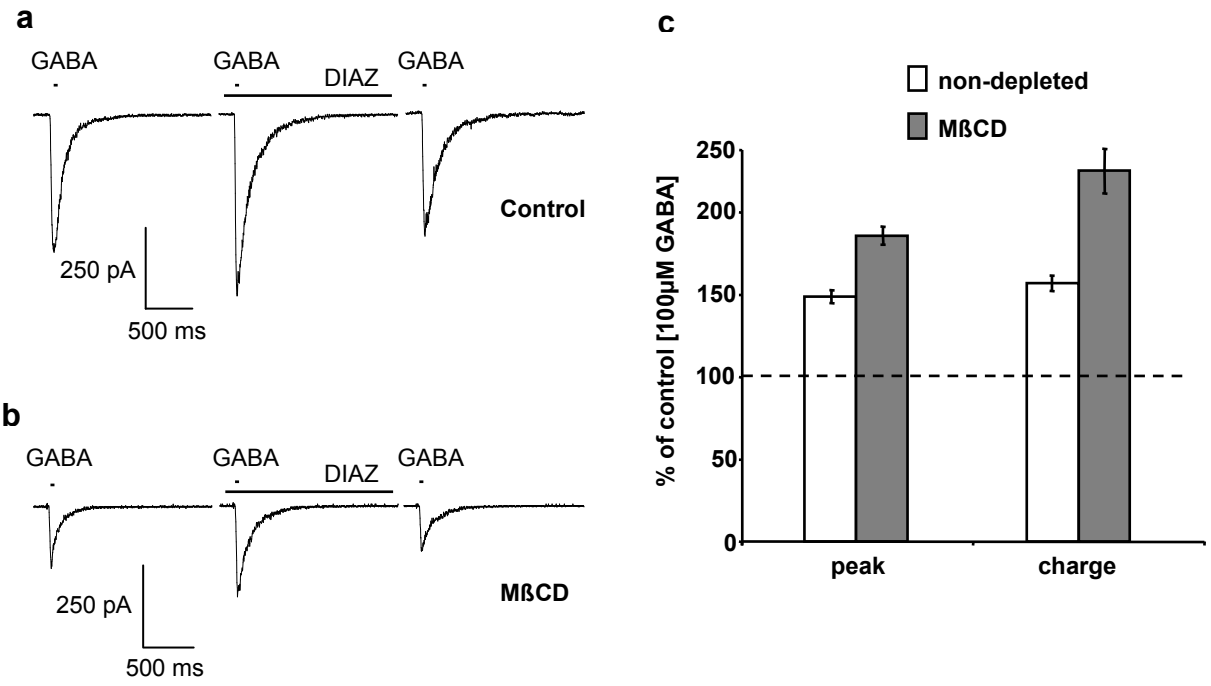

Fig.16. Potentiation of GABA-evoked currents by diazepam after MßCD treatment of WSS-1 cells is increased. Chloride currents were recorded in the whole-cell voltage-clamp configuration. GABA (100µM) was applied for 10ms in the absence or presence of 1µM Diaz. **(a)** Potentiating effect of Diaz on the $GABA_A$ receptor in non depleted cells. Representative recordings before and after application of Diaz and subsequent washout are shown. **(b)** Effect of Diaz after MßCD treatment. Cells were treated with 0.5mM MßCD for 12h before the recordings. **(c)** Quantification of the effect of Diaz on peak amplitude and charge of GABA-evoked currents in non depleted cells (white bars) and after treatment with MßCD (grey bars). n=6 independent experiments for each condition and data are shown as mean±SEM% of "control" values obtained in absence of Diaz. Diaz enhanced peak amplitude and charge significantly under depleted conditions. Diaz effect in non-depleted cells: Peak=148.52±4.06%, Charge=156.76±4.76%. Diaz effect in depleted cells: Peak=185±5.41% (p=0.018), Charge=224.96±13.40% (p=0.027).

The potentiation of Diaz effect after depletion with MßCD could be reproduced after changing the agonist application time to 500ms (Fig. 11d). To determine whether the enhancement of the Diaz effect after cholesterol depletion is correlated to the general reduction of GABA currents, a dose-response relationship including maximum receptor efficacy and the Diaz effect at lower concentrations was necessary to test if Schild regression was feasible. Due to insufficient cell stability during the recordings in depleted cells, the MßCD concentration had to be reduced to 0.25mM.

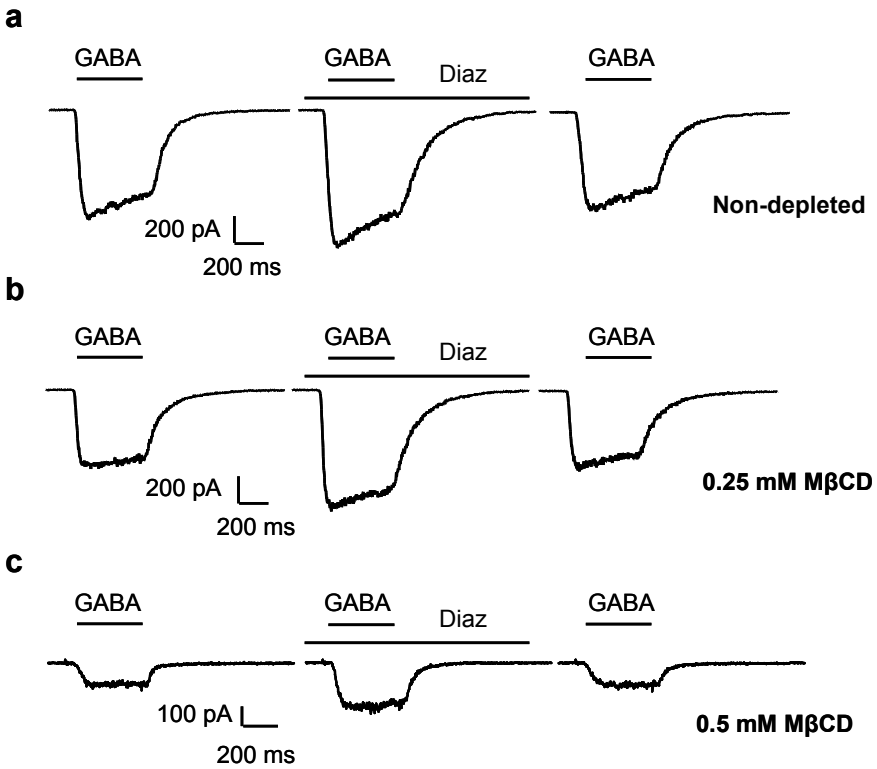

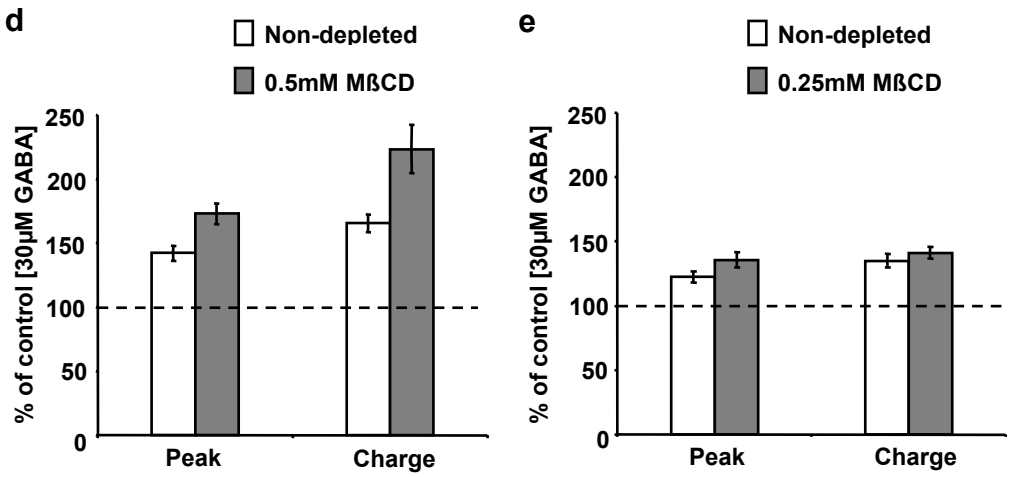

Fig.17. Potentiation of GABA evoked currents by diazepam after treatment with different MßCD concentrations. Chloride currents were recorded in the whole-cell voltage-clamp configuration. GABA (30µM) was applied for 500ms in the absence or presence of 1µM diazepam (Diaz). **(a)** Potentiating effect of Diaz on $GABA_A$ receptor in non-depleted cells. Representative recordings before and after application of Diaz and subsequent washout are shown. **(b)** Effect of Diaz after treatment with reduced concentration of MßCD. Cells were treated with 0.25mM MßCD for 12h before the recordings. **(c)** Effect of Diaz after treatment with normal concentration of MßCD. Cells were treated with 0.5mM MßCD for 12h before the recordings. **(d)** Quantification of the effect of Diaz on peak amplitude and charge of the GABA-evoked currents in non depleted cells (white bars) and after treatment with 0.5mM MßCD for 12h (grey bars). n=6 independent experiments for each condition and data are shown as mean±SEM% of "control" values obtained in absence of Diaz. Non-depleted cells cells (white bars) showed a potentiating effect of Diaz (Peak=142.23±5.84%, charge=165.46±6.74%). Diaz enhanced peak amplitude and charge significantly under depleted conditions. 0.5mM MßCD compared to non depleted cells: Peak=172.79±7.85% (p=0.013), Charge=223.42±19.01% (p=0.021). **(e)** Quantification of the effect of Diaz on peak amplitude and charge of GABA-evoked currents in non depleted cells (white bars) and after treatment with 0.25mM MßCD for 12h. n=6 independent experiments for each condition and data are shown as mean±SEM% of "control" values obtained in absence of Diaz. 0.25mM MßCD compared to non depleted cells (Peak=122.49±4.18%, Charge=135.02±5.35%): Peak=135.55±5.81% (p=0.177), Charge=141.19±4.47% (p=0.176).

Cholesterol depletion with MßCD for 12h dose-dependently diminished GABA-evoked chloride currents (Fig. 17a-c). After treatment with a lower MßCD concentration, the Diaz effect was still enhanced, but to a lower extent compared to depleted cells with 0.5 mM MßCD. However, the maximal Diaz-induced potentiation of receptor currents did not change (Fig. 18b) when currents were normalized to

maximal $GABA_A$ receptor activation at saturating GABA concentration. Effect of diazepam at close to maximum $GABA_A$ activation is less pronounced than in submaximal GABA concentrations in non-depleted cells. In contrast currents through GABAA receptors in MßCD-treated cells were more potentiated in the presence of Diaz (Fig. 18c), although the lower MßCD concentration seemed not efficient enough (Fig. 18a) to shift the GABA dose response relation compared to the experiments with 0.5mM MßCD (Fig. 15b).

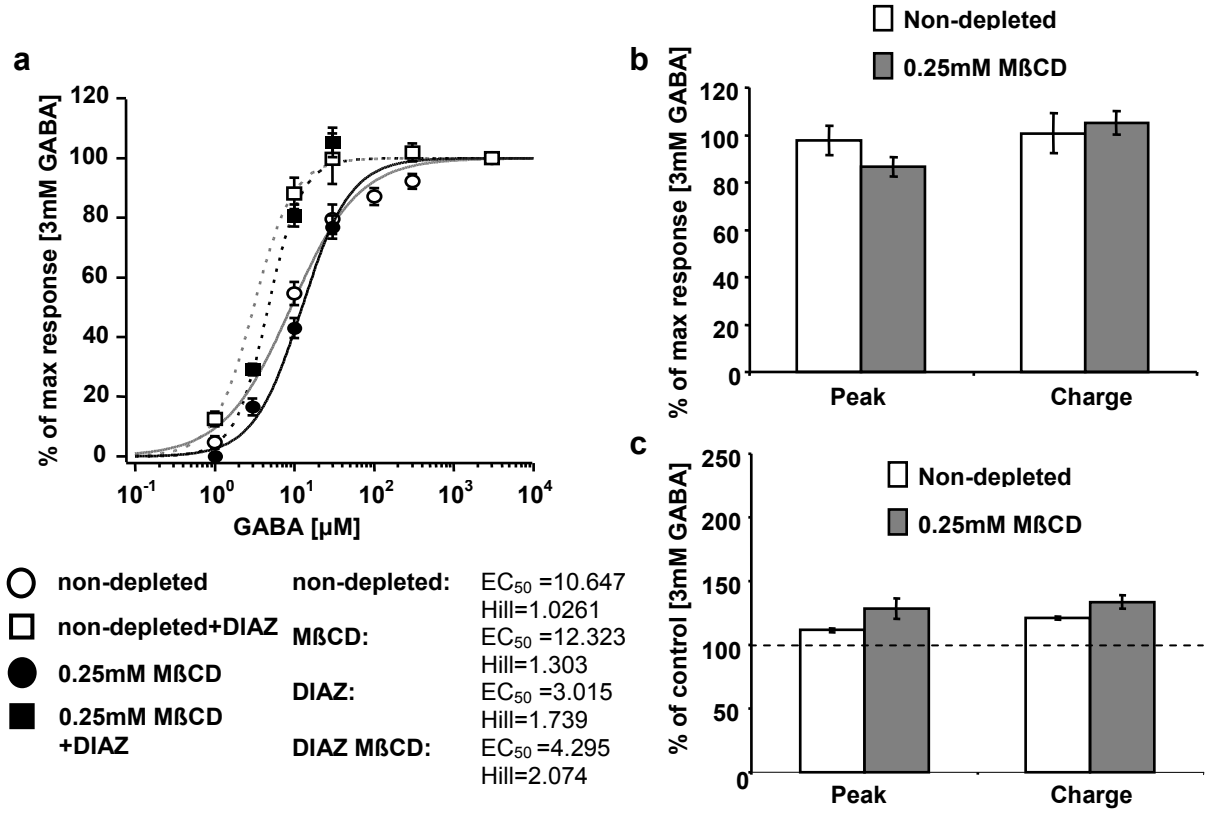

Fig.18. Impact of MßCD-induced cholesterol depletion of WSS-1 cells on GABA-evoked chloride currents and their modulation by Diaz. (a) Dose-response relationship of the GABA-evoked current charge in non depleted WSS-1 cells (open circles; grey curve) and in WSS-1 cells treated with 0.25mM MßCD (solid circles; black curve). Results are normalized to the maximum receptor current induced by 3mM GABA and presented as mean±EM of 5 independent experiments. Open squares, dashed grey curve: Mean±SEM of normalized charges in non-depleted WSS-1 cells treated with 1µM DIAZ of 4 independent experiments. Solid squares, dashed black curve: Mean±SEM of normalised charges in WSS-1 cells depleted with 0.25mM MßCD and treated with 1µM Diaz of 4 independent experiments. 0.25mM MßCD: EC_{50} 12.32±1.13 compared to non-depleted: EC_{50} 10.65±2.07 (p=0.872); 0.25mM MßCD+DIAZ: EC_{50} 4.30±0.063 compared to non depleted+DIAZ: EC_{50} 3.02±0.40 (p=0.128). **(b)** Quantification of the effect of Diaz on peak amplitude and charge of GABA-evoked currents (expressed in % of the maximal answer obtained with 3mM GABA) in non-

depleted cells (white bars) and after treatment with 0.25mM MßCD for 12h (grey bars). n=6 independent experiments for each condition and data are shown as mean±SEM% of “control” values obtained in absence of Diaz. Non-depleted cells (white bars): Peak=97.91±6.18%, Charge=100.78±8.38%. 0.25mM MßCD compared to non-depleted cells: Peak=86.64±4.19% (p=0.064), Charge=105.23±4.87% (p=0.822). **(c)** Diaz potentiation at 3mM GABA concentration. Quantification of the effect of Diaz on peak amplitude and charge of GABA-evoked currents in non-depleted cells (white bars) and after treatment with 0.25mM MßCD for 12h (grey bars). n=6 independent experiments for each condition and data are shown as mean±SEM% of “control” values obtained in absence of Diaz. Non-depleted cells (white bars): Peak=111.54±1.39%, Charge=121.10±1.07% compared to 0.25mM MßCD: Peak=128.44±7.83% (p=0.064), Charge=133.58±5.28% (p=0.822).

4.1.5 Effects of cholesterol depletion on NMDA receptor function and the antagonistic effects of desipramine

To study the influence of cholesterol depletion on the NMDA receptor, the use of hippocampal neurons was necessary because stably transfected cell lines were not favourable for the depletion process due to low responses with the agonist.

The antidepressant desipramine (DMI) reduced NMDA-evoked cation currents in acutely dissociated hippocampal neurons (Fig. 19a, b). Treatment of primary hippocampal neurons with 0.1mM MßCD for 12h did not significantly affect NMDA/D-serine-evoked currents and also did not alter the inhibitory effect of DMI on these currents (Fig. 19b, c).

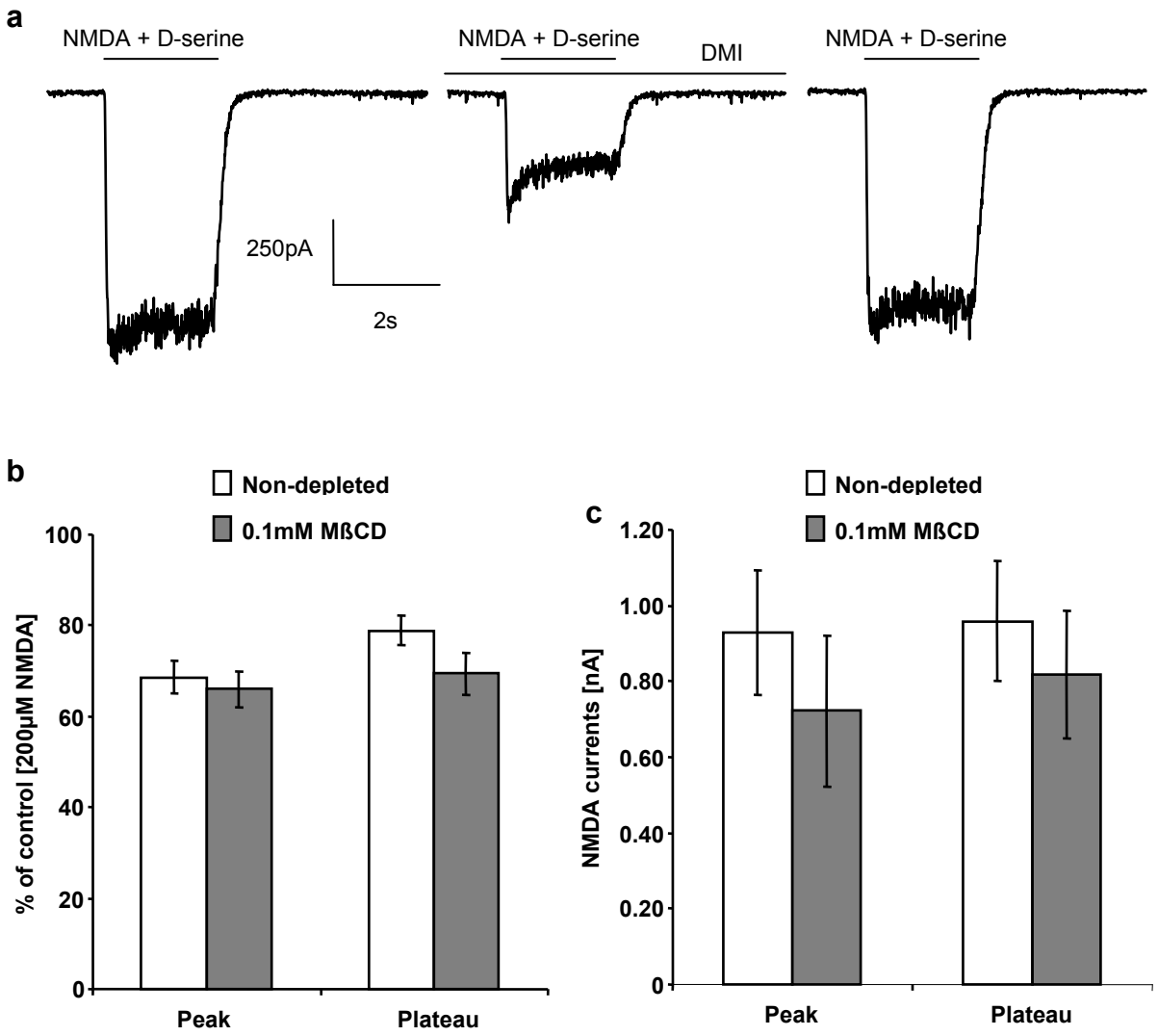

Fig.19. Effects of cholesterol depletion on NMDA receptor function and on the antagonistic effects of desipramine in hippocampal neurons. NMDA currents were recorded in the whole-cell voltage-clamp configuration. 200µM NMDA and 5µM of the co-

agonist D-serine were applied for 2s in the absence or presence of 3µM desipramine (DMI). **(a)** Antagonistic effect of DMI on the NMDA receptor. Representative recordings before and after application of DMI and subsequent washout are shown. **(b)** Antagonistic effect of DMI after MßCD treatment. Cells were treated with 0.1mM MßCD for 12h before the recordings. Quantification of the effect of DMI on peak amplitude and plateau of NMDA-evoked currents in non depleted cells (white bars) and after treatment with 0.1mM MßCD for 12h (grey bars). n=9 independent experiments for each conditions and data are shown as mean±SEM% of "control" values obtained in absence of DMI (Peak=68.66±3.53%, Plateau=78.91±3.99%). DMI reduced peak amplitude and plateau to a similar extent in both experimental conditions. 0.1mM MßCD compared to non depleted cells: Peak=65.94±3.38% (p=0.142), Plateau=69.35±4.58% (p=0.079). **(c)** Treatment with MßCD (0.1mM) did not significantly affect NMDA-evoked currents in hippocampal neurons. Peak amplitude and plateau [nA] in non depleted cells (white bars) and after treatment with 0.1mM MßCD for 12h (grey bars) in the presence of 200µM NMDA and 5µM D-serine. n=9 independent experiments for each condition. Data are shown as mean±SEM of NMDA-induced cation currents [nA]. 0.1mM MßCD compared to control (Peak=0.93±0.16nA, Plateau=0.96±0.19nA): Peak=0.72±0.16nA (p=0.304), Plateau=0.82±0.17nA (p=0.321).

4.1.6 Supplementary data

The effects of depletion we observed on the different currents we recorded might come from a direct effect of the MßCD treatment. To exclude a pharmacological effect of MßCD and to make sure that these effects are solely caused by cholesterol depletion alone, MßCD and Simvastatin were acutely applied to N1E-115 cells (Fig. 20a, b). MßCD showed a concentration dependent acute effect.

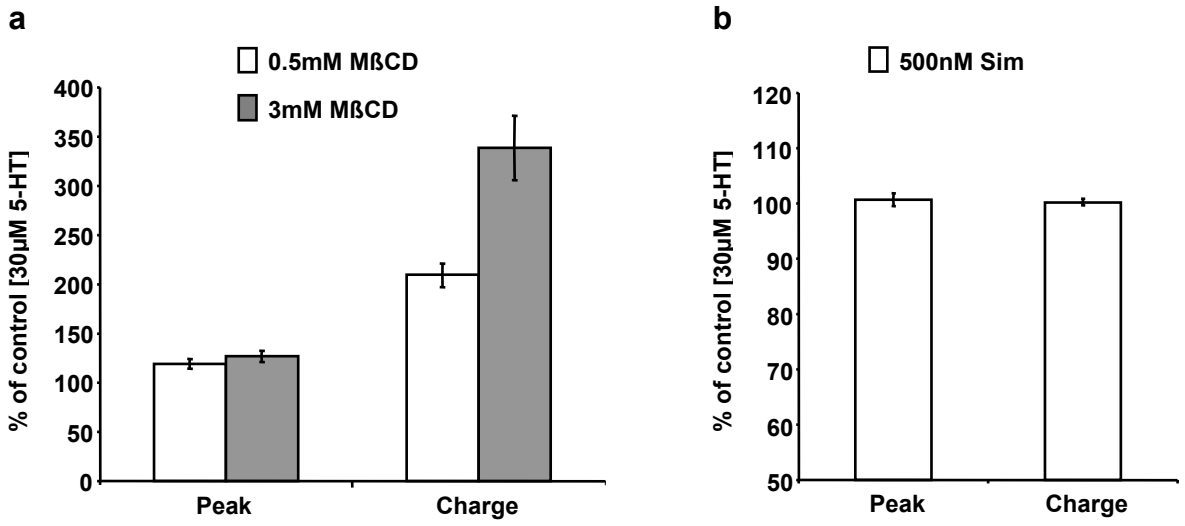

Fig.20. Acute effects of MßCD and Simvastatin (Sim) on serotonin-evoked currents in N1E-115 cells. 5-HT (30µM) was applied for 2s. Results are normalised to the maximum current induced by 30µM 5-HT application alone and presented as mean±SEM. n=3 independent experiments for each condition. **(a)** Acute application of MßCD dose-dependently potentiates 5-HT-evoked currents in N1E-115 cells. Peak amplitude and charge after 0.5mM MßCD (white bars) and 3mM MßCD (grey bars) treatments. 0.5mM MßCD compared to control: Peak=119.32±4.98% (p=0.111), Charge=209.23±11.83% (p=0.023); 3mM MßCD compared to control: Peak=127.06±5.83% (p=0.082), Charge=338.40±32.58% (p=0.035). **(b)** Acute application of 500nM Sim has no effect on serotonin-evoked currents in N1E-115 cells. Peak amplitude and charge after 500nM Sim application (white bars). 500nM Sim compared to control: Peak=100.72±1.17% (p=0.707), Charge=100.21±0.56% (p=0.817).

The depletion of N1E-115 cells with MßCD showed no significant changes in the pharmaceutical effects of Fluox and DMI. Additionally to these experiments, a HEK293 cell line stably transfected with 5-HT_3 receptor was used for a control experiment. DMI was applied after treatment of HEK293 cells with MßCD under the same conditions. As shown in the N1E-115 cells, the DMI effect was not altered after depletion (Fig. 21).

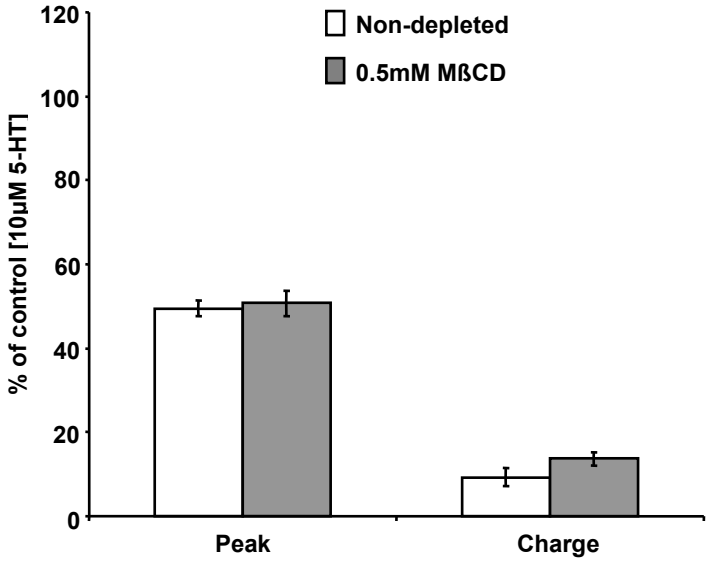

Fig.21. The modulation of serotonin-evoked currents by DMI is retained after MßCD treatment of HEK293 cells stably transfected with 5-HT_3 receptor. Cation currents were recorded in the whole-cell voltage-clamp configuration. 5-HT (10µM) was applied for 2s in the absence or presence of 10µM DMI. Antagonistic effect of DMI after MßCD treatment. Cells were treated with 0.5mM MßCD for 12h before the recordings. Quantification of the effect of DMI on peak amplitude and charge of serotonin-evoked currents in non depleted cells (white bars) and after treatment with 0.5mM MßCD for 12h (grey bars). n=7 independent

experiments for each condition and data are shown as mean±SEM% of “control” values obtained in absence of DMI. DMI reduced peak amplitude and charge to a similar extent than in N1E-115 cells in both experimental conditions. DMI effect in non depleted cells: Peak=49.49±1.85%, Charge=9.28±2.18%. 0.5mM MßCD compared to non depleted cells: Peak=50.69±2.95% (p=0.770), Charge=13.67±1.69% (p=0.193).

4.2 Effects of the antidepressant desipramine on synaptic plasticity related mechanisms

4.2.1 Acutely applied desipramine inhibits LTP

Previous studies have shown that desipramine (DMI induced a decrease in long-term potentiation (LTP) magnitude in rat hippocampal slices (Watanabe, Saito *et al.* 1993). Here the same kind of experiments were performed in acute hippocampal brain slices from CD1 mice. DMI also diminished, in a concentration dependent manner, CA1-LTP triggered by high frequency stimulus (HFS) of the Schaffer collaterals. Incubation of the slices for 1h prior HFS in DMI (3μM) decreased LTP magnitude by at least 60% (Fig. 22b), whereas incubation of the slices in 10μM DMI nearly abolished LTP (Fig. 22a, b).

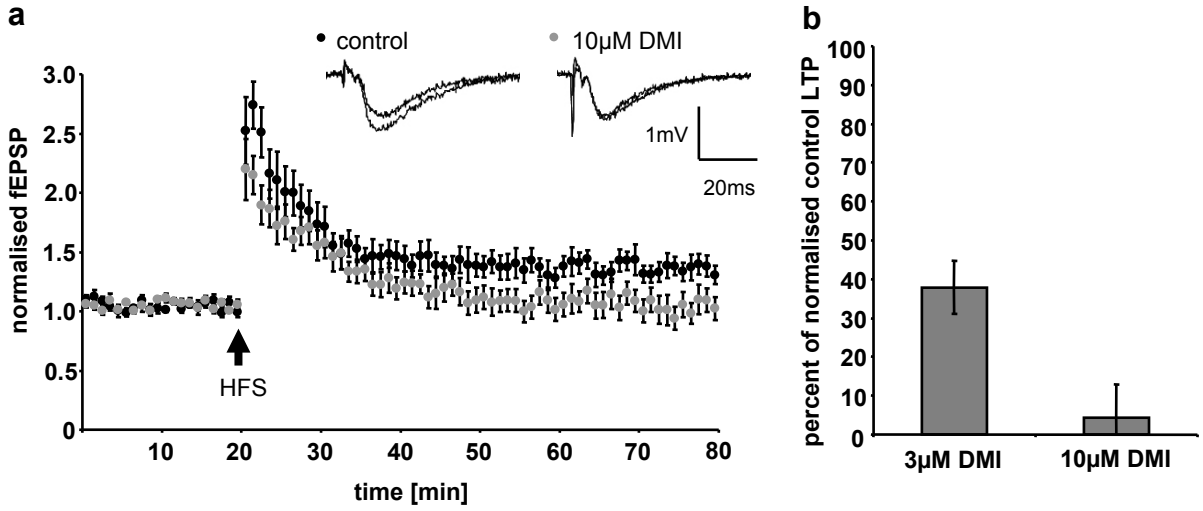

Fig.22. Inhibition of LTP by despiramine (DMI). (a) Graph illustrating LTP under control conditions (black) or after 1h of slice incubation prior to HFS in DMI (10μM grey). Field excitatory postsynaptic potentials (fEPSP) slope was recorded for 1h after HFS and slope values were normalized to the mean of the slope of the last 5min of baseline (before HFS). Representative fEPSPs before and after LTP induction for both conditions are presented above the graph. **(b)** Dose-dependent inhibition of LTP by DMI. The effect of LTP was reduced to 37.83 ± 6.83% (n=4, $p<0.001$) with 3μM DMI and nearly abolished with 10μM DMI (4.21 ± 8.60%, n=4, $p<0.001$). LTP magnitudes under DMI are shown as percent of LTP magnitude obtained for control slices, and data are shown as mean ± SEM%.

4.2.2 Influence of desipramine on the activity of pMAPK before and after LTP induction

In order to investigate the activation of the Mitogen-Activated Protein Kinase (MAPK) signalling pathway, hippocampal brain slices were stained with DAPI and a phospho-p44/42MAP (phosphor Extracellular-Regulated protein Kinase 1/2, pERK 1/2) antibody after 1h incubation with either DMI alone, after LTP induction, or after LTP induction after 1h of DMI treatment. Cells were counted in the *stratum pyramidale* (Pyr) and *stratum radiatum* (Rad) of the CA1 area at different time points after DMI treatment and LTP induction respectively. The number of pERK positive cells was normalized to the total cell number (=DAPI positive cells) in all conditions. To induce a maximal inhibition of LTP, DMI was used at 10µM concentration.

In brain slices incubated with DMI, the onset of pERK 1/2 activation was observed in Pyr after 15min of treatment and reached a maximum after 30min (Fig. 23a). After 1h of incubation in DMI, the number of pERK1/2-positive cells dropped down to basal level again (Fig. 23a). On the contrary, in the Rad of the CA1 subfield, no significant changes in the number of pERK 1/2-positive cell bodies could be observed along time (Fig. 23a). LTP induction caused a transient but steep increase in the number of pERK 1/2-positive cells 5min after HFS which dropped to basal level after 10min, whereas in the Pyr, the number of activated cells remained unchanged (Fig. 23b). Finally after 1h incubation of slices in DMI, LTP was abolished and the corresponding increase in pERK 1/2-positive cells in the Rad, induced by HFS, was completely blocked (Fig. 23c).

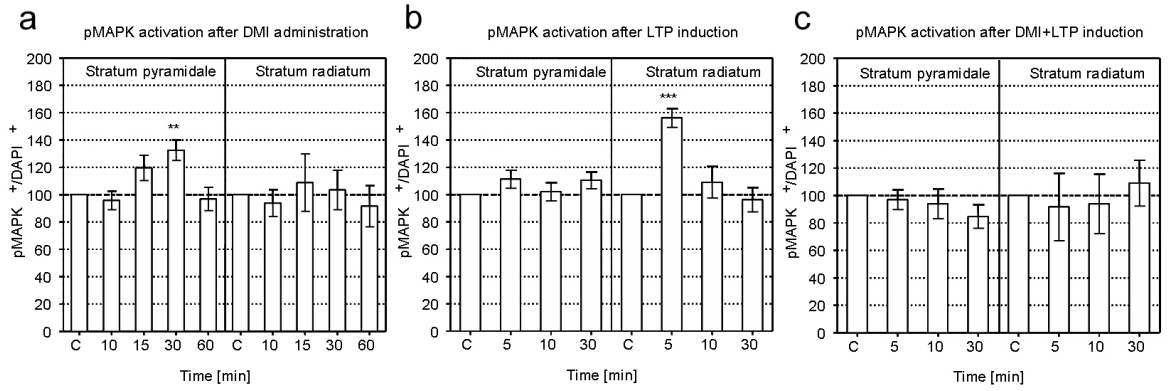

Fig.23. Quantification of the effect of LTP and DMI on the number of pERK 1/2-positive (pMAPK) cells in the Pyr and Rad of the CA1 subfield. The number of pERK 1/2-positive cell bodies was normalized to the total number of cells (DAPI staining) and expressed as mean ± SEM% of the number of cells in control condition **(a)** Acute brain slices incubated

with 10µM DMI showed an increase (19.5 ± 9.2%, n=4) in the number of pERK 1/2-positve cell bodies in the *stratum pyramidale* (Pyr) after 15 min of DMI incubation. This increase was maximal after 30min of incubation (32.5 ± 7.4%, n=4, p=0.003) and dropped down to basal level after 60min of incubation. In *stratum radiatum* (Rad), no significant changes have been observed. **(b)** After LTP induction, the number of pERK 1/2-positive cell bodies did not significantly change in Pyr, while a transient and steep increase (56 ± 6.9%, n=5, p<0.001) was observed in Rad 5min after HFS. **(c)** Pre-incubation of slices in DMI for 1h prior to LTP induction prohibited the increase in the number of pERK 1/2-positive cell bodies in the Rad after HFS and had overall no significant influence on the total number of pERK-positive cells (Pyr: p=0.549, Rad: p=0.9).

4.2.3 Modifications of neuronal activity in the CA1 subfield of the hippocampus, showed by *Arc* activation, by LTP and desipramine treatment

An increase in the number of activated neurons in CA1 Pyr after LTP induction could not be observed with pERK 1/2 immunostaining. To monitor LTP-induced neuronal activation and the effect of DMI on such activation, the neuronal activity marker *Arc* expression was studied using fluorescent *in situ* hybridization for *Arc* mRNA. The total cell number was determined by DAPI staining and *Arc*-positive cells by the cytosolic signal of the fluorescent probe directed against *Arc* mRNA.

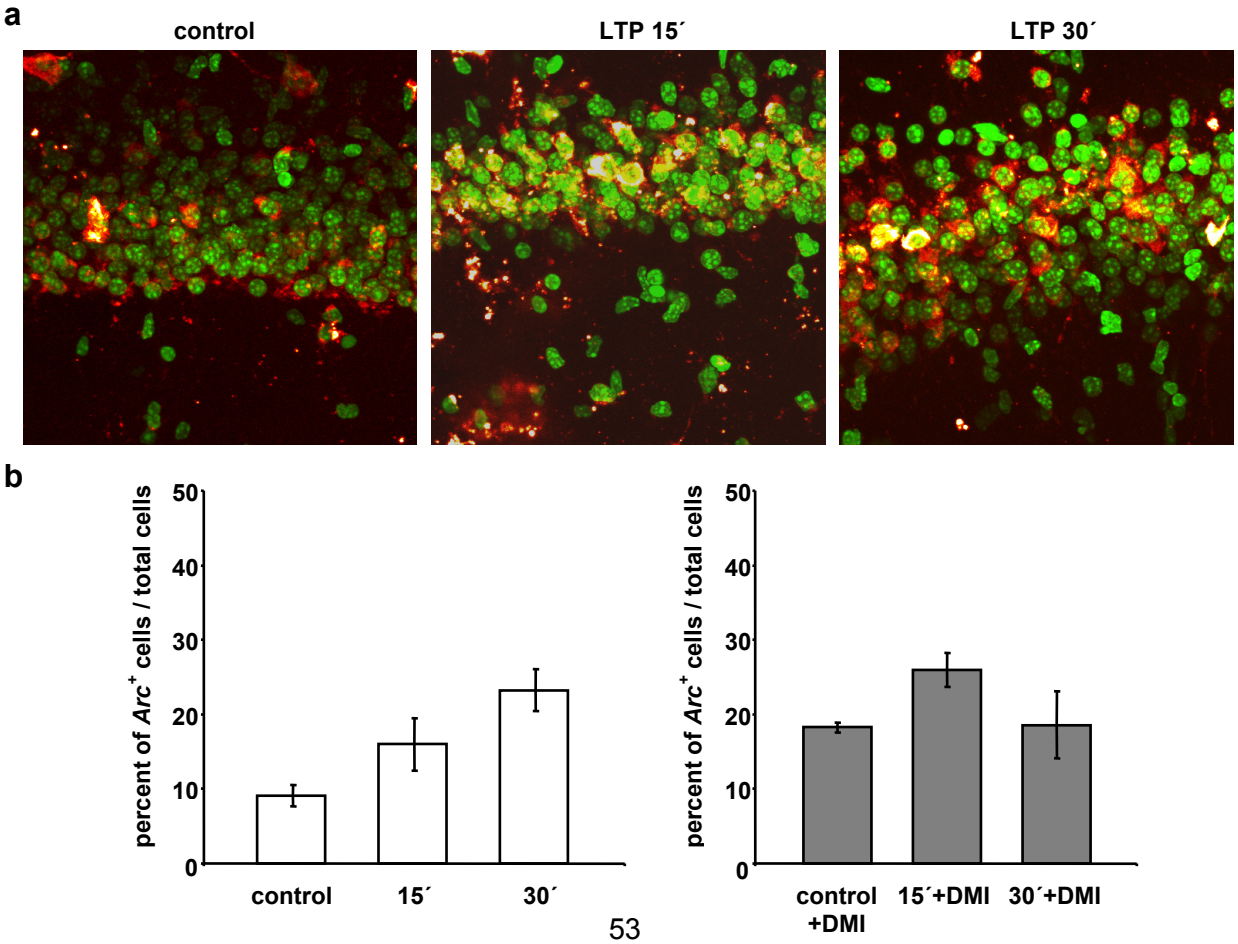

Fig.24. Neuronal activation before and after LTP induction in the presence or absence of DMI, measured by *Arc* mRNA expression. (a) Representative pictures of *in situ* hybridization showing *Arc* mRNA expression in the CA1 hippocampus before (control), 15min and 30min after LTP induction. For reasons of presentation “false” colours were used: DAPI staining (original blue) is shown in green, *Arc* mRNA probe (original red) is depicted in a merged colour channel ("orange"). n=4 independent experiment. **(b) Left panel:** Neuronal activation by counting of *Arc*-positive cells during baseline recording (alternating stimuli every 15s) is 9.1±1.4% while 15min after LTP induction 16.0±3.5% (p=0.018) cells showed Arc expression. 30min after LTP induction this number reached 23.3±2.9% (p<0.001) **Right panel:** Effect of DMI on LTP-induced neuronal activation. During baseline under DMI, neuronal activation is higher than in non-treated slices (control, left panel: 18.3±0.7%). 15min after HFS, the number of *Arc*-positive cells increased to 25.9±2.3% (p=0.003) but, on the contrary to non-treated slices, dropped down to basal level after 30min (18.7±4.5%, p=0.9). The number of *Arc*-positive cells is normalized to the total number of cells (DAPI cell count). n=4 independent experiments.

Arc mRNA expression increased after LTP induction and the number of *Arc*-positive cells was doubled 30min after HFS compared to before HFS (Fig. 24a, b left panel). After 1h of DMI treatment and prior to LTP induction, the number of *Arc*-positive neurons is significantly higher than in non-treated slices (Fig. 24b, right panel). The LTP-induced increase in the number of Arc-positive neurons can still be observed (25% percent increase) 15min after HFS in slices incubated in DMI. However this increase disappeared 30min after HFS, and the number of *Arc*-positive neurons dropped down to basal levels, contrary to non-treated slices (Fig. 24b).

4.2.4 Effect of desipramine on neuron-astrocyte signalling *via* phosphorylation of EphA4 receptor (preliminary data)

The activation of pERK 1/2 in *stratum radiatum* after LTP induction indicates a possible involvement of a mechanism that is linked to the communication between astrocytes and neurons. Indeed, astrocytes are mainly located in the stratum radiatum in the hippocampus where their processes embed the CA3-CA1 synapses, which are stimulated during LTP induction (Ventura and Harris 1999). EphrinA3 and the EphA4 receptor have been shown to promote this communication and play a major role during LTP (Filosa, Paixao *et al.* 2009). To investigate whether ADs could

influence this communication, DMI was acutely applied to brain slices for 1h, alone or prior to incubation of EphrinA3.

The phosphorylation of the EphA4 receptor was then analysed by immunoprecipitation of phosphorylated EphA4 from CA1 hippocampus extracts. Preliminary results might indicate decreased phosphorylation of the EphA4 receptor by the ligand EphrinA3 after DMI treatment.

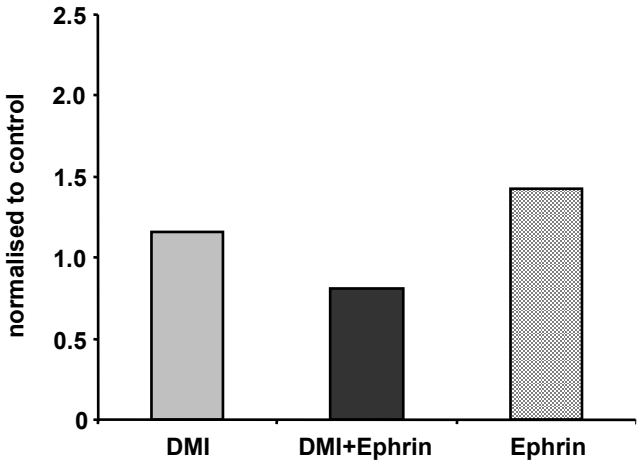

Fig.25. Phosphorylation of EphA4 receptor by its ligand EphrinA3 shown with immuno-precipitation in CA1 region of hippocampal slices. Preliminary results (mean of two experiments) showed a decreased phosphorylation (not significant) of EphA4 after 1h incubation with DMI. Further experiments have to be performed.

5 Discussion

5.1 Impact of lipid raft integrity on ionotropic receptor function and its modulation by psychopharmacological compounds

The influence of lipid raft integrity on ligand-gated ion channel function has been shown for a variety of receptors (for review see Allen *et al.*, 2007). Lipid rafts are important for the maintenance of synaptic morphology and density, whereas lipid raft disruption, for example, reduced the stability of lipid raft-associated surface AMPA receptors in rat hippocampal neurons (Hering, Lin *et al.* 2003). Specifically, $GABA_A$ and nicotinic acetylcholine receptor function has been shown to be affected by the cholesterol content of the membrane (Sooksawate and Simmonds 2001; Barrantes 2007). Cholesterol depletion resulted in a reduced ligand binding and G-protein coupling of the serotonin 1A ($5\text{-}HT_{1A}$) receptor in bovine hippocampal membranes (Pucadyil and Chattopadhyay 2004). Moreover in rat dorsal root ganglia, electrical currents through the vanilloid receptor subtype 1 (TRPV1) were diminished after cholesterol depletion (Liu, Huang *et al.* 2006). Since some ADs are enriched in lipid rafts in low buoyant densitiy (LBD) fractions of sucrose density gradients, and their concentrations within these fractions are related to their antagonistic potency against $5\text{-}HT_3$ receptors, it might be hypothesized that lipid raft integrity is an important determinant for the allosteric modulation of certain ionotropic receptors by psychopharmacological compounds (Eisensamer, Uhr *et al.* 2005).

In this work the impairment of lipid raft integrity was accomplished by the cholesterol depleting agent MßCD in N1E-115 mouse neuroblastoma cells and HEK 293 cells stably expressing the human $5\text{-}HT_{3A}$ receptor, as well as WSS1-cells expressing the $GABA_A$ receptor and hippocampal neurons containing the NMDA receptor. The experimental conditions used in this work still allowed the characterization of serotonin-evoked cation currents through $5\text{-}HT_3$ receptors, although the cholesterol content of cell membranes was shown to be reduced to less than 50% by this method (Nothdurfter, Tanasic *et al.* 2010). The same parameters were used for the depletion of WSS1 cells, but had to be changed (decreased concentration of MßCD) for hippocampal neurons due to reasons of cell viability.

The issue of ‘lipid raft disruption’ by MßCD is controversially discussed since no firm guidelines exist to properly prove lipid raft disruption. Only partial removal of cholesterol from cell membranes can be achieved by MßCD under conditions that

retain cell viability (Kilsdonk, Yancey *et al.* 1995; Yancey, Rodrigueza *et al.* 1996; Christian, Haynes *et al.* 1997; London 2005). This is in line with the results of this work, though it would be advisable to refer to 'lipid raft impairment' rather than to complete 'lipid raft disruption'. However, the existence of different raft populations with a different sensitivity to cholesterol depletion cannot be completely excluded.

Lipid raft impairment under our experimental conditions was verified by immunocytochemistry analysis of the membrane distribution of the lipid raft marker protein flotillin-1 in N1E-115 cells. The treatment with 0.5mM MßCD caused a more diffuse membrane distribution of flotillin-1 together with an apparent signal enhancement of flotillin-1, which was not due to a higher expression of the protein but might reflect an increased availability of the flotillin-1 epitope for detection by the respective antibody (Nothdurfter, Tanasic *et al.* 2010). Thus, cholesterol depletion affects lipid raft integrity, but a complete lipid raft disruption remains questionable.

To shift flotillin-1 to the high buoyant densitiy (non-raft) fractions of sucrose density gradients a 15-fold higher concentration of MßCD would be required, which does not allow whole-cell voltage-clamp recordings anymore, due to severe cell damage. These results suggest that impairment of lipid rafts by cholesterol depletion is not necessarily detected by sucrose density gradients under experimental conditions needed to perform functional investigations such as electrophysiological recordings (Nothdurfter, Tanasic *et al.* 2010).

With regard to 5-HT_3 receptor function, a significant reduction in peak amplitude and charge of serotonin-evoked currents were observed after cholesterol depletion with 0.5mM MßCD, in spite of a prolongation of receptor desensitization and deactivation (Fig. 12). Depletion with Sim, by inhibiting the synthesis of endogenous cholesterol, is considered as an alternative approach for lipid raft impairment and exerted similar effects on serotonin-evoked currents (Table 1) (Sjogren, Hamblin *et al.* 2006; Ponce, de la Ossa *et al.* 2008).

To rule out potential direct pharmacological effects of MßCD on serotonin-evoked currents, independently from cholesterol depletion, 0.5mM and 3mM MßCD, as well as 500nM Sim were applied acutely to N1E-115 cells (Fig. 20). Although MßCD had only little effect on the peak amplitude, it prolonged the decay for deactivation and thus had a huge impact on the charge parameter. The acute application of Sim had no effect at all (Fig. 20b). This suggests that the pronounced

reduction of the peak amplitude and prolonged desensitisation after cholesterol depletion by MßCD was indeed due to cholesterol depletion.

To partially counteract cholesterol depletion N1E-115 cells were kept in medium supplemented with 10% FCS before and during MßCD. The effects of MßCD on serotonin-evoked currents under these experimental conditions were far less pronounced and clearly distinguishable from those of cholesterol depletion without FCS (Fig. 12, Table 1). These findings support the hypothesis that the function of the 5-HT_3 receptor largely depends on the cholesterol content of the membrane, even if there is no complete raft disruption under cholesterol-depleted conditions (Nothdurfter, Tanasic *et al.* 2010). Nevertheless, lipid raft integrity might be important for the physiological function of this receptor in context with the colocalisation of psychopharmacological compounds and this ligand-gated ion channel in raft-like domains, as shown in sucrose density gradients (Eisensamer, Uhr *et al.* 2005).

Unexpectedly, the antagonistic potency of the ADs desipramine (DMI) and fluoxetine (Fluox) on serotonin-evoked currents was retained following cholesterol depletion by either MßCD or Sim, in spite of a pronounced overall reduction of serotonin-evoked currents. This is further supported by the observation that both DMI and Fluox accelerated receptor desensitization even under conditions of cholesterol depletion (Fig. 13+14, Table 2+3). Similar results were obtained for DMI, using cloned HEK 293 cells with a stably transfected 5-HT_3 receptor (Fig. 21).

In contrast to the findings obtained with sucrose density gradients, immuno-cytochemistry revealed only a coincidental degree of colocalization of the 5-HT_3 receptor and flotillin-1 in the absence of cholesterol-depleting agents (Nothdurfter, Tanasic *et al.* 2010). In conclusion only a minor proportion of 5-HT_3 receptors could be constantly present in lipid rafts. However this minor proportion of 5-HT3 seems to be ideally located to interact with ADs, which are preferentially enriched in lipid rafts.

Because lipid rafts are thought to be highly dynamic structures, finding whether a distinct protein is raft-associated or not is a technical challenge, which largely relies on the respective technique employed. Several studies have reported a lower rate of colocalization of ‘raft candidate proteins’ and even an underestimation of raft association by means of immunocytochemistry when compared with biochemical methods such as sucrose density gradient centrifugation (Kusumi and Suzuki 2005; Nothdurfter, Tanasic *et al.* 2010).

These conflictive findings may be due to the heterogeneity of the experimental protocols used to detect raft-like domains along with raft-associated proteins in the different studies. A combination of different methodological approaches would probably give a more realistic picture than just relying on a single method.

The results of this work challenged the hypothesis that 5-HT_3 receptor integration within lipid rafts is an indispensable prerequisite for the non-competitive antagonistic effects of antidepressants or antipsychotics and that these effects are predominantly conferred through an interaction of 5-HT_3 receptors with raft-like domains (Eisensamer, Rammes *et al.* 2003; Rammes, Eisensamer *et al.* 2004). The observation that the functional antagonistic effects of ADs on the 5-HT_3 receptor are retained in spite of cholesterol depletion, together with the results from immunocytochemistry, argue against the hypothesis that receptor integration within lipid rafts is the major determinant for these modulatory effects (Nothdurfter, Tanasic *et al.* 2010).

In conclusion, it could not be determined if 5-HT_3 receptors appear to be raft or non-raft associated within a dynamic system. Moreover, lipid raft integrity did also not seem to be a prerequisite for the allosteric modulation of this ligand-gated ion channel by the ADs desipramine and fluoxetine.

With regard to lipid raft association, the α_1 subunit of $GABA_A$ receptors was shown to be almost exclusively associated with lipid rafts after purification from rat cerebellar granule cells with the detergent Brij 98 (Dalskov, Immerdal *et al.* 2005). After solubilisation of rat forebrain tissue with Triton X-100, distinct $GABA_A$ receptor subunit combinations have been allocated to different cell membrane compartments. α and β subunits in the absence of γ subunits, which might represent extrasynaptic receptors, have been detected in detergent-resistant membranes/lipid rafts. In contrast, synaptic assemblies containing α and β subunits together with the γ_2 subunit showed only negligible lipid raft association (Li, Serwanski *et al.* 2007).

The NR1A subunit of the NMDA receptor has been found in non-raft membrane fractions of rat forebrain, when using an Optiprep gradient without detergent solubilisation (Wu, Butz *et al.* 1997). Furthermore, a non raft-association has been reported for the NR1, NR2A and NR2B subunits using Triton X-100 as a detergent (Suzuki, Ito *et al.* 2001). In contrast Bessoh *et al.* found lipid-raft association of the NR2A subunit under detergent-containing conditions, whereas the

NR2B subunit in rat brain tissue shifted from postsynaptic densities to lipid rafts with increasing age (Besshoh, Chen *et al.* 2007). A study by Ponce et al. suggested an important role of lipid raft integrity for NMDA receptor function, showing that the reduction of cholesterol levels by simvastatin might protect from NMDA-induced neuronal damage by reducing the association of the NR1 subunit with lipid rafts (Ponce, de la Ossa *et al.* 2008).

In a study of Nothdurfter *et al.*, the use of Triton X-100 as detergent shifted NMDA and $GABA_A$ receptor subunits to the HBD fractions of sucrose gradients. However, when using a detergent-free protocol, a much more differential distribution pattern of ionotropic receptors within the cell membrane could be observed. NMDA (NR1A subunit) and $GABA_A$ receptor (α_1, β_2, and γ_2 subunits) were distributed both over the LBD and the HBD fractions of the sucrose gradient (Nothdurfter *et al*., 2012, currently under revision). This data might indicate at least a partial localisation of both receptors in lipid rafts.

The tricyclic antidepressant DMI is a functional antagonist of NMDA receptor and, as mentioned before, was shown to colocalise in fractions containing lipid rafts (Sernagor, Kuhn *et al.* 1989; Watanabe, Saito *et al.* 1993; Eisensamer, Uhr *et al.* 2005; Szasz, Mike *et al.* 2007). Due to technical challenges, it was not possible to perform patch clamp experiments on cells transfected with NMDA receptor. The alternative to deplete acutely dissociated hippocampal neurons was only possible at a much lower concentration of MßCD due to reasons of cell viability. MßCD (0.1mM) was not sufficient to show a significant change in receptor modulation (Fig. 19). Methodological issues such as an insufficient amount of cell material also made a cholesterol assay unfeasable. The possible involvement of lipid rafts in NMDA receptor function and its modulation by DMI could not be shown.

The benzodiazepine diazepam (Diaz) colocalised with $GABA_A$ receptor subunits in HBD fractions, which supports the hypothesis that synaptic $GABA_A$ receptors, that are sensitive to benzodiazepines, are located predominantly within non-raft fractions (Li, Serwanski *et al.* 2007). Therefore lipid raft impairment should not alter the Diaz effect. Diaz markedly potentiated GABA-evoked currents, which was shown in previous studies (Davies, Hoffmann *et al.* 2000). Impairment of lipid raft integrity by MßCD diminished $GABA_A$ receptors currents per se, similarly to the results previously found for the 5-HT_3 receptor (Fig. 15) (Nothdurfter, Tanasic *et al.* 2010). Surprisingly the potentiating effect of Diaz appeared to be enhanced at lower

GABA concentrations under cholesterol depleting conditions (Fig. 17d). To investigate whether this effect was due to the diminished receptor response to GABA, shown by the GABA dose-response analysis in depleted cells (Fig. 15b), a dose-response relation of the Diaz effect had to be included. Although it was necessary to lower the concentration of MßCD for reasons of cell stability during dose-response measurements, the trend for an increased Diaz effect could be shown (Fig. 18a). This effect got lost when normalised to the Diaz response at maximal GABA concentrations (Fig. 18b). However, due to technical limitations owed to cholesterol depletion, Schild regression analysis could not be performed which would have provided definite clarity about the effects of benzodiazepines at the $GABA_A$ receptor under conditions of cholesterol depletion (Nothdurfter *et al* 2012, currently under revision). Additionally, the depleted cells showed still an increased potentiation (but not significant) by Diaz at 3mM GABA (Fig. 18c), maybe indicating that lipid raft integrity does not determine the modulatory potency of the benzodiazepine Diaz at the $GABA_A$ receptor.

In conclusion the cholesterol content of the cell membrane appears to be an important determinant for the overall function of the $GABA_A$ receptor, whereas the increased effectiveness by Diaz is more likely affected by the lowered agonist affinity caused by cholesterol depletion.

5.2 Acute effects of the antidepressant desipramine on synaptic plasticity-related mechanisms

Synaptic plasticity depends on a variety of mechanisms which contribute to the maintenance of neuronal networks and to the functionality of neuronal signal transduction. These mechanisms include for example remodelling of neuronal connections, regulation of synaptic receptor homeostasis *via* Arc protein, communication or crosstalk between neurons and astrocytes, and activation of intracellular signalling pathways, such as the MAPK pathway (Chowdhury, Shepherd *et al.* 2006; Bloomer, VanDongen *et al.* 2008; Klein 2009).

The second part of this work dealt with the potential influences and the immediate effects of the antidepressant DMI on these mechanisms. LTP is a cellular correlate of learning and memory and supposedly a synaptic plasticity-related mechanism (Bliss and Collingridge 1993), therefore an appropriate tool to investigate possible effects of DMI.

The dose-dependent inhibition of LTP by DMI has been previously shown (Watanabe, Saito *et al.* 1993) and is confirmed by the results in this work (Fig. 22). Several studies have pointed out the importance of the MAPK pathway in the CA1 region of the hippocampus during LTP and in synaptic plasticity. Especially ERK 1/2 has been shown to be activated after LTP induction and stimulation of NMDA receptors in the CA1 region. These findings led to the hypothesis that MAPK signalling pathways might regulate processes which are important for synaptic plasticity including second messenger generation (e.g. phospholipase A_2), cytoskeletal modulation (e.g. MAP2 protein) and transcription (e.g. Elk-1 transcription factor) (Brugg and Matus 1991; Lin, Wartmann *et al.* 1993; English and Sweatt 1996).

The results of this work showed a clear and steep increase in the number of pERK 1/2-positive cells immediately after LTP induction (Fig. 23) and verified the reported activation of MAPK. Interestingly the number of pERK1/2-positive cells only increased in the *stratum radiatum* of the CA1 area. This was not shown in former studies since mostly Western blot analysis was used to quantify the phosphorylation (*i.e.* activation) of ERK 1/2 pathway. After 1h of incubation with 10µM DMI, LTP induction was inhibited and the increase in the number of pERK 1/2-positive cells at the 5min time point could not be observed anymore as it was in untreated slices.

Other studies have shown the necessity of ERK 1/2 activation for LTP. The use of specific MEK (the upstream kinase of ERK 1/2) inhibitors (U0126 and PD

98059), blocking ERK 1/2 phosphorylation, prevented LTP induction in the CA1 region of the hippocampus (English and Sweatt 1996; English and Sweatt 1997; Rosenkranz, Frick *et al.* 2009). Rosenkranz *et al.* have suggested the blockade of ERK 1/2 activation to prevent changes in dendritic excitability, supposedly caused by its influence on A-type K^+ channels that are important regulators for this mechanism. They hypothesised that ERK 1/2 blockade lead to an indirect modulation of synaptic plasticity by functional changes in the dendrites, also referred to as dendritic plasticity (Rosenkranz, Frick *et al.* 2009).

Our findings suggest the involvement of cells located in *stratum radiatum* which seem to play a major role during LTP induction in regards of pERK1/2 activation, rather than pyramidal neurons. Nevertheless, an activation of this pathway in the *stratum pyramidale* cannot be excluded since only the number of additionally recruited cells and not the total pERK 1/2 amount in individual cells was quantified.

Interestingly during the incubation with DMI 1h before application of HFS, a time-dependent increase in the number of pERK 1/2-positive cells was also observed in the pyramidal layer, dropping down to basal level again at 60min of incubation time (Fig. 23a). Only few studies have shown an involvement of ERK1/2 signalling during treatment with ADs. In a recent publication, it has been observed that DMI acts as a signalling potentiator for the α_{2A} adrenergic receptor in combination with its specific agonist norepinephrine, by activating ERK 1/2 via G protein in a selective manner. They concluded that DMI may not interact in a classical agonist/antagonist relation but in a far more complex way than other associated ligands on this receptor (Cottingham, Jones *et al.* 2012). Duman *et al.* demonstrated that acute blockade of ERK 1/2 signalling resulted in a depressive-like phenotype and blocked behavioural actions of the antidepressants DMI and sertraline in mice. They postulated a relationship between the brain-derived growth factor (BDNF) signalling cascade, ERK 1/2 pathway and ADs (Duman, Schlesinger *et al.* 2007).

In *post mortem* tissue of patients that suffered from major depressive disorder, a significant increase in the expression of MAPK phosphatase-1, which acts as a negative regulator of MAPK, was found in hippocampal subfields (Duric, Banasr *et al.* 2010). This suggests that the activation of MAPK through DMI, as shown in this work, is substantial for its mode of action. However, the selectivity of activation and deactivation of ERK 1/2 in different regions and different states of neuronal activity remains yet unclear. One explanation may be the targeting of different cell types,

regulating various neuronal functions and thus activating different signalling pathways which rely on ERK 1/2.

The surprising result of no additional recruitement of pERK 1/2-positive cells in *stratum pyramidale* is conflictive with the postulate that NMDA and AMPA receptors activate gene expression *via* Ca^{2+} and ERK1/2 activation after LTP induction. It was demonstrated that NMDA receptor activation is a fundamental step for LTP induction, and ERK 1/2 is an important mediator of NMDA-induced gene transcription (Rao, Pintchovski *et al.* 2006; Tzingounis and Nicoll 2006). DMI is a potent NMDA-evoked current inhibitor as shown in this work (Fig. 19a, b) and previous studies (Tohda, Urushihara *et al.* 1995; Kiss, Szasz *et al.* 2012). This suggests that the acute inhibition of LTP observed here is due to a blockade of NMDA receptor after incubation with DMI 1h prior to HFS. Nevertheless, mRNA expression of *Arc* is increased during baseline time points as well as after LTP induction following incubation with DMI (Fig. 24b, right panel). This might be in conflict with the hypothesis of an *Arc*-mediated regulation of synapse formation, growth and stabilisation *via* NMDA-dependent activation of ERK 1/2 in neuronal cells (Fig. 26).

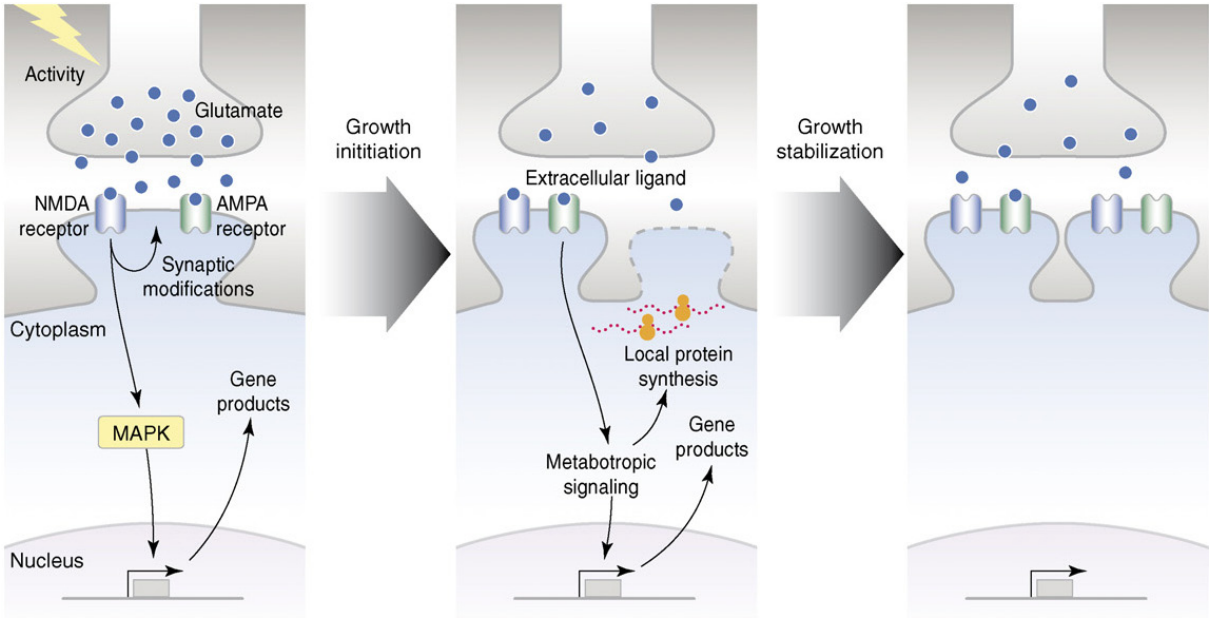

Fig.26. NMDA and AMPA receptors regulate synapse formation, growth and stabilisation. During bouts of synaptic activity, NMDA receptors activate signalling cascades, leading to modifications of the stimulated synapse and activation of MAPK and nuclear gene expression. Nascent gene products promote the formation of new synapses , represented as a second dendritic spine apposed to the presynaptic terminal. In this model, signalling by synaptic AMPA receptors regulates transcription and dendritic mRNA

translation, thereby promoting the growth and stabilization of the newly formed spine (Rao, Pintchovski *et al.* 2006).

Several studies have shown that Arc is able to affect AMPA receptors trafficking by directly interacting with the endocytotic machinery (Chowdhury, Shepherd *et al.* 2006). AMPA receptors present a highly dynamic motility at the cell surface and undergo rapid shuffling between the plasma membrane and internal recycling pools (Zhang, Etherington *et al.* 2012). LTP, as well as LTD, involves the regulation of exo- and endocytosis of AMPARs respectively (Shepherd, Rumbaugh *et al.* 2006).

Arc overexpression in cultures of hippocampal neurons and in slices result in a downregulation and accelerated endocytosis of surface AMPARs. The exact molecular mechanism and the role of *Arc*/ARC in the control of AMPAR homeostasis still remain unknown. Neither ARC nor the associated proteins endophilin and dynamin interact directly with AMPA receptors. It is also not clear how Arc can influence the function of the endophilin and dynamin complex, even though the possibility that the catalysis of endosome formation mediated by *Arc* exist. *Arc*/ARC seems to act as a modulator of specifically localized or concentrated endocytotic proteins at sites where AMPA receptors endocytosis can occur (Shepherd and Bear 2011).

Until now, only few data on the influence of ADs on *Arc* expression have been published. The increase of *Arc* mRNA expression after 1h of DMI treatment is in favour of an acute effect of this AD. That questions the argument in a work of Pei *et al.* from 2003 where they rule out an acute activation of *Arc* by DMI (Pei, Zetterstrom *et al.* 2003). This may be on account of the method they used: a single intraperitoneal injection of DMI in rats and an analysis of *Arc* mRNA by means of *in situ* hybridisation 18h later. This experimental design might not be suitable to represent the "acute" effects of an antidepressant on the activation of an IEG such as the method used in this work.

The regulation of neuronal plasticity is one of *Arc*'s main functions and it seems that a persistent increase in neuronal activity is compensated by scaling down AMPA receptors, as a result of an increase in ARC protein. On the contrary, a persistent decrease in neuronal activity is compensated by scaling up AMPA receptors under conditions of low network activity and scaling down AMPA receptors under conditions of increased network excitability (Turrigiano 2008). This underlines

the hypothesis of a very sensitive feedback mechanism regulating AMPA and NMDA receptor homeostasis and *Arc* expression in a bidirectional way. Moreover, it may explain the observed downregulation of *Arc* mRNA after 15min of LTP in slices treated with DMI (Fig. 24b, right panel).

Activation of NMDA receptors and/or voltage-sensitive calcium channels induces a rapid synthesis of *Arc* mRNA while the activation of metabotropic glutamate receptors (mGluRs) generates a delayed increase in *Arc* transcription after 1-2h (Park, Park *et al.* 2008). In conclusion, *Arc* may be activated by more than one signalling pathway and at different time points, depending on which pathway is stimulated. A direct link between *Arc* function and LTP maintenance has yet to be made. It is still possible that *Arc* is important for LTP stabilisation in an indirect way that may be a result of other homeostatic processes. This could also be an explanation for the finding that DMI shows a potentiating effect on LTP after 7 days of treatment in rats (Levkovitz, Grisaru *et al.* 2001). The initial and supposed steady increase in *Arc* expression under DMI incubation may act as a compensatory effect for the DMI-mediated inhibition of NMDA receptors and the consequential acute inhibition of LTP.

Nevertheless, these results suggest that maintenance of LTP requires sustained *Arc* mRNA synthesis during a specific time window and DMI is acutely affecting the course of events involved in this mechanism.

5.3 Summary and future outlook

The results of this work show once more that the mode of action of ADs is still a complex topic where a lot of questions remain unanswered. The involvement of molecular targets such as lipid rafts and their possible association with specific ligand-gated ion channels still remain disputable. In this work, it was shown that experiments on the modulation and targeting of receptors supposedly embedded in raft-like domains by psychopharmacological compounds are a methodological challenge. Due to the heterogeneity of the methods used in analysis and detection of lipid rafts in the scientific community, it is difficult to approach this field of study from a correct point of view. Electrophysiological methods, as used in this work, seemed not usable to detect changes in modulatory effects of the antidepressants DMI and Fluox, or the benzodiazepine Diaz. Nevertheless, the importance of cholesterol content for

receptor function was proven. This given fact together with the assumption that lipid rafts consist in much higher cholesterol content than the rest of the cell membrane can imply that the general function of ligand-gated ion channels, localised in lipid rafts, may be affected. Hence, the effect of psychopharmacological compounds on these raft-located receptors differs in comparison to non-raft receptors.

Until now, basic pharmacological research does not take in account that receptors located in cell membrane compartments with a different lipid composition might have different mode of action. Even though, some studies have shown the involvement of lipid rafts in neurological and psychiatric diseases, the conflictive findings of the localisation of some receptors in raft-like domains challenge the reliability of these results (Allen, Halverson-Tamboli *et al.* 2007). It would be necessary to standardise lipid raft imaging and analysis to include this important factor into the research in drug development. This, however, would only be possible with the use of new and advanced techniques giving reliable and reproducible results. Furthermore, it would be interesting if certain cell types show differences in lipid raft abundance and if this may vary in subjects suffering from mental disorders or other diseases.

Antidepressants are known to acutely increase synaptic concentrations of monoamines, but clinical efficacy requires several weeks of daily and continuous treatment, suggesting that time-dependent neural adaptation, perhaps induced by acute synaptic actions, are important for therapeutic efficacy (Duman and Monteggia 2006).

Acute effects of DMI on synaptic plasticity-related mechanisms such as activation of ERK 1/2 and *Arc* signalling pathway during LTP were chosen as an experimental design to investigate new potential targets or a link between known mechanisms influenced by ADs. Although a number of studies showed the influence of ADs, such as DMI, on the activation of MAPK (see previous chapter) a more detailed inspection upon their activation patterns has yet to be made. Most studies still use Western blot analysis which may depict a general activation, but is considered as a "crude" method. For example, it is only possible to differentiate between areas in the brain that can be isolated by manual preparation. In addition, a distinction between the different cell types expressing pERK 1/2 is not possible with this method.

In this work, LTP induction and application of DMI produced a very complex activation pattern of ERK 1/2 in different regions of CA1 in the hippocampus. While

DMI alone increased the number of pERK 1/2-positive cells in the *stratum pyramidale*,it abolished the HFS-induced activation of ERK 1/2 in the *stratum radiatum*. This may lead to the hypothesis of different cell types targeted by DMI and responsible for different functions during synaptic plasticity. A possible influence of astrocytes cannot be ruled out as they are the most abundant cell type in *stratum radiatum* (Ventura and Harris 1999). Indeed, this may be very likely since astrocytes are shown to become more and more important in the field of synaptic plasticity regulation (Hamilton and Attwell 2010). For a clear analysis, the discrimination between neuronal and glial cells has to be made. A possible approach would be to use an immunofluorescence staining with neuronal markers, such as NeuN, and astrocytic markers, like S100ß and GFAP. Alternatively GFP-expressing cells could be used to ascertain the cell types activated during these processes. The next step would be to focus on the upstream mechanism that activates ERK 1/2, which may lead to the direct targets of DMI.

Basal levels of *Arc* mRNA were elevated after 1h of DMI treatment suggesting an effect on the transcription of this gene. As stated in the chapter above, Arc is a mediator of AMPA and NMDA receptor homeostasis (Shepherd, Rumbaugh *et al.* 2006; Turrigiano 2008). DMI has been shown to increase GluR1 levels in the hippocampus, indicating an increased trafficking of AMPA receptors (Martinez-Turrillas, Del Rio *et al.* 2005).

The activation of mGluRs can induce a delayed *Arc* transcription (1-2h) and DMI potentiates adrenergic receptor activity, both processes involving phosphorylation of ERK 1/2 (Shepherd and Bear 2011; Cottingham, Jones *et al.* 2012). This may be an explanation for the increase in basal levels of *Arc* mRNA and the activation of ERK 1/2 in the *stratum pyramidale* during DMI incubation. A more thorough investigation of *Arc* during this 1h has to be made. Incubation of slices with DMI alone and specific time points analysis of *Arc* mRNA expression, as performed for ERK 1/2, as well as a subsequent *in situ* analysis could exclude or even underline the involvement of mGluRs or α_{2A} adrenergic receptor. Furthermore, the results of this work speak for an ERK 1/2-independent activation of *Arc* in the neuronal layer of *stratum pyramidale* after LTP induction. However, as stated before, the method used shows only *a posteriori* recruited cells and gives no information about the total amount of pERK 1/2 in the cells. The mechanism of *Arc* induction, either through LTP or DMI, still remains

unclear, nevertheless the results presented provide a solid basis for further and deeper investigations.

As mentioned before, the involvement of astrocytes in these mechanisms cannot be excluded. They are thought to play many important and diverse roles in the CNS, including guiding development, regulating extracellular concentrations of ions, metabolites, and neurotransmitters, and supporting neuronal and synaptic function (Bushong, Martone *et al.* 2002). Astrocytes have also been shown to respond to glutamate released from synaptic terminals in the hippocampal CA1 region by increases in intracellular Ca^{2+} *via* the activation of metabotropic and ionotropic glutamate receptors expressed at their membrane (Porter and McCarthy 1996; Zhou and Kimelberg 2001). Preliminary results showed a possible influence of DMI on astrocyte-neuron communication by inhibiting the EphrinA3-mediated phosphorylation of EphA4. This recently discovered pathway may play a key role in immediate changes in synaptic plasticity and in the acute effects of ADs. Whether the blockade of pERK 1/2 in the *stratum radiatum* after DMI application is somehow connected to EphA4/EphrinA3 signalling has still to be investigated by additional experiments. This would be a novelty in ADs research and may add a whole new pathway to the mode of action of psychopharmacological drugs.

Although we supposedly know a lot of ADs, being the operator, and their possible targets, being the operands, the consequential equation and its solution remains a scientific matter yet to be elucidated.

6 References

Adams, J. P. and S. M. Dudek (2005). "Late-phase long-term potentiation: getting to the nucleus." Nat Rev Neurosci **6**(9): 737-743.

Allen, J. A., R. A. Halverson-Tamboli, et al. (2007). "Lipid raft microdomains and neurotransmitter signalling." Nat Rev Neurosci **8**(2): 128-140.

Allen, N. J. and B. A. Barres (2005). "Signaling between glia and neurons: focus on synaptic plasticity." Curr Opin Neurobiol **15**(5): 542-548.

Alme, M. N., K. Wibrand, et al. (2007). "Chronic fluoxetine treatment induces brain region-specific upregulation of genes associated with BDNF-induced long-term potentiation." Neural Plast **2007**: 26496.

Andersen, P. (2007). The hippocampus book. Oxford ; New York, Oxford University Press.

Anderson, W. W. and G. L. Collingridge (2001). "The LTP Program: a data acquisition program for on-line analysis of long-term potentiation and other synaptic events." J Neurosci Methods **108**(1): 71-83.

Barnes, N. M. and T. Sharp (1999). "A review of central 5-HT receptors and their function." Neuropharmacology **38**(8): 1083-1152.

Barrantes, F. J. (2007). "Cholesterol effects on nicotinic acetylcholine receptor." J Neurochem **103 Suppl 1**: 72-80.

Barres, B. A. (2008). "The mystery and magic of glia: a perspective on their roles in health and disease." Neuron **60**(3): 430-440.

Barria, A., D. Muller, et al. (1997). "Regulatory phosphorylation of AMPA-type glutamate receptors by CaM-KII during long-term potentiation." Science **276**(5321): 2042-2045.

Baumann, P., J. M. Gaillard, et al. (1983). "Relationships between brain concentrations of desipramine and paradoxical sleep inhibition in the rat." J Neural Transm **56**(2-3): 105-116.

Bergles, D. E. and C. E. Jahr (1998). "Glial contribution to glutamate uptake at Schaffer collateral-commissural synapses in the hippocampus." J Neurosci **18**(19): 7709-7716.

Besshoh, S., S. Chen, et al. (2007). "Developmental changes in the association of NMDA receptors with lipid rafts." J Neurosci Res **85**(9): 1876-1883.

Bianchi, M., J. J. Hagan, et al. (2005). "Neuronal plasticity, stress and depression: involvement of the cytoskeletal microtubular system?" Curr Drug Targets CNS Neurol Disord **4**(5): 597-611.

Birnstiel, S. and H. L. Haas (1991). "Acute effects of antidepressant drugs on long-term potentiation (LTP) in rat hippocampal slices." Naunyn Schmiedebergs Arch Pharmacol **344**(1): 79-83.

Bliss, T., G. Collingridge, et al. (2007). Synaptic plasticity in the hippocampus. The hippocampus book. P. Anderson, R. Morris, D. Amaral, T. Bliss and J. O´Keef, Oxford University Press**:** 343-474.

Bliss, T. V. and G. L. Collingridge (1993). "A synaptic model of memory: long-term potentiation in the hippocampus." Nature **361**(6407): 31-39.

Bliss, T. V. and T. Lomo (1973). "Long-lasting potentiation of synaptic transmission in the dentate area of the anaesthetized rabbit following stimulation of the perforant path." J Physiol **232**(2): 331-356.

Bloomer, W. A., H. M. VanDongen, et al. (2008). "Arc/Arg3.1 translation is controlled by convergent N-methyl-D-aspartate and Gs-coupled receptor signaling pathways." J Biol Chem **283**(1): 582-592.

Bourgin, C., K. K. Murai, et al. (2007). "The EphA4 receptor regulates dendritic spine remodeling by affecting beta1-integrin signaling pathways." J Cell Biol **178**(7): 1295-1307.

Bourne, J. N. and K. M. Harris (2008). "Balancing structure and function at hippocampal dendritic spines." Annu Rev Neurosci **31**: 47-67.

Bramham, C. R., M. N. Alme, et al. (2010). "The Arc of synaptic memory." Exp Brain Res **200**(2): 125-140.

Bramham, C. R., P. F. Worley, et al. (2008). "The immediate early gene arc/arg3.1: regulation, mechanisms, and function." J Neurosci **28**(46): 11760-11767.
Breitinger, H. G., N. Geetha, et al. (2001). "Inhibition of the serotonin 5-HT3 receptor by nicotine, cocaine, and fluoxetine investigated by rapid chemical kinetic techniques." Biochemistry **40**(28): 8419-8429.
Brown, D. A. and J. K. Rose (1992). "Sorting of GPI-anchored proteins to glycolipid-enriched membrane subdomains during transport to the apical cell surface." Cell **68**(3): 533-544.
Brugg, B. and A. Matus (1991). "Phosphorylation determines the binding of microtubule-associated protein 2 (MAP2) to microtubules in living cells." J Cell Biol **114**(4): 735-743.
Bushong, E. A., M. E. Martone, et al. (2002). "Protoplasmic astrocytes in CA1 stratum radiatum occupy separate anatomical domains." J Neurosci **22**(1): 183-192.
Castren, E., V. Voikar, et al. (2007). "Role of neurotrophic factors in depression." Curr Opin Pharmacol **7**(1): 18-21.
Chowdhury, S., J. D. Shepherd, et al. (2006). "Arc/Arg3.1 interacts with the endocytic machinery to regulate AMPA receptor trafficking." Neuron **52**(3): 445-459.
Christian, A. E., M. P. Haynes, et al. (1997). "Use of cyclodextrins for manipulating cellular cholesterol content." J Lipid Res **38**(11): 2264-2272.
Citri, A. and R. C. Malenka (2008). "Synaptic plasticity: multiple forms, functions, and mechanisms." Neuropsychopharmacology **33**(1): 18-41.
Collingridge, G. L., S. J. Kehl, et al. (1983). "Excitatory amino acids in synaptic transmission in the Schaffer collateral-commissural pathway of the rat hippocampus." J Physiol **334**: 33-46.
Cottingham, C., A. Jones, et al. (2012). "Desipramine selectively potentiates norepinephrine-elicited ERK1/2 activation through the alpha2A adrenergic receptor." Biochem Biophys Res Commun **420**(1): 161-165.
Dagestad, G., S. D. Kuipers, et al. (2006). "Chronic fluoxetine induces region-specific changes in translation factor eIF4E and eEF2 activity in the rat brain." Eur J Neurosci **23**(10): 2814-2818.
Dalskov, S. M., L. Immerdal, et al. (2005). "Lipid raft localization of GABA A receptor and Na+, K+-ATPase in discrete microdomain clusters in rat cerebellar granule cells." Neurochem Int **46**(6): 489-499.
Davies, P. A., E. B. Hoffmann, et al. (2000). "The influence of an endogenous beta3 subunit on recombinant GABA(A) receptor assembly and pharmacology in WSS-1 cells and transiently transfected HEK293 cells." Neuropharmacology **39**(4): 611-620.
Davies, S. P., D. Carling, et al. (1989). "Tissue distribution of the AMP-activated protein kinase, and lack of activation by cyclic-AMP-dependent protein kinase, studied using a specific and sensitive peptide assay." Eur J Biochem **186**(1-2): 123-128.
Deckersbach, T., C. R. Savage, et al. (2005). "Spontaneous and directed application of verbal learning strategies in bipolar disorder and obsessive-compulsive disorder." Bipolar Disord **7**(2): 166-175.
Di Benedetto, B., M. Kallnik, et al. (2009). "Activation of ERK/MAPK in the lateral amygdala of the mouse is required for acquisition of a fear-potentiated startle response." Neuropsychopharmacology **34**(2): 356-366.
Donati, R. J., Y. Dwivedi, et al. (2008). "Postmortem brain tissue of depressed suicides reveals increased Gs alpha localization in lipid raft domains where it is less likely to activate adenylyl cyclase." J Neurosci **28**(12): 3042-3050.
Donati, R. J. and M. M. Rasenick (2005). "Chronic antidepressant treatment prevents accumulation of gsalpha in cholesterol-rich, cytoskeletal-associated, plasma membrane domains (lipid rafts)." Neuropsychopharmacology **30**(7): 1238-1245.
Duman, C. H., L. Schlesinger, et al. (2007). "A role for MAP kinase signaling in behavioral models of depression and antidepressant treatment." Biol Psychiatry **61**(5): 661-670.
Duman, R. S., J. Malberg, et al. (1999). "Neural plasticity to stress and antidepressant treatment." Biol Psychiatry **46**(9): 1181-1191.

Duman, R. S. and L. M. Monteggia (2006). "A neurotrophic model for stress-related mood disorders." Biol Psychiatry **59**(12): 1116-1127.
Duric, V., M. Banasr, et al. (2010). "A negative regulator of MAP kinase causes depressive behavior." Nat Med **16**(11): 1328-1332.
Eisensamer, B., G. Rammes, et al. (2003). "Antidepressants are functional antagonists at the serotonin type 3 (5-HT3) receptor." Mol Psychiatry **8**(12): 994-1007.
Eisensamer, B., M. Uhr, et al. (2005). "Antidepressants and antipsychotic drugs colocalize with 5-HT3 receptors in raft-like domains." J Neurosci **25**(44): 10198-10206.
English, J. D. and J. D. Sweatt (1996). "Activation of p42 mitogen-activated protein kinase in hippocampal long term potentiation." J Biol Chem **271**(40): 24329-24332.
English, J. D. and J. D. Sweatt (1997). "A requirement for the mitogen-activated protein kinase cascade in hippocampal long term potentiation." J Biol Chem **272**(31): 19103-19106.
Fan, P. (1994). "Inhibition of a 5-HT3 receptor-mediated current by the selective serotonin uptake inhibitor, fluoxetine." Neurosci Lett **173**(1-2): 210-212.
Filosa, A., S. Paixao, et al. (2009). "Neuron-glia communication via EphA4/ephrin-A3 modulates LTP through glial glutamate transport." Nat Neurosci **12**(10): 1285-1292.
Fletcher, S. and N. M. Barnes (1998). "Desperately seeking subunits: are native 5-HT3 receptors really homomeric complexes?" Trends Pharmacol Sci **19**(6): 212-215.
Frank, C., A. M. Giammarioli, et al. (2004). "Cholesterol perturbing agents inhibit NMDA-dependent calcium influx in rat hippocampal primary culture." FEBS Lett **566**(1-3): 25-29.
Fritschy, J. M. and I. Brunig (2003). "Formation and plasticity of GABAergic synapses: physiological mechanisms and pathophysiological implications." Pharmacol Ther **98**(3): 299-323.
Fu, W. Y., Y. Chen, et al. (2007). "Cdk5 regulates EphA4-mediated dendritic spine retraction through an ephexin1-dependent mechanism." Nat Neurosci **10**(1): 67-76.
Fukazawa, Y., Y. Saitoh, et al. (2003). "Hippocampal LTP is accompanied by enhanced F-actin content within the dendritic spine that is essential for late LTP maintenance in vivo." Neuron **38**(3): 447-460.
Fukunaga, K., L. Stoppini, et al. (1993). "Long-term potentiation is associated with an increased activity of Ca2+/calmodulin-dependent protein kinase II." J Biol Chem **268**(11): 7863-7867.
Georgotas, A., M. Krakowski, et al. (1982). "Controlled trial of zimelidine, a 5-HT reuptake inhibitor, for treatment of depression." Am J Psychiatry **139**(8): 1057-1058.
Gould, E. and P. Tanapat (1999). "Stress and hippocampal neurogenesis." Biol Psychiatry **46**(11): 1472-1479.
Greger, R. (1996). Membranpotential. "Lehrbuch der Physiologie", Klinke, R., Silbernagl, S. (Hrsg.). Stuttgart, Georg Thieme Verlag**:** 47-58.
Guirland, C., S. Suzuki, et al. (2004). "Lipid rafts mediate chemotropic guidance of nerve growth cones." Neuron **42**(1): 51-62.
Guzowski, J. F., G. L. Lyford, et al. (2000). "Inhibition of activity-dependent arc protein expression in the rat hippocampus impairs the maintenance of long-term potentiation and the consolidation of long-term memory." J Neurosci **20**(11): 3993-4001.
Halassa, M. M., T. Fellin, et al. (2007). "The tripartite synapse: roles for gliotransmission in health and disease." Trends Mol Med **13**(2): 54-63.
Hamill, O. P., A. Marty, et al. (1981). "Improved patch-clamp techniques for high-resolution current recording from cells and cell-free membrane patches." Pflugers Arch **391**(2): 85-100.
Hamilton, N. B. and D. Attwell (2010). "Do astrocytes really exocytose neurotransmitters?" Nat Rev Neurosci **11**(4): 227-238.
Hannon, J. and D. Hoyer (2008). "Molecular biology of 5-HT receptors." Behav Brain Res **195**(1): 198-213.
Hering, H., C. C. Lin, et al. (2003). "Lipid rafts in the maintenance of synapses, dendritic spines, and surface AMPA receptor stability." J Neurosci **23**(8): 3262-3271.

Hirschfeld, R. M. (2000). "History and evolution of the monoamine hypothesis of depression." J Clin Psychiatry **61 Suppl 6**: 4-6.
Hussy, N., W. Lukas, et al. (1994). "Functional properties of a cloned 5-hydroxytryptamine ionotropic receptor subunit: comparison with native mouse receptors." J Physiol **481 (Pt 2)**: 311-323.
Hyttel, J. (1977). "Neurochemical characterization of a new potent and selective serotonin uptake inhibitor: Lu 10-171." Psychopharmacology (Berl) **51**(3): 225-233.
Johnston, G. A. (1996). "GABAA receptor pharmacology." Pharmacol Ther **69**(3): 173-198.
Kandel, E. R., T. D. Albright, et al. (2000). "Neural science: a century of progress and the mysteries that remain." Neuron **25 Suppl**: S1-55.
Karson, C. N., J. E. Newton, et al. (1993). "Human brain fluoxetine concentrations." J Neuropsychiatry Clin Neurosci **5**(3): 322-329.
Kayser, M. S., M. J. Nolt, et al. (2008). "EphB receptors couple dendritic filopodia motility to synapse formation." Neuron **59**(1): 56-69.
Kilsdonk, E. P., P. G. Yancey, et al. (1995). "Cellular cholesterol efflux mediated by cyclodextrins." J Biol Chem **270**(29): 17250-17256.
Kiss, J. P., B. K. Szasz, et al. (2012). "GluN2B-containing NMDA receptors as possible targets for the neuroprotective and antidepressant effects of fluoxetine." Neurochem Int **60**(2): 170-176.
Klein, R. (2009). "Bidirectional modulation of synaptic functions by Eph/ephrin signaling." Nat Neurosci **12**(1): 15-20.
Klinke, R. (1996). Erregungsübertragung in Zellverbänden. "Lehrbuch der Physiologie", Klinke, R., Silbernagl, S. (Hrsg.). Stuttgart, Georg Thieme Verlag.
Krishnan, V. and E. J. Nestler (2008). "The molecular neurobiology of depression." Nature **455**(7215): 894-902.
Kubik, S., T. Miyashita, et al. (2007). "Using immediate-early genes to map hippocampal subregional functions." Learn Mem **14**(11): 758-770.
Kusumi, A. and K. Suzuki (2005). "Toward understanding the dynamics of membrane-raft-based molecular interactions." Biochim Biophys Acta **1746**(3): 234-251.
Lang, D. M., S. Lommel, et al. (1998). "Identification of reggie-1 and reggie-2 as plasmamembrane-associated proteins which cocluster with activated GPI-anchored cell adhesion molecules in non-caveolar micropatches in neurons." J Neurobiol **37**(4): 502-523.
Lankiewicz, S., N. Lobitz, et al. (1998). "Molecular cloning, functional expression, and pharmacological characterization of 5-hydroxytryptamine3 receptor cDNA and its splice variants from guinea pig." Mol Pharmacol **53**(2): 202-212.
Lee, H. K., M. Barbarosie, et al. (2000). "Regulation of distinct AMPA receptor phosphorylation sites during bidirectional synaptic plasticity." Nature **405**(6789): 955-959.
Levkovitz, Y., N. Grisaru, et al. (2001). "Transcranial magnetic stimulation and antidepressive drugs share similar cellular effects in rat hippocampus." Neuropsychopharmacology **24**(6): 608-616.
Li, X., D. R. Serwanski, et al. (2007). "Two pools of Triton X-100-insoluble GABA(A) receptors are present in the brain, one associated to lipid rafts and another one to the post-synaptic GABAergic complex." J Neurochem **102**(4): 1329-1345.
Liao, D., R. H. Scannevin, et al. (2001). "Activation of silent synapses by rapid activity-dependent synaptic recruitment of AMPA receptors." J Neurosci **21**(16): 6008-6017.
Lin, L. L., M. Wartmann, et al. (1993). "cPLA2 is phosphorylated and activated by MAP kinase." Cell **72**(2): 269-278.
Link, W., U. Konietzko, et al. (1995). "Somatodendritic expression of an immediate early gene is regulated by synaptic activity." Proc Natl Acad Sci U S A **92**(12): 5734-5738.
Liu, J., K. Fukunaga, et al. (1999). "Differential roles of Ca(2+)/calmodulin-dependent protein kinase II and mitogen-activated protein kinase activation in hippocampal long-term potentiation." J Neurosci **19**(19): 8292-8299.
Liu, M., W. Huang, et al. (2006). "TRPV1, but not P2X, requires cholesterol for its function and membrane expression in rat nociceptors." Eur J Neurosci **24**(1): 1-6.

London, E. (2005). "How principles of domain formation in model membranes may explain ambiguities concerning lipid raft formation in cells." Biochim Biophys Acta **1746**(3): 203-220.
Lopez de Heredia, M. and R. P. Jansen (2004). "mRNA localization and the cytoskeleton." Curr Opin Cell Biol **16**(1): 80-85.
Lu, W., H. Man, et al. (2001). "Activation of synaptic NMDA receptors induces membrane insertion of new AMPA receptors and LTP in cultured hippocampal neurons." Neuron **29**(1): 243-254.
Lyford, G. L., K. Yamagata, et al. (1995). "Arc, a growth factor and activity-regulated gene, encodes a novel cytoskeleton-associated protein that is enriched in neuronal dendrites." Neuron **14**(2): 433-445.
Lynch, M. A. (2004). "Long-term potentiation and memory." Physiol Rev **84**(1): 87-136.
Malenka, R. C., J. A. Kauer, et al. (1989). "An essential role for postsynaptic calmodulin and protein kinase activity in long-term potentiation." Nature **340**(6234): 554-557.
Malenka, R. C., B. Lancaster, et al. (1992). "Temporal limits on the rise in postsynaptic calcium required for the induction of long-term potentiation." Neuron **9**(1): 121-128.
Martin, S. J., P. D. Grimwood, et al. (2000). "Synaptic plasticity and memory: an evaluation of the hypothesis." Annu Rev Neurosci **23**: 649-711.
Martinez-Turrillas, R., J. Del Rio, et al. (2005). "Sequential changes in BDNF mRNA expression and synaptic levels of AMPA receptor subunits in rat hippocampus after chronic antidepressant treatment." Neuropharmacology **49**(8): 1178-1188.
Matsuzaki, M., N. Honkura, et al. (2004). "Structural basis of long-term potentiation in single dendritic spines." Nature **429**(6993): 761-766.
McHugh, T. J., K. I. Blum, et al. (1996). "Impaired hippocampal representation of space in CA1-specific NMDAR1 knockout mice." Cell **87**(7): 1339-1349.
Messaoudi, E., T. Kanhema, et al. (2007). "Sustained Arc/Arg3.1 synthesis controls long-term potentiation consolidation through regulation of local actin polymerization in the dentate gyrus in vivo." J Neurosci **27**(39): 10445-10455.
Miyamoto, E. (2006). "Molecular mechanism of neuronal plasticity: induction and maintenance of long-term potentiation in the hippocampus." J Pharmacol Sci **100**(5): 433-442.
Murai, K. K., L. N. Nguyen, et al. (2003). "Control of hippocampal dendritic spine morphology through ephrin-A3/EphA4 signaling." Nat Neurosci **6**(2): 153-160.
Nicolau, D. V., Jr., K. Burrage, et al. (2006). "Identifying optimal lipid raft characteristics required to promote nanoscale protein-protein interactions on the plasma membrane." Mol Cell Biol **26**(1): 313-323.
Nothdurfter, C., S. Tanasic, et al. (2010). "Impact of lipid raft integrity on 5-HT3 receptor function and its modulation by antidepressants." Neuropsychopharmacology **35**(7): 1510-1519.
Numberger , D. (1996). Patch-Clamp-Technik, Spektrum Akademischer Verlag GmbH, Heidelberg Berlin Oxford.
Park, S., J. M. Park, et al. (2008). "Elongation factor 2 and fragile X mental retardation protein control the dynamic translation of Arc/Arg3.1 essential for mGluR-LTD." Neuron **59**(1): 70-83.
Pasquale, E. B. (2008). "Eph-ephrin bidirectional signaling in physiology and disease." Cell **133**(1): 38-52.
Pei, Q., T. S. Zetterstrom, et al. (2003). "Antidepressant drug treatment induces Arc gene expression in the rat brain." Neuroscience **121**(4): 975-982.
Pike, L. J. (2003). "Lipid rafts: bringing order to chaos." J Lipid Res **44**(4): 655-667.
Pike, L. J. (2004). "Lipid rafts: heterogeneity on the high seas." Biochem J **378**(Pt 2): 281-292.
Pines, M., A. A. Oplinger, et al. (2005). Inside the cell. Bethesda, Md.?, U.S. Dept. of Health and Human Services, Public Health Service, National Institutes of Health, National Institute of General Medical Sciences.

Pita-Almenar, J. D., M. S. Collado, et al. (2006). "Different mechanisms exist for the plasticity of glutamate reuptake during early long-term potentiation (LTP) and late LTP." J Neurosci **26**(41): 10461-10471.
Plath, N., O. Ohana, et al. (2006). "Arc/Arg3.1 is essential for the consolidation of synaptic plasticity and memories." Neuron **52**(3): 437-444.
Ponce, J., N. P. de la Ossa, et al. (2008). "Simvastatin reduces the association of NMDA receptors to lipid rafts: a cholesterol-mediated effect in neuroprotection." Stroke **39**(4): 1269-1275.
Porter, J. T. and K. D. McCarthy (1996). "Hippocampal astrocytes in situ respond to glutamate released from synaptic terminals." J Neurosci **16**(16): 5073-5081.
Pucadyil, T. J. and A. Chattopadhyay (2004). "Cholesterol modulates ligand binding and G-protein coupling to serotonin(1A) receptors from bovine hippocampus." Biochim Biophys Acta **1663**(1-2): 188-200.
Ramirez-Amaya, V., A. Vazdarjanova, et al. (2005). "Spatial exploration-induced Arc mRNA and protein expression: evidence for selective, network-specific reactivation." J Neurosci **25**(7): 1761-1768.
Rammes, G., B. Eisensamer, et al. (2004). "Antipsychotic drugs antagonize human serotonin type 3 receptor currents in a noncompetitive manner." Mol Psychiatry **9**(9): 846-858, 818.
Rao, V. R., S. A. Pintchovski, et al. (2006). "AMPA receptors regulate transcription of the plasticity-related immediate-early gene Arc." Nat Neurosci **9**(7): 887-895.
Reeves, D. C. and S. C. Lummis (2006). "Detection of human and rodent 5-HT3B receptor subunits by anti-peptide polyclonal antibodies." BMC Neurosci **7**: 27.
Rial Verde, E. M., J. Lee-Osbourne, et al. (2006). "Increased expression of the immediate-early gene arc/arg3.1 reduces AMPA receptor-mediated synaptic transmission." Neuron **52**(3): 461-474.
Rodriguez, J. J., H. A. Davies, et al. (2005). "Long-term potentiation in the rat dentate gyrus is associated with enhanced Arc/Arg3.1 protein expression in spines, dendrites and glia." Eur J Neurosci **21**(9): 2384-2396.
Rosenkranz, J. A., A. Frick, et al. (2009). "Kinase-dependent modification of dendritic excitability after long-term potentiation." J Physiol **587**(Pt 1): 115-125.
Sakimura, K., T. Kutsuwada, et al. (1995). "Reduced hippocampal LTP and spatial learning in mice lacking NMDA receptor epsilon 1 subunit." Nature **373**(6510): 151-155.
Schildkraut, J. J. (1965). "The catecholamine hypothesis of affective disorders: a review of supporting evidence." Am J Psychiatry **122**(5): 509-522.
Sernagor, E., D. Kuhn, et al. (1989). "Open channel block of NMDA receptor responses evoked by tricyclic antidepressants." Neuron **2**(3): 1221-1227.
Sheng, M. and M. E. Greenberg (1990). "The regulation and function of c-fos and other immediate early genes in the nervous system." Neuron **4**(4): 477-485.
Shepherd, J. D. and M. F. Bear (2011). "New views of Arc, a master regulator of synaptic plasticity." Nat Neurosci **14**(3): 279-284.
Shepherd, J. D., G. Rumbaugh, et al. (2006). "Arc/Arg3.1 mediates homeostatic synaptic scaling of AMPA receptors." Neuron **52**(3): 475-484.
Simons, K. and D. Toomre (2000). "Lipid rafts and signal transduction." Nat Rev Mol Cell Biol **1**(1): 31-39.
Singer, S. J. and G. L. Nicolson (1972). "The fluid mosaic model of the structure of cell membranes." Science **175**(4023): 720-731.
Sjogren, B., M. W. Hamblin, et al. (2006). "Cholesterol depletion reduces serotonin binding and signaling via human 5-HT(7(a)) receptors." Eur J Pharmacol **552**(1-3): 1-10.
Sogaard, R., T. M. Werge, et al. (2006). "GABA(A) receptor function is regulated by lipid bilayer elasticity." Biochemistry **45**(43): 13118-13129.
Sooksawate, T. and M. A. Simmonds (2001). "Effects of membrane cholesterol on the sensitivity of the GABA(A) receptor to GABA in acutely dissociated rat hippocampal neurones." Neuropharmacology **40**(2): 178-184.

Steward, O., C. S. Wallace, et al. (1998). "Synaptic activation causes the mRNA for the IEG Arc to localize selectively near activated postsynaptic sites on dendrites." Neuron **21**(4): 741-751.
Steward, O. and P. F. Worley (2001). "A cellular mechanism for targeting newly synthesized mRNAs to synaptic sites on dendrites." Proc Natl Acad Sci U S A **98**(13): 7062-7068.
Suzuki, T., J. Ito, et al. (2001). "Biochemical evidence for localization of AMPA-type glutamate receptor subunits in the dendritic raft." Brain Res Mol Brain Res **89**(1-2): 20-28.
Szasz, B. K., A. Mike, et al. (2007). "Direct inhibitory effect of fluoxetine on N-methyl-D-aspartate receptors in the central nervous system." Biol Psychiatry **62**(11): 1303-1309.
Tagawa, Y., P. O. Kanold, et al. (2005). "Multiple periods of functional ocular dominance plasticity in mouse visual cortex." Nat Neurosci **8**(3): 380-388.
Tohda, M., H. Urushihara, et al. (1995). "Inhibitory effects of antidepressants on NMDA-induced currents in Xenopus oocytes injected with rat brain RNA." Neurochem Int **26**(1): 53-58.
Trushina, E., J. Du Charme, et al. (2006). "Neurological abnormalities in caveolin-1 knock out mice." Behav Brain Res **172**(1): 24-32.
Tsui-Pierchala, B. A., M. Encinas, et al. (2002). "Lipid rafts in neuronal signaling and function." Trends Neurosci **25**(8): 412-417.
Turrigiano, G. G. (2008). "The self-tuning neuron: synaptic scaling of excitatory synapses." Cell **135**(3): 422-435.
Tzingounis, A. V. and R. A. Nicoll (2006). "Arc/Arg3.1: linking gene expression to synaptic plasticity and memory." Neuron **52**(3): 403-407.
Tzingounis, A. V. and J. I. Wadiche (2007). "Glutamate transporters: confining runaway excitation by shaping synaptic transmission." Nat Rev Neurosci **8**(12): 935-947.
van Hooft, J. A. and H. P. Vijverberg (2000). "5-HT(3) receptors and neurotransmitter release in the CNS: a nerve ending story?" Trends Neurosci **23**(12): 605-610.
Vazdarjanova, A., V. Ramirez-Amaya, et al. (2006). "Spatial exploration induces ARC, a plasticity-related immediate-early gene, only in calcium/calmodulin-dependent protein kinase II-positive principal excitatory and inhibitory neurons of the rat forebrain." J Comp Neurol **498**(3): 317-329.
Ventura, R. and K. M. Harris (1999). "Three-dimensional relationships between hippocampal synapses and astrocytes." J Neurosci **19**(16): 6897-6906.
Videbech, P. and B. Ravnkilde (2004). "Hippocampal volume and depression: a meta-analysis of MRI studies." Am J Psychiatry **161**(11): 1957-1966.
Wallace, C. S., G. L. Lyford, et al. (1998). "Differential intracellular sorting of immediate early gene mRNAs depends on signals in the mRNA sequence." J Neurosci **18**(1): 26-35.
Waltereit, R., B. Dammermann, et al. (2001). "Arg3.1/Arc mRNA induction by Ca2+ and cAMP requires protein kinase A and mitogen-activated protein kinase/extracellular regulated kinase activation." J Neurosci **21**(15): 5484-5493.
Walters, R. J., S. H. Hadley, et al. (2000). "Benzodiazepines act on GABAA receptors via two distinct and separable mechanisms." Nat Neurosci **3**(12): 1274-1281.
Watanabe, Y., H. Saito, et al. (1993). "Tricyclic antidepressants block NMDA receptor-mediated synaptic responses and induction of long-term potentiation in rat hippocampal slices." Neuropharmacology **32**(5): 479-486.
Wu, C., S. Butz, et al. (1997). "Tyrosine kinase receptors concentrated in caveolae-like domains from neuronal plasma membrane." J Biol Chem **272**(6): 3554-3559.
Yamada, S. and W. J. Nelson (2007). "Synapses: sites of cell recognition, adhesion, and functional specification." Annu Rev Biochem **76**: 267-294.
Yancey, P. G., W. V. Rodrigueza, et al. (1996). "Cellular cholesterol efflux mediated by cyclodextrins. Demonstration Of kinetic pools and mechanism of efflux." J Biol Chem **271**(27): 16026-16034.
Yasuda, M., M. Fukuchi, et al. (2007). "Robust stimulation of TrkB induces delayed increases in BDNF and Arc mRNA expressions in cultured rat cortical neurons via distinct mechanisms." J Neurochem **103**(2): 626-636.

Zhang, H., L. A. Etherington, et al. (2012). "Regulation of AMPA receptor surface trafficking and synaptic plasticity by a cognitive enhancer and antidepressant molecule." Mol Psychiatry.
Zhou, M. and H. K. Kimelberg (2001). "Freshly isolated hippocampal CA1 astrocytes comprise two populations differing in glutamate transporter and AMPA receptor expression." J Neurosci **21**(20): 7901-7908.

7 Figure Index

7.1 Tables

8 Abbreviation Index

5-HT = serotonine

τ_{on} = onset

τ_{off} = offset

τ_{des} = desensitisation

AD = antidepressant

AMPA = α-Amino-3-hydroxy-5-methyl-4-isoxazolepropionic acid

Arc/Arg3.1 = (activity-regulated cytoskeleton-associated protein/activity regulated gene 3.1)

BDNF = brainderived neurotrophic factor

BSA = bovine serum albumin

CA region = *cornu ammonis* region

CaMK = Calmodulin kinase

Cdk5 = cyclin-dependent kinase 5

CREB = cyclic AMP (cAMP) response element binding protein

DAPI = 4`,6-Diamidino-2-phenylindole dihydrochlorid

DHPG = dihydroxyphenylglycine

Diaz = diazepam

DMEM = Dulbecco's Modified Eagle's Medium

DMI = desipramine

ERK1/2 = Extracellular-regulated protein Kinase 1/2

EDTA = Ethylenediaminetetraacetic acid

EGTA = ethylene glycol tetraacetic acid

FCS = fetal calf serum

fEPSP = field excitatory postsynaptic potential

FISH = fluorescent *in situ* hybridisation

Fluox = fluoxetine

GABA = gamma-aminobutyric acid

GPI = glycosylphosphatidylinositol

HEPES = 4-(2-hydroxyethyl)-1-piperazineethanesulfonic acid

HBD = high buoyant densitiy

HFS = high frequency stimulation

LBD = low buoyant densitiy

LGC = ligand-gated channel

L-Glu = L-glutamate

LTP = long-term potentiation

MAOI = monoamine oxidase inhibitor

MAPK = mitogen-activated protein kinase

MßCD = methyl-ß-cyclodextrine

mGluR = metabotropic glutamate receptor

mRNP = messenger ribonucleoprotein

NMDAR = N-methyl-D aspartate receptor

PFA = paraformaldehyd

PBS = Phosphate buffered saline

RhoA = Ras homolog gene family member A

SSC/DEPC H_2O = Standard Saline Citrat/Diethylpyrocarbonate water

Sccp = Schaffer collateral commissural pathway

SSRI = selective serotonine reuptake inhibitor

SV = presynaptic vesicles

TrkB = tyrosine kinase B

TRPV1 = vanilloid receptor subtype 1

9 Acknowledgements

Ich danke meinen Gutachtern, Prof. Dr. Martin Klingenspor und inbesondere Prof. Dr. Jochen Graw, für ihr entgegengebrachtes Interesse und vor allem ihre große Geduld. Großer Dank gilt auch Prof. Dr. Gerhard Rammes für die Einführung in Elektrophysiologie.

Ich danke der gesamten Arbeitsgruppe Rupprecht, besonders aber Dr. Barbara Di Benedetto für viele fruchtbare Diskussionen und entscheidende Hilfestellungen, sowie Eva Wagner für die Unterstützung bei den molekularbiologischen Methoden.
Ich bedanke mich bei Prof. Dr. Rainer Rupprecht für die Aufnahme und die Unterstützung in seiner Arbeitsgruppe und bei Dr. Caroline Nothdurfter für die Zusammenarbeit.

Ich danke Dr. Julien Dine für die vielen fachlichen Diskussionen während der Kaffeepausen und das Korrekturlesen meiner Arbeit.

Ich danke meiner Familie für Ihre Unterstützung weit ins "Erwachsenenalter" hinein.